

Anionic living polymerization of useful monomers that can provide intermolecular chemical links

メタデータ	言語: English 出版者: 公開日: 2008-01-07 キーワード (Ja): キーワード (En): 作成者: SE, Kazunori メールアドレス: 所属:
URL	http://hdl.handle.net/10098/1398

The Revised Manuscript: August 13, 2002

The First Manuscript: May 26, 2001

**Anionic living polymerization of useful monomers
that can provide intermolecular chemical links**

Kazunori SE*

*Department of Materials Science and Engineering, Faculty of Engineering,
Fukui University, Bunkyo 3-9-1, Fukui 910-8507, Japan*

RUNNING HEAD: Anionic living polymerization of useful monomers

* Tel: +81-776-27-8957; fax: +81-776-27-8767

* *E-Mail address:* se@matse.fukui-u.ac.jp

Contents

1. Introduction	7
2. Polyaminostyrenes, PAS.....	8
2. 1 Poly(tertiary aminostyrene)s, PtAS	9

2. 1. 1	Polymerization of tertiary aminostyrenes, tAS	10
2. 1. 2.	General aspect for preparing monodispersed polymers ...	12
2. 1. 3.	Quaternization of PtAS	14
2. 1. 4	The degree of quaternization	14
2. 1. 5.	Preparation of cross-linked films of PtAS with <i>p</i> , p'-bis(chloromethyl)azobenzene, CAB	16
2. 1. 6.	Photochemical isomerization of crosslinked films of PtAS with CAB	18
2. 1. 7.	Photochemical isomerization of crosslinked films of poly(<i>N</i> , <i>N</i> -dimethyl-4-vinylphenethylamine)- <i>block</i> -polystyrene with CAB	20
	(a)Kinetics	21
	(b)Reversible optical recording materials	22
2. 2.	Poly(secondary aminostyrene).....	24
2. 2. 1	Polymerization of secondary aminostyrene, ISBA	24
2. 2. 2.	Removal of a trimethylsilyl group	26
2. 2. 3.	Anionic reactivity of aminostyrenes	27
2. 2. 4.	Grafting of oligopeptides	29
2. 2. 5.	Blood compatibility of PAS- <i>graft</i> -oligopeptides	31
3.	Block-graft copolymers	34
3. 1.	Poly(4-vinylphenyl)dimethylvinylsilane, PVS	35
3. 1. 1	Polymerization of (4-vinylphenyl)dimethylvinylsilane, VS ...	36
	(a)Initiators	36
	(b)Solvents	37

(c) Polymerization times	38
3. 1. 2 Lithographic characterization	39
3. 1. 3 Preparation	of
[poly(4-vinylphenyl)dimethylvinylsilane- <i>graft</i> -polyisoprene]- <i>block</i> -polystyrene, (PVS- <i>g</i> -PIs)- <i>b</i> -PS	42
3. 1. 4. Molecular characteristics of (PVS- <i>g</i> -PIs)- <i>b</i> -PS	43
3. 1. 5. Morphology	46
3. 2. Poly(<i>p</i> -hydroxystyrene), PHSt	49
3. 2. 1 Polymerization of <i>p-tert</i> -butoxystyrene, BSt	50
3. 2. 2. Preparation	of
polystyrene- <i>block</i> -[poly(<i>p</i> -hydroxystyrene- <i>graft</i> -poly(ethylene oxide))- <i>block</i> -polystyrene, PS- <i>b</i> -(PHSt- <i>g</i> -PEO)- <i>b</i> -PS	
.....	52
3. 2. 3. Molecular characteristics of PS- <i>b</i> -(PHSt- <i>g</i> -PEO)- <i>b</i> -PS ...	53
(a) Block-graft copolymers, $M_n^{\text{block-graft}}$	53
(b) Grafts, M_n^{graft}	54
(c) Metallation efficiency, f_{metal}	55
(d) Number of grafts, N^{graft}	56
3. 2. 4. Morphology	57
4. Concluding remarks: anionic living polymerization of new monomers.....	61
References	63

Abstract

Anionic living polymerization of four new monomers that serve as intermolecular chemical links between polymer chains are described, along with the wide applications of the resultant polymer alloys. Examples of the first monomer include three tertiary aminostyrenes. The corresponding poly(tertiary aminostyrene)s (PtAS) having a desired molecular weight and narrow molecular weight distribution were prepared. Crosslinked films of PtAS with *p*, *p'*-bis(chloromethyl)azobenzene (CAB) were prepared by quaternization. Photochemical isomerization of CAB incorporated in PtAS was investigated. The second monomer discussed is *N*-isopropyl-*N*-trimethylsilyl-4-vinylbenzylamine (ISBA). ISBA was anionically polymerized and subsequent deprotection of the trimethylsilyl protecting group produced poly(*N*-isopropyl-4-vinylbenzylamine) (PIBA) with a secondary amino group. The non-thrombogenic behavior of the corresponding poly(aminostyrene)-*graft*-oligopeptide graft copolymers was evaluated. The third monomer, (4-vinylphenyl)dimethylvinylsilane (VS), contains a silylvinyl group. To carry out a

chemoselective polymerization of the styryl group of VS, a systematic study on anionic polymerization was carried out. Lithographic characterization shows the resultant polymer (PVS) acting as a negative working resist. Three (PVS-*graft*-polyisoprene)-*block*-polystyrene block-*graft* copolymers were prepared by a “grafting onto” process. The fourth monomer discussed is *p*-butoxystyrene. The deprotection of the *tert*-butyl protecting group from the corresponding polymer produces poly(*p*-hydroxystyrene) (PHSt). Two polystyrene-*block*-[PHSt-*graft*-poly(ethylene oxide)]-*block*-polystyrene block-*graft* copolymers were prepared by a “grafting from” process. Benzene-cast films formed clear and specific lamellar structures in which poly(ethylene oxide) is not crystallized.

Keywords: Anionic living polymerization; Poly(tertiary aminostyrene)s; Photochemical isomerization; Poly(*n*-isopropyl-4-vinylbenzylamine); Poly(aminostyrene)s-*graft*-oligopeptides; Poly(4-vinylphenyldimethylvinylsilane); Negative working resists; Block-*graft* copolymers; Poly(*p*-hydroxystyrene)

1. Introduction

Recently, a number of highly functionalized polymers with interesting physical properties and high performance polymers have been prepared [1-3]. However, it appears that homopolymers and/or simple linear block copolymers may not be useful in the fabrication of polymeric devices [4-6] exhibiting more sophisticated physical phenomena [7-9]. An example of this is provided by polymer alloys [10, 11] consisting of two or more different polymers combined by chemical links [12-14]. Thus, a new type of polymer alloy based on block copolymers is required [15, 16]. When preparing such polymer alloys, anionic living polymerization [17-19] provides a means to obtain the desired molecular weights and narrow molecular weight distributions (MWDs), although cationic and radical living techniques have been rapidly advancing [20-23]. Therefore, a key step is the design and synthesis of new monomers that contain a vinyl group and another functional group: The vinyl group is polymerized by the anionic living mechanism and the functional group remains unaltered during the anionic polymerization to subsequently provide intermolecular chemical links between two polymers.

We propose four new monomers, with vinyl and functional groups, as shown in **Fig. 1**. The first monomers are tertiary aminostyrenes (tAS) that contain a functional tertiary amino group. Poly(tertiary aminostyrene)s can be used as prepolymers of crosslinked polymers by quaternization of the tertiary amino groups. The second monomer is *N*-isopropyl-*N*-trimethylsilyl-4-vinylbenzylamine (ISBA) that contains a trimethylsilyl

protecting group. The deprotection from the corresponding polymers produces poly(secondary aminostyrene) that can be used as the backbone chains of graft copolymers by amidation of the secondary amino group. The third monomer is a (4-vinylphenyl)dimethylvinylsilane (VS) that contains a silylvinyl group. Poly(4-vinylphenyl)dimethylvinylsilane has a silylvinyl group that can be used as crosslinked points and/or grafting points. The fourth is a *p*-butoxystyrene (BSt) that contains a *tert*-butyl protecting group. Furthermore, the deprotection from the corresponding polymer produces poly(*p*-hydroxystyrene). Poly(*p*-hydroxystyrene) has a hydroxyl group that can be changed to alkoxide ions as initiators by metallation. The corresponding macromolecular initiators are candidates for the synthesis of new graft copolymers.

Anionic living polymerization of the four useful monomers is described in this review. The description thus provides a general method of performing anionic living polymerization of new monomers, having a vinyl group and another functional group. Wide applications and physical properties of the resultant polymer alloys are also described.

2. Polyaminostyrenes, PAS

As shown in **Fig. 2**, poly(aminostyrene)s (PAS) may have amino groups classified as primary, secondary, or tertiary amino groups [24, 25]. In this review, the amino group substituents of special interest include the phenyl, benzyl, or phenethyl groups. The resultant PAS may show a decrease in the electron density on the nitrogen atom of the amino group in the sequence; phenethyl, benzyl, and phenyl amine. Tertiary aminostyrenes should polymerize by the anionic living mechanism without too much difficulty. For example,

using three tertiary aminostyrenes, a general approach to polymerize new monomers by anionic living mechanism will be described in chapter 2. 1.

By contrast, primary and secondary aminostyrenes can not be polymerized by anionic living mechanisms, because the propagating carbanionic species rapidly react with the labile protons of the amino groups to terminate the polymerization. In these cases, the amino groups must be protected during anionic polymerization, and the protecting group must be rapidly and completely removed after the polymerization [26-28]. The resultant poly(primary aminostyrene)s seem unsuitable for backbone chains of graft copolymers and for introducing other functions, because the complete utilization of two labile protons on each nitrogen atom of the primary aminostyrenes appears impossible. From a view point of the next reactions, poly(secondary aminostyrene) seems suitable for providing intermolecular chemical links [29]. As an example, using a secondary aminostyrene, a general approach to polymerize new monomers having a labile proton by anionic living mechanism will be described in chapter 2. 2.

2. 1. Poly(tertiary aminostyrene)s, PtAS

As shown in Fig. 2, three tertiary aminostyrenes: *N, N*-dimethyl-4-vinylphenylamine, DPA, $\text{CH}_2=\text{CHPhN}(\text{CH}_3)_2$; *N, N*-dimethyl-4-vinylbenzylamine, DBA, $\text{CH}_2=\text{CHPh}(\text{CH}_2)\text{N}(\text{CH}_3)_2$; and *N, N*-dimethyl-4-vinylphenethylamine, DPTA, $\text{CH}_2=\text{CHPh}(\text{CH}_2)(\text{CH}_2)\text{N}(\text{CH}_3)_2$; may be polymerized by an anionic living mechanism [24, 25]. Quaternization of three poly(tertiary aminostyrene)s (PtAS) with alkyl halides was investigated [30], followed by the preparation of crosslinked films by quaternization of PtAS or their block copolymers with *p, p*-bis(chloromethyl)azobenzene (CAB),

$\text{ClCH}_2\text{Ph-N=N-PhCH}_2\text{Cl}$ [31]. Photochemical isomerization of the crosslinked films was investigated to prepare the reversible recording materials [32].

2. 1. 1. Polymerization of tertiary aminostyrenes, tAS

Three monomers of DPA, DBA, and DPTA were prepared according to our previous procedures [24]. The polymerization was carried out in a sealed glass apparatus under a pressure of 10^{-6} mmHg [33, 34]. The results of the polymerization for DPA are shown in **Table 1**. When a *sec*-butyllithium (*sec*-BuLi)/benzene (Bz) system was used as the initiator/solvent, the polymerization solution showed a light red color at room temperature, corresponding to a characteristic color of living carbanions. The solution gradually changed from light red to colorless, and then finally remained colorless after 15 h. This finding suggests that the living carbanions might abstract a proton from the methyl groups on the amino groups to be deactivated during the chain propagation. For suppressing the abstraction reaction, a lower temperature is preferable to the anionic living polymerization. When a *n*-butyllithium (*n*-BuLi)/ tetrahydrofuran (THF) system was used at -78°C , the polymerization solution showed a yellow color. The color remained unchanged overnight. However, the GPC chromatogram had a broad peak ($M_w/M_n = 1.2_2$), as shown in **Fig. 3**. When a cumylcesium (Cumyl Cs)/THF system was used at -78°C , the polymerization solution remained red overnight. In spite of the low polymer conversion (40%-85%), the molecular weight observed (M_n) was close to the kinetic molecular weight expected from the amounts of monomer and initiator (M_k). As shown in Fig. 3, the GPC chromatogram had a sharp peak ($M_w/M_n = 1.0_9$). When a cumylpotassium (Cumyl K)/THF system was used at -78°C , the polymer conversion was 100%. We succeeded in preparing nearly all

monodispersed poly(*N, N*-dimethyl-4-vinylphenylamine) (PDPA) having $M_n = 2.8 \times 10^4 - 2.6 \times 10^5$.

The results of the polymerization for DBA are shown in **Table 2**. When a *n*-BuLi/THF system was used, the polymerization solution remained yellow overnight. Also, the GPC chromatogram had a broad peak. However, using Cumyl K or Cumyl Cs as an initiator, we prepared poly(*N, N*-dimethyl-4-vinylbenzylamine) (PDBA) having a narrow MWD in 100% polymer conversion.

The results of the polymerization for DPTA are also shown in Table 2. When *n*-BuLi was used, the polymer solution remained yellow overnight. However, the M_w/M_n value was more than 1.2. When Cumyl K or Cumyl Cs was used as an initiator, poly(*N, N*-dimethyl-4-vinylphenethylamine) (PDPTA) having a narrow MWD was prepared.

2. 1. 2. General aspect for preparing monodispersed polymers

To obtain polymers having narrow MWDs, three conditions must be fulfilled in preparing the polymers by an anionic living mechanism:

- (a) a "living" polymerization proceed,
- (b) the carbanion responsible for anionic polymerization must be stable enough and not react with solvent and side chains of the polymers,
- (c) the overall time period required for propagation must be much greater than the time period required for all chains to initiate.

The polymerization solutions showed characteristic colors of carbanions, and block copolymers of tertiary aminostyrenes and styrene were quantitatively obtained in preliminary preparations. These facts suggest that the "living" polymerization of tertiary aminostyrenes proceeded. Except for the *sec*-BuLi/Bz/PDPA system, the present data fulfilled the

condition (a).

The experimental proofs fulfilling the condition (b) are: (1) a 100 % polymer conversion is attained and (2) the M_n value is in good agreement with the M_k value. Excluding a *sec*-BuLi/Bz/PDPA system and a Cumyl Cs/THF/PDPA system, the present data fulfilled the experimental proofs of (1) and (2); namely, condition (b).

Particular attention should be directed to the low polymer conversion of a Cumyl Cs/THF/PDPA system. If the rate of initiation is much faster than that of propagation, the polymerization rate can be expressed by

$$-\ln(1-x) = k_{ap} [LE] t \quad (1)$$

where k_{ap} is an apparent rate constant; [LE] is a molar concentration of the living end, and x is the polymer conversion, respectively.

The first-order plots of the Cumyl Cs/THF systems and the Cumyl K/THF systems for PDPA are shown in **Fig. 4**. The kinetic characteristics are shown in **Table 3**. From a comparison of the k_{ap}^K and the k_{ap}^{Cs} values for PDPA with the apparent rate constant of a Na ion for styrene [17, 35], the k_{ap}^K and k_{ap}^{Cs} values were found to be very small. Due to a small k_{ap}^{Cs} value, the polymer conversion of the cumyl Cs/THF/PDPA system was less than 85%; namely, the condition (b) was fulfilled in this system.

The experimental proof fulfilling condition (c) is: (3) the MWD is sharp. It was difficult to prepare nearly monodispersed polymers having M_n much more than 10^6 , because of the viscous polymerization solutions. Hence, an additional proof fulfilling the condition (c) is: (4) the polymer having a narrow MWD can be prepared in a wide range of molecular weight from 10^4 to 10^6 .

When *n*-BuLi was used as the initiator, the amino group of PtAS may participate in the solvation of a Li ion during the propagation because of the high affinity of the amino group

for the Li ion. However, when Cumyl K and Cumyl Cs were used as initiators, the experimental proof (3) was fulfilled. Because of the low k_{ap}^K and k_{ap}^{Cs} values, we succeeded in preparing PDPA samples having $M_n = 2.7 \times 10^4 - 2.6 \times 10^5$, and their M_w/M_n values were less than 1.0₅. In conclusion, three conditions of (a), (b) and (c) were fulfilled in the present data, except for the *sec*-BuLi/Bz/PDPA system and the *n*-BuLi/THF/three PtAS systems. Therefore, the three PtAS having narrow MWDs were prepared by an anionic living mechanism using Cumyl K and Cumyl Cs as initiators.

2. 1. 3. Quaternization of PtAS

Tertiary amino groups react with *n*-butyl bromide to produce quaternary ammonium salts by the Menshutkin reaction [36]. The M_n and M_w/M_n values of the quaternized PtAS are found the same as those of the corresponding PtAS. These results suggest that neither intermolecular crosslinkage nor degradation of PtAS occurred during quaternization. The quaternized PtAS were a new type of cationic polyelectrolytes [37]. As an example, **Fig 5** shows the resultant neutralization curve of the quaternized PDBA (QPDBA) treated with an anion-exchange resin (Amberlite IRA-400).

2. 1. 4. The degree of quaternization

Three poly(tertiary aminostyrene)s were quaternized with *n*-butyl bromide at 60°C for 1 h - 6 h. The molar ratio of *n*-butyl bromide to the tertiary amino group was five. **Fig. 6** shows the reaction time dependence of the degree of quaternization (DQ). The DQ value of PDPA was much smaller than those of PDBA and PDPTA over the entire reaction time.

The quaternization of PDPA, PDBA, and PDPTA was carried out for 6 h at a constant temperature varied from 0°C to 120°C. As shown in **Fig. 7**, quaternization reactivity

increases in the order of PDPA, PDBA, and PDPTA. The DQ values of the three PtAS could be controlled from 0% to nearly 100% by choosing the appropriate reaction time and temperature. The resultant quaternized PtAS that had DQ values of more than 60% were found easily soluble in water.

Since the Menschutkin reaction is regarded to be a bimolecular reaction [36] of an amino group and an alkyl halide, its rate of reaction can be represented by the following equation:

$$\ln [C_0^h (C_0^a - C_t^q) / C_0^a (C_0^h - C_t^q)] / (C_0^a - C_0^h) = k_a t \quad (2)$$

where C_0^a and C_0^h represent the initial concentrations of amine and halide, respectively, C_t^q represents the concentration of the resultant quaternary ammonium salts at a given reaction time, and k_a is an apparent reaction rate constant. Further, from Eq. (2), the k_a value was estimated. Several k_a values were also estimated at temperatures at which quaternization was carried out. As shown in **Fig. 8**, temperature dependence of the k_a values of PDPA, PDBA, and PDPTA can be determined by an Arrhenius' equation:

$$\ln k_a = \ln A^* - (\Delta E_a^* / RT) \quad (3)$$

where A^* and ΔE_a^* represent a frequency factor and an activation energy, respectively. The resultant kinetic characteristics of A^* and ΔE_a^* are listed in **Table 4**.

As shown in Table 4, the E_a^* values of PDPTA and PDBA were identical, and the A^* value of PDPTA was three times as large as that of PDBA. This phenomenon is probably caused by steric hindrance in the vicinity of nitrogen of the *N,N*-dimethylamino group, and is consistent with the distance between the nitrogen and aromatic ring of PDPTA that is longer than that of PDBA. In contrast, the ΔE_a^* and the A^* values of PDPA were much smaller than those of PDBA and PDPTA. The low reactivity of quaternization of PDPA with *n*-butyl bromide is caused by two factors: One is a drop in electron density on the nitrogen

atom of the *N, N*-dimethylamino group due to the resonance effect between the phenyl group and nitrogen, the other is a steric hindrance in the vicinity of the nitrogen atom which is directly attached to the aromatic ring. The quaternization of the three PtAS with alkyl dibromides or alkyl dichlorides should permit preparation of cross-linked polymers such as a model network.

2. 1. 5. Preparation of cross-linked films of PtAS with *p, p'*-bis(chloromethyl) azobenzene, CAB

We could control the degree of quaternization of the three PtAS from 0% to 100% by using the appropriate reaction time and temperature [30]. Hence, on mercury or on cover glasses floated on mercury, cross-linked films (10 - 40 μm thickness) were prepared by evaporation of the solvent from a mixed solution of PtAS and *p, p'*-bis(chloromethyl)azobenzene (CAB) for 2 days at 25°C [31]. After drying the films in a vacuum, they were annealed at 90°C for more than 10 h. **Fig. 9** schematically shows a structural formula of the crosslinked films. The cross-linked films are designated as PDPA(CAB)_Y, PDDBA(CAB)_Y, and PDPTA(CAB)_Y, respectively, where Y is a molar % of chloromethyl groups for CAB to *N, N*-dimethylamino groups of PtAS.

In order to confirm the formation of the cross linkage, we carried out a swelling equilibrium test of the films. The films were submerged in methanol or THF as a swelling solvent for 6 h at 25°C. The films were actualized in an equilibrium state before at least 6 h, because the swollen gels did not increase in weight until 36 h. The result of the swelling tests is shown in **Table 5**. The degree of swelling (Q_r) decreased by increasing the amount of CAB. An apparent effective-network-concentration (ν'_e) could be calculated from the amount of CAB and the polymer. The ν'_e values are also described in Table 5.

Next, an effective network concentration ν_e was estimated from the swelling of the crosslinked films. A crosslinked polymer is insoluble in methanol but swells with methanol by the suppression of elasticity due to network structures. In the swelling equilibrium state, the following modified Flory-Rehner's equation is valid [38, 39],

$$\nu_e = \frac{-2[v + \mu v^2 + \ln(1 - v)]}{V_s (2v^{1/3} - v)} \quad (4)$$

where V_s is a molar volume of solvent, μ is a polymer-solvent interaction parameter, and v is a volume fraction of polymer in a gel, which is the reciprocal of Q_r ($= 1/v$) [36]. When $v^{1/3} \gg v/2$ (Q_r is large), Eq. (4) can be rewritten as

$$\nu_e = \frac{1}{Q_r^{5/3} V_s} (1/2 - \mu) \quad (5)$$

The μ is expressed as [40, 41]

$$\mu = \mu_z + (V_s/RT) (\delta_s - \delta_p) \quad (6)$$

where δ_s and δ_p are solubility parameters of solvent and polymer, respectively; and μ_z is a small constant (empirically 0.2) assumed in the entropy calculation. The solubility parameter of THF, δ_s is 9.1. Thus, the μ value was estimated at 0.34 ($\delta_p = 9.7$ by Small) [41] or 0.32 ($\delta_p = 9.8$ by Hoy) [41]. When the μ value is known, ν_e can be calculated from Eq. (5) and the results are listed in Table 5. As shown in **Fig. 10**, both values of ν_e determined from a Small's number and a Hoy's number for the same film seem somewhat larger than that of ν_e' . This discrepancy probably comes from a difference in μ estimated by a Small's method or a Hoy's method. It is concluded that all of the CAB added to PDBA form the cross linkage between the amino groups of PDBA. Differential scanning calorimetric (DSC) thermograms of the three PtAS and the resultant crosslinked films also present clear evidence supporting the formation of crosslinked films.

2. 1. 6. Photochemical isomerization of crosslinked films of PtAS with CAB

Photochromism is a reversible photochemical exchange in molecular structure that results in remarkable changes in the absorption spectra [42, 43]. Much attention has been devoted to investigating this phenomenon for its usage as reversible recording materials. When a photochromic compound is used as the reversible recording material, thermal stability is an important problem to overcome because the reverse thermal reactions occur in most organic photochromic compounds [44, 45].

Fig. 11 shows the UV spectra of CAB in methanol. When the solution was irradiated with a UV light ($300 \text{ nm} < \lambda_1 < 380 \text{ nm}$), the absorbances at 330 nm and 220nm decreased, but increased with an increase of irradiation time, respectively. This is attributed to the photochemical isomerization of *trans* to *cis* form of CAB. When a visible light ($420 \text{ nm} < \lambda_2$) was used or the solution was allowed to stand in darkness, the UV spectrum was restored to the original spectrum. This behavior arises from the photochemical isomerization of *cis* to *trans* form of CAB. Moreover, isosbestic points were observed at 385nm and 280nm. Observation of isosbestic points indicates that there is no side reaction.

A similar behavior was observed in the crosslinked films of PDBA(CAB)_{1,5}, as shown in **Fig. 12**. Hence, a change in absorbance of PDBA(CAB)_{1,5} at 320 nm was measured to determine the fraction of *trans* to *cis* form of CAB. **Fig. 13** shows a change in photochemical isomerization of *trans* to *cis* form with time. The degree of isomerization was detected as the ratio of A_t/A_0 , where A_0 and A_t are the initial absorbance and absorbance at time t , respectively. In the case of CAB dispersed in polystyrene (PSt), PSt(CAB)_{1,5} [31, 46]. CAB was isomerized in a 65% conversion (*cis* form) after the irradiation of λ_1 for 30 min. When CAB was incorporated in the films of PDPTA(CAB)_{1,3}, CAB was isomerized in a 15%

conversion (*cis* form). These facts indicate that the thermal freedom of CAB was suppressed by cross-linked polymers in a glassy state.

At temperatures above T_g , the cross-linked films are in a rubbery state. Therefore, it is expected that CAB in a rubbery state can be isomerized more than in a glassy state [46]. However, as shown in Fig. 13, the *trans* fractions of PDPTA(CAB)_{1,3} did not decrease with an increasing irradiation time at 60°C. Furthermore, an unexpected behavior was observed: The *trans* fractions of CAB appeared to increase with UV irradiation. This behavior may be attributed to the deformation of the films due to conformational changes in the crosslinked polymer chain. The process should also be utilized to induce photostimulated mechanical motions such as bending, twisting [47, 48], and expansion. In order to suppress the deformation of the films above the T_g of PDPTA (T_g^{PDPTA}), the block copolymer was prepared.

2. 1. 7. Photochemical isomerization of crosslinked films of poly(N, N-dimethyl-4-vinylphenethylamine)-block-polystyrene with CAB

Table 6 shows the experimental conditions and results of the preparation of the poly(N, N-dimethyl-4-vinylphenethylamine)-*block*-polystyrene block copolymer (PDPTA-*b*-PSt) by anionic living copolymerization. From the common morphological results of the block copolymers [1, 7], the phases of PSt (53 wt%) and PDPTA were expected to form the lamellar structure. Crosslinked films of PDPTA-*b*-PSt with CAB were prepared according to the same procedure [31]. As shown in Figure 13, CAB of the (PDPTA-*b*-PSt)(CAB)_{2,5} film was isomerized in a 27% conversion (*cis* form) at 60°C for 30 min. We succeeded in measuring the photochemical isomerization of CAB in the block copolymer at 60°C, which is a higher temperature than T_g^{PDPTA} [31].

(a) Kinetics

As shown in **Fig. 14**, a plot of $-\ln[(C_t - C_e)/(C_0 - C_e)]$ versus t for each film of (PDPTA-*b*-PSt)(CAB)_Y was not linear within most of the range of t , where C_0 , C_t , and C_e are *trans* fractions at the initial state ($t = 0$), time t , and equilibrium state ($t = \infty$), respectively. Such deviation from the first-order plots has been qualitatively discussed on the basis of a distribution of a free volume [49-51]. The departures from the first-order kinetics in polymer matrices have been analyzed quantitatively by Saito et al. [52] and Tomioka et al. [53] using a phenomenological procedure based on the Kohlraush-Williams-Watts (KWW) equation [54]. A time-dependent reaction rate constant, k_t , can be defined as

$$-d \ln [(C_t - C_e) / (C_0 - C_e)] / dt = k_t \quad (7)$$

By using a KWW equation, k_t can be expressed as

$$k_t = \kappa t^{\alpha-1} \quad (8)$$

Substituting the above expression for k_t in Eq. (7) and the subsequent integration of Eq. (7) yields,

$$-\ln [(C_t - C_e) / (C_0 - C_e)] = (\kappa/\alpha) t^\alpha \quad (9)$$

When a parameter α takes unity, k_t becomes κ corresponding to an inherent reaction rate constant and the resultant Eqs. (7) and (9) become an equation of the first-order kinetics. Thus, the parameter α concerns itself with the deviation of reaction kinetics from the first order reactions. **Fig. 15** showed the relationship between the thus-obtained parameter α and temperature, at which the photochemical isomerization from *trans* to *cis* form of CAB proceeded in the polymer matrices. The resultant temperature dependence of the α values is the same as those of spirooxazine in poly(*n*-butyl methacrylate) reported by Saito et al. [52], and of spyropyrans in poly(methyl methacrylate) reported by Tomioka et al. [53]. Namely,

segmental motions of matrix polymers affect the molecular environment around CAB. Thus, the parameter α increased and progressively reached to unity with increasing temperature.

Particular attention should be paid to the half-life period ($\tau_{1/2}$) and a three fourths-life period ($\tau_{3/4}$) of the photochemical isomerization from *trans* to *cis* form of CAB. Both values were determined from the times at which the $(C_t - C_e) / (C_0 - C_e)$ values attained 50% and 75%, respectively. **Fig. 16** shows the resultant temperature dependence of $\tau_{1/2}$ and $\tau_{3/4}$ of (PDPTA-*b*-PSt)(CAB)_Y. Photochemical isomerization from *trans* to *cis* form of CAB was suppressed by the cross-linked films below T_g^{PDPTA} (~30°C) and the suppression was discontinuously removed from CAB at T_g^{PDPTA} . The photochemical isomerization of CAB proceeded in a homogeneous molecular environment above T_g^{PDPTA} .

(b)Reversible optical recording materials

When the films are used as reversible optical recording materials, a process of optical recording, of retention of the records, and of deletion of the records must be considered carefully. The process of optical recording corresponds to the photochemical isomerization from *trans* to *cis* form of CAB that was described in the previous paragraph. The other two processes are related to the photochemical isomerization from *cis* to *trans* form of CAB.

As shown in **Fig. 17**, a film of (PDPTA-*b*-PSt)(CAB)_{1.5} was first irradiated with an UV light at 60°C > T_g^{PDPTA} for 2 h. After 2 h under the irradiation with an UV light, the *trans* fractions of (PDPTA-*b*-PSt)(CAB)_{1.5} became 72% at 60°C. After 3 h under irradiation with visible light (420 nm < λ_2) at 20°C, the *trans* fractions of the film varied to 82%. *Trans* fraction of the film also varied to 79% after storing the film in darkness at room temperature for 180 h. Hence, approximately 20% of the CAB remained in the *cis* form. In conclusion,

the retention of the *cis* form (corresponding to the retention of the records) was achieved using PDPTA-*b*-PSt below T_g^{PDPTA} .

The deletion of the *cis* form was also studied by the measurement of the photochemical isomerization of *cis* to *trans* form of CAB in (PDPTA-*b*-St)(CAB)_{1.5} after irradiation with a visible light at 90°C. As shown in Fig. 17, when the film was irradiated with a visible light at 90°C > T_g^{PDPTA} for 3 h after irradiation with a UV light at 60°C for 2 h, the *trans* fraction increased from approximately 72% to 100%. The *cis* form can be deleted completely by irradiation with a visible light at 90°C, although 18% of the *cis* form remained at 20°C. Therefore, the retention and/or deletion of the *cis* form (the records) was controlled by alternation of the thermal motion of PPTA below and above the T_g^{PDPTA} of the PDPTA-*b*-PSt block copolymer.

2. 2. Poly(secondary aminostyrene)

Secondary aminostyrenes could not be polymerized by anionic living mechanisms because the propagating carbanionic species readily react with the labile proton of the secondary amino group. The confliction of the labile proton and anionic polymerization can be overcome by using a protective technique. The amino groups should be protected during anionic polymerization, and the protecting group can be promptly and completely removed after polymerization to prepare the corresponding polymer.

2. 2. 1. Polymerization of secondary aminostyrene, ISBA

N-isopropyl-*N*-trimethylsilyl-4-vinylbenzylamine (ISBA),
 $\text{CH}_2=\text{CHPhCH}_2\text{N}[\text{Si}(\text{CH}_3)_3][\text{CH}(\text{CH}_3)_2]$, was synthesized according to our procedure [29]. ISBA was dried with calcium hydride (CaH_2), octylbenzophenone sodium,

(C₈H₁₇)-Ph-(CO)⁻-Ph Na⁺ (C₈BP-Na) [19], and *sec*-butylmagnesium bromide (BuMgBr) as purging reagents in the order at 10⁻⁶mmHg. Thus-purified ISBA could not be polymerized by *n*-BuLi. The anionic initiator was found to be deactivated by *N*-isopropyl-4-vinylbenzylamine (IBA), which was a pre-product of ISBA.

In order to purge IBA from ISBA, the THF solution of ISBA was dried over BuMgBr at room temperature because of a low solubility of BuMgBr in ISBA. After the removal of THF, ISBA was distilled from the mixture of ISBA and BuMgBr. When the ISBA was added to an initiator solution, the solution showed a yellow color, however the color disappeared immediately. The ISBA was dried twice over BuMgBr/THF and the corresponding solution showed a yellow color, which remained unchanged for 3 h. As shown in **Table 7**, the resultant poly(*N*-isopropyl-*N*-trimethylsilyl-4-vinylbenzylamine), PISBA was prepared in a 17% conversion. The ISBA dried 3 times was polymerized for 24 h to yield PISBA in an 100% conversion. As shown in **Fig. 18**, GPC chromatograms became sharp with the number of purifications using BuMgBr. By using thus-purified ISBA, well-defined PISBA ($0.60 \times 10^4 < M_n < 16 \times 10^4$, $1.0_3 < M_w/M_n < 1.0_7$) was successfully prepared.

Initiation efficiency of the initiator (*f*) was calculated as follows;

$$f = M_k / M_n^{\text{PISBA}}_{\text{OSM}} \quad (10)$$

where the $M_n^{\text{PISBA}}_{\text{OSM}}$ value was determined by membrane osmometry. As shown in Table 7, the *f* values were not 1.0 but approximately 0.9; namely, the values did not decrease with an increasing M_k . This result suggests that the deactivation of the initiator should occur not in a process of polymerization but during storage in a refrigerator. This result occurs sometimes when carrying out the anionic polymerization, and is not a serious problem but an experimental one that should be overcome.

After ISBA was polymerized by *n*-BuLi in THF at -78°C , St was added to the polymerization solution to yield poly(*N*-isopropyl-*N*-trimethylsilyl-4-vinylbenzylamine)-*block*-polystyrene (PISBA-*b*-PSt). In contrast, after St was polymerized by *n*-BuLi in THF at -78°C , ISBA was added to the polymerization solution to yield PSt-*b*-PISBA. Thus, two block copolymers of PISBA and PSt were prepared. As shown in **Table 8**, the polymer conversions were 100%, the M_n values were close to the M_k values, and the compositions of the block copolymers were nearly equal to those fed in the polymerization solutions. Both block copolymers seemed to be prepared precisely. However, as shown in **Fig. 19**, PISBA-*b*-PSt shows a sharp GPC peak ($M_w/M_n = 1.0_5$) and PSt-*b*-PISBA shows a broad peak ($M_w/M_n = 1.2_5$). The sequence of the addition of the two monomers is thought to be important for preparing a well-defined block copolymer of PSt and PISBA. The reason will be described in chapter 2. 2. 3.

2. 2. 2. Removal of a trimethylsilyl group

The removal of the trimethylsilyl group from PISBA proceeded completely in methanol at 30°C during a period of 1 h. **Fig. 20** shows the NMR spectra of PISBA and the deprotected product of poly(*N*-isopropyl-4-vinylbenzylamine) (PIBA), $-\text{[CH}_2\text{-CHPhCH}_2\text{NH}\{\text{CH}(\text{CH}_3)_2\}]_n$ [55]. **Fig. 21** shows the GPC chromatograms of PISBA and the resultant PIBA. The chromatogram of PIBA shifted to a lower molecular weight on the side of the corresponding PISBA. Molecular heterogeneity of both the polymers were approximately the same; specifically, the deprotection did not cause any degradation or cross-linkage of the polymer chains of PISBA and PIBA. Removal of the trimethylsilyl group from PISBA-*b*-PSt and PSt-*b*-PISBA block copolymers was also fulfilled to produce new diblock copolymers having a poly(secondary aminostyrene) as a block.

2. 2. 3. Anionic reactivity of aminostyrenes

Special attention should be directed to an anionic reactivity of aminostyrenes and basic properties of the corresponding polymers. When a tertiary aminostyrene of DPA was anionically polymerized by *n*-BuLi or Cumyl K in THF at -78°C , the resultant PDPA sample had a M_w/M_n value of 1.3₈ or 1.0₉. During the propagation, the tertiary amino group at the growing polymer end may participate in the solvation of the Li ion [17, 35, 36]. Structural heterogeneity of the living end with the Li ion induced broadening of MWD of the final polymer. In contrast, a weak anionic initiator of Cumyl K may play no role of solvation with the amino group, hence the initiator may produce the final polymer with a narrow MWD. In the case of ISBA, the amino group has a bulky isopropyl group and a trimethyl group on the nitrogen atom. According to this steric hindrance, the amino group at the growing polymer end may not participate in the solvation of the Li ion. The structural homogeneity of the living end with the Li or K ion should produce PISBA with a narrow MWD.

A substituent effect of the amino groups on an anionic reactivity of the vinyl group should be attributed to not only a steric effect but also an electronic effect. The electronic effect of the vinyl group can be estimated from a ^{13}C chemical shift of a β -carbon in the vinyl group [56]. As shown in **Table 9**, the ^{13}C chemical shifts of the β -carbon in the aminostyrenes decreased from that of St due to the electron-releasing ability of the amino groups. A decrease in the ^{13}C chemical shift corresponds to an increase in the electron density on the β -carbon of the vinyl group, further corresponding to a lower anionic reactivity of aminostyrene, relative to that of St. Hence, the anionic reactivity of ISBA is expected to be lower than that of St. The aminostyryl living end of PISBA can easily initiate St, whereas the styryl living end of PSt has difficulty initiating ISBA. Thus, the PISBA-*b*-PSt

block copolymer has a M_w/M_n value of 1.0₅, while the PSt-*b*-PISBA block copolymer has a M_w/M_n value of 1.2₅.

In order to investigate the anionic reactivity of *N*, *N*-bis(trimethylsilyl)-4-vinylphenylamine (SPA) [57, 58], diblock copolymerizations of SPA and St were also carried out. The resultant PSPA-*b*-PSt block copolymer ($M_n = 10 \times 10^4$) has an M_w/M_n value of 1.0₉, whereas the PSt-*b*-PSPA block copolymer ($M_n = 4.7 \times 10^4$) has an M_w/M_n value of 1.2₆. These results are well explained by the same electronic effect as mentioned above.

The removal of the trimethylsilyl group from PISBA proceeded completely in methanol at 30°C during a period of 1 h, while the removal of the trimethylsilyl group from poly(*p*-*N*, *N*-bis(trimethylsilyl)-4-vinylphenylamine), (PSPA), $-\text{[CH}_2\text{-CHPhN}\{\text{Si}(\text{CH}_3)_3\}\{\text{Si}(\text{CH}_3)_3\}\text{-}$ proceeded in the THF-methanol (9:1 v/v) solution at a reflux temperature during a period of 3 h. The nitrogen-silicon bond of PISBA seems to be unstable, compared with that of PSPA. The difference in the removal of the trimethylsilyl group can be explained by the difference in basicity; namely, the electron density on the nitrogen of the amino group and steric hindrance in the vicinity of the nitrogen atom. Therefore, PISBA has high basicity because it has high electron density on the nitrogen atom and a small ethylene group (compared to a large phenyl group for PSPA) as a steric hindrance in the vicinity of the nitrogen atom.

2. 2. 4. Grafting of oligopeptides

The carboxylic acids should react with the amines of PAS to form an amide and/or peptide bond. This coupling reaction is expected to be useful for preparing high-performance graft copolymers that have oligopeptides (OP) [59], because the peptide

bond is formed by a covalent bond, thereby becoming more stable than the quaternized salts [30]. The resultant graft copolymer will be applied to biocompatible materials [60], biomedical polymers [61], and polymer catalysts with enzyme-like activities [6].

We carried out the coupling reaction of PAS with N-protected and C-free OP [62]. Three OP were used: *t*-butyloxycarbonyl-glycine (Boc-Gly), benzyloxycarbonyl-glycyl-proline (Z-Gly-Pro) and benzyloxycarbonyl-glycyl-L-prolyl-L-Leucyl-glycyl-L-proline (Z-Gly-Pro-Leu-Gly-Pro), where Boc ((CH₃)₃C-O-CO-) and Z (C₆H₅-CH₂-O-CO-) are the amino-protecting groups of OP. These OPs contain glycine, proline, and glycyl-prolyl forms, which are the main components of collagen [63]. **Table 10** shows the molecular characteristics of the two PASs used in this chapter.

Dicyclohexylcarbodiimide (DCC), C₆H₁₁-N=C=N-C₆H₁₁, is an efficient, nonacidic dehydrating agent that was used for a coupling of PAS with OP. DCC was added to a solution of OP in the mixed solvent of DMF and methylene chloride (CH₂Cl₂) at 0°C [64]. A solution of PAS was added to the resultant solution in order for it to react with OP.

Boc-Gly reacted with PPA to yield poly(4-vinylphenylamine)-*graft*-(Gly-Boc) (PPA-*g*-(Gly-Boc)) at 0°C for 2 h. **Fig. 22** shows a ¹³C-NMR spectrum of the resultant polymer. As compared with the ¹³C-NMR spectra of PPA and Boc-Gly, we discovered a peptide bond was found to be forming between the amino group of PPA and the carboxylic acid of Boc-Gly, thereby yielding a graft copolymer. The degree of grafting (DOG) of OP on a PAS molecule was defined as follows:

$$\text{DOG} / \% = ([\text{OP}] / [\text{AS}]) \times 100 \quad (11)$$

where [OP] and [AS] are, respectively, the molar concentrations of OP and of the aminostyrene monomer unit of PAS. To determine the DOG of PPA-*g*-(Gly-Boc), a ¹H-NMR spectrum of PPA-*g*-(Gly-Boc) was measured.

The coupling reaction was carried out at 45°C with the molar ratio of [Boc-Gly] / [AS] at 1.0 in the reactant. As shown in **Fig. 23**, the coupling reaction using DCC was found to be fast even at 0°C and quantitatively proceeded.

The coupling reaction was performed at 0°C for 2 h with a change in the molar ratio of [Boc-Gly] / [AS] from 0.5 to 4. As shown in **Fig. 24-(A)**, the DOG value increases in proportion to the [Boc-Gly] / [AS] value from 0 to 1, and remained constant at 100%. Identical behaviors were observed in the coupling reactions of Z-Gly-Pro (**Fig. 24-(B)**) and Z-Gly-Pro-Leu-Gly-Pro (**Fig. 24-(C)**). The coupling reaction quantitatively proceeds; namely, PPA-*g*-(OP) graft copolymers were quantitatively prepared. The DOG values of the resultant graft copolymers could be controlled by changing the molar ratio of [OP] / [AS].

Boc-Gly reacted with PIBA having a secondary amino group to yield poly(*N*-isopropyl-4-vinylbenzylamine)-*graft*-(Gly-Boc) (PIBA-*g*-(Gly-Boc)). The DOG value increased in proportion to the [Boc-Gly] / [AS] value from 0 to 1, and remained constant at 100% even when the [Boc-Gly] / [AS] value increased from 1 to 2, which was the same as that of Fig. 24.

The four graft copolymers having OP acting as the grafts were prepared. The DOG value could be controlled in the range of 0% to 100% by changing the molar ratio of [OP] to [AS]. DOG was revealed to be independent from the length of OP (from a mono-peptide to a pentapeptides) and to be independent of the differences in both polymers (PPA with the primary phenylamine and PIBA with the secondary benzylamine) as well.

2. 2. 5 Blood compatibility of PAS-graft-oligopeptides

Many biomedical applications of polymers have been reported in literature [65, 66]. From a clinical point of view, blood compatibility appears to be the most important characteristic when applying the sample to biomedical applications. Two tests should be conducted as the preliminary experiments for blood compatibility: One is a contact angle determination, and the other is a characterization of non-thrombogenicity at surfaces of the samples.

Hydrophilicity might play an important role to improve the blood compatibility of the samples [65]. PPA was insoluble in methanol, however PPA-g-(Gly-Boc) was soluble in methanol. An introduction of Boc-Gly to PPA was found to hydrophilize PPA. The contact angles of the samples were measured (**Table 11**). PPA showed an increase in hydrophilicity in comparison with PSt. An introduction of OP to PPA shows an increase in hydrophilicity in the sequence of Gly-Boc and Pro-Gly-Leu-Pro-Gly-Z in comparison with PPA.

PPA-g-(Pro-Gly-Leu-Pro-Gly-Z) exhibited a time dependence of the contact angle, which has never been observed for PPA and PPA-g-(Gly-Boc). After 10 minutes, the contact angle approached a constant value of 36 degrees that is a 50% decrease in the initial value. TecoflexTM is a cycloaliphatic poly(ether urethane) derivative, which is already in use for a catheter system [65]. The contact angle of TecoflexTM is reported to be 55 degrees [65]. PPA-g-(Pro-Gly-Leu-Pro-Gly-Z), that was in contact with water for 10 minutes, appears to have a good hydrophilic property in comparison with TecoflexTM.

A preliminary non-thrombogenic test for the four samples shown in Table 11 was conducted. The inside surface of a 'Pyrex' test tube was coated with each film of the corresponding graft copolymers. Fresh human whole blood (HWB) of 1 ml was introduced

into the test tube. After the test tube was left standing at 37°C for 5 minutes, the test tube was tipped to observe whether or not HWB flows at intervals of 30 seconds. When HWB was found not to flow by tipping the test tube, the resultant time was evaluated as a Lee-White clotting time [67, 68]. The Lee-White clotting time of a 'Pyrex' glass was measured at 11-12 minutes as a reference. By dividing the Lee-White clotting time of the sample by that of a 'Pyrex' glass, the Lee-White relative clotting time (L-WRCT) was determined. The resultant L-WRCT values of the samples are shown in **Fig. 25**. PSt and poly(vinyl chloride) were also measured to indicate the L-WRCT values of 2.3 and 2.0-2.5, respectively [69]. Many block copolymers for biomedical applications have been prepared; for example, charge-mosaic membranes [70] which were prepared from pentablock copolymers of an ABACA type by selectively introducing an anion or a cation exchange group into each phase of the micro-separated phases, and poly(amino acid) derivative-*block*-polystyrene block copolymers. Even in the case of these block copolymers that have the special groups depressing the thrombocyte adhesion, they indicated the L-WRCT values of 2.0-3.0 [69-71].

As shown in Fig. 25, PPA and PPA-*g*-(Pro-Gly-Leu-Pro-Gly-Z) having a DOG value of 100% indicate the L-WRCT values of 2.5. Especially, PPA-*g*-(Gly-Boc) was found to indicate a L-WRCT value of 3.7. Furthermore, the graft copolymers prepared in this study might show the higher qualities of the non-thrombogenicity. The mechanism of modifying the non-thrombogenic property of PPA-*g*-(Gly-Boc) is not well known at the moment [67, 72].

3. Block-graft copolymers

Block copolymers and graft copolymers are thought to be chemically linked pairs of homopolymers. According to chemical bonding between different polymer species, block copolymers form a unique structure; namely a microphase-separated structure (MS structure) [7, 73, 74]. The relationship between the MS structure and physical properties of block copolymers has been systematically studied in detail [7, 11, 75].

In contrast, few studies have investigated the relationship between the MS structure and physical properties of graft copolymers, because well-defined graft copolymers have not been available [13, 76, 77]. As a result, we created and employed a model graft copolymer; specifically one in which the backbone has a narrow MWD, the graft has a narrow MWD, the number of grafts per backbone has a narrow distribution, and one where the position and spacing of grafts on a backbone are well defined. This graft copolymer is termed a block-graft copolymer because it is formed *via* a synthetic route of anionic living polymerization.

Thus, the block-graft copolymers must contain grafts that exist in a desirable position of the backbone chain such as the terminal or a central position shown in **Fig. 26**. In order to prepare this block-graft copolymer, an AB-type block copolymer or an ABA-type block copolymer is prepared first; wherein the "A" polymer contains no functional groups that provide intermolecular chemical links of grafts; whereas the "B" polymer contains these functional groups. Subsequently, the "C" polymers are attached as grafts to the "B" polymer of an AB-type or an ABA-type block copolymer to yield a block-graft copolymer. (4-Vinylphenyl)dimethylvinylsilane (VS) and *p*-butoxystyrene (BSt) were employed as the "B" monomers for preparing the block-graft copolymers.

In order to prepare such block-graft copolymers *via* anionic living polymerization, two approaches have generally been proposed: The first one is a "grafting onto" process (a

backbone coupling) and next is a "grafting from" process (a backbone initiation) [12, 80]. The two approaches will be described in this chapter.

3. 1. Poly[(4-vinylphenyl)dimethylvinylsilane], PVS

Polymers that contain a vinyl group as a side chain are interesting stable intermediates of final polymers, because they can be used as backbone chains of graft copolymers and prepolymers of cross-linked polymers. Thus, VS was designed by the present authors. As shown in Fig. 1, VS contains two vinyl groups, a styryl group and a silylvinyl group. Although the silylvinyl group of VS is thought to be much less reactive than the styryl group of VS under an anionic condition, both vinyl groups are capable of polymerizing anionically in a polar solvent. To prepare a well-defined poly[(4-vinylphenyl)dimethylvinylsilane] (PVS), a chemoselective anionic polymerization should be carried out [78].

The polymers themselves form intermolecular cross-linkages, and thus can be used as negative working resists. Ensuing, lithographic evaluation was accomplished [79]. VS was used as the B monomer for preparing block-graft copolymers *via* a "grafting onto" process (a backbone coupling) [80].

3. 1. 1. Polymerization of (4-vinylphenyl)dimethylvinylsilane, VS

When VS was polymerized by Cumyl K in THF at -50°C , the polymerization solution became viscous and a gel-like product was obtained. Both vinyl groups were found to be simultaneously polymerized.

When a new monomer is polymerized by an anionic polymerization technique to yield a so-called monodispersed polymer, particular attention should be directed to (a) an initiator, (b) a solvent, (c) a polymerization time, (d) a polymerization temperature, (e) a concentration

of initiator, and (f) a concentration of monomer. The first three factors are more influential than the latter three. Although the details of the mechanism is not known, a lower temperature is favorable for suppressing side reactions. Hence, a polymerization temperature was set at -78°C , while a concentration of initiator was approximately 10^{-3}mol/l and a concentration of monomer was approximately $2 \times 10^{-1}\text{mol/l}$; that is to say, a kinetic molecular weight, M_k , fell within the range of $3 \times 10^4 - 4 \times 10^4$. On a basis of these experimental conditions, the first three factors of (a), (b) and (c) were systematically studied to prepare a well-defined PVS having a high molecular weight and a narrow MWD.

(a) Initiators

The styryl group of VS was first anionically polymerized using THF as a solvent and 3 h as a polymerization time. When *n*-BuLi was used, the polymer conversion was 60% (**Table 12**) and the corresponding GPC chromatogram showed a single but broad peak (**Fig. 27**). The styryl living end prepared by *n*-BuLi is deactivated step by step before chain propagation completely finishes. This deactivation is thought to be attributed to abstraction of a labile proton from the methyl group on the silicon atom (an abstraction mechanism).

When Cumyl K and Cumyl Cs were used as initiators, the polymer conversion was nearly 100%. The corresponding GPC chromatograms show sharp double and/or triple peaks. The molecular weight of each peak from a lower molecular weight side of double and/or triple peaks was found to correspond to M_k , $2M_k$ (a dimer), or $3M_k$ (a trimer). After chain propagation completely finishes, as a result the styryl living end may become attached to the silylvinyl group of the side chain of another polymer chain (an addition mechanism).

(b) Solvents

VS was polymerized by Cumyl K or Cumyl Cs using 0.5 h–2 h as a polymerization time in diethyl ether (Ether), 2-methyltetrahydrofuran (Me-THF), THF, or 4, 4-dimethyl-1, 3-dioxane (1, 3-DX) as a solvent. The polymerization results are shown in **Table 13**. When Ether and Me-THF were used, the polymer conversions were approximately 0% and 30%, respectively. When THF was used, PVS was prepared at a 90% conversion, and its chromatogram showed two peaks. As shown in **Fig. 28**, the respective M_n of the lower molecular weight peak and higher molecular weight peak corresponds to M_k and $2M_k$, respectively.

When 1, 3-DX was used as a solvent, PVS was prepared in a conversion of 100%, and its chromatogram showed two peaks. The M_n values of the two peaks were found much larger than the M_k value and $2M_k$ value, respectively. The freezing point of 1, 3-DX is -88.5°C , hence, this solvent became viscous at -78°C . VS could not be polymerized homogeneously, however it was polymerized on the interface between the initiator solution and monomer solution to yield PVS that had a higher M_n . To reduce the high viscosity of 1, 3-DX at -78°C , a mixed solvent of Ether and 1, 3-DX were used. The polymerization was performed homogeneously, and after 30 minutes, the corresponding GPC chromatogram of PVS showed a sharp peak containing a small shoulder at the higher molecular weight side (**Fig. 29**).

(c) Polymerization times

Cumyl Cs was used as an initiator and a 1:2 or a 1:1 mixture ratio of Ether/1, 3-DX (a volume fraction) was used as a solvent. To suppress the addition mechanism, a dependence of polymerization times for VS was studied. The polymerization results are shown in **Table 14** and Figure 29. The GPC chromatogram of each PVS shows one sharp peak having a

small shoulder at the higher molecular weight side, and the size of the shoulder was found to increase with polymerization time. The addition mechanism was believed to occur after chain propagation completely finished. The M_w/M_n value of each GPC main peak increased with polymerization time from 1.0₃ (30 minutes) to 1.1₁ (2h). This is the result of another addition of the styryl living end to the silylvinyl group of the same polymer molecule. Lastly, ring formation might occur, and its extent increased slightly with time.

These results indicate that the propagation of VS can completely finish in 30 minutes, and the styryl living end has to be terminated as soon as possible. Next, four PVS samples were prepared under the optimum condition. As shown in **Table 15**, the polymer conversion of the four PVS samples are 100% and the M_n value for each of the four samples is in good agreement with the corresponding M_k value. The M_n values are in a range of 2.5₀ x 10⁴ – 1.3₆ x 10⁵ and the M_w/M_n values are less than 1.0₈.

3. 1. 2. Lithographic characterization

PVS containing a silylvinyl group as a side chain forms intermolecular cross-linkages, and thus can be used as a negative working resist [58, 81, 82]. Silicon-based resists can be applied to multi-layer resists and *submicron* lithography, due to the fabricated substrate surface. From a DSC measurement, PVS is not a semicrystalline polymer but it is an amorphous one, and the glass transition temperature, T_g , of PVS was approximately 303K. Thus, PVS is easier to handle when carrying out a lithographic evaluation compared to ordinary cyclized polyisoprene negative resists [83, 84].

The PVS samples used in the lithographic characterization are shown in Table 15. The PVS film was deposited onto a silicon wafer by spin-coating a xylene polymer solution (20 wt%) at 500 rpm for 30 seconds. After exposure for 30 seconds to an ultraviolet (UV) light

having a wavelength of 405 nm (12.0 mW/cm²), the spin-coated film was developed. No gel was observed in the exposed area. PVS could not act as a negative resist for a UV light.

Following exposure to a deep UV light of intensity from 135 mJ/cm² to 186 mJ/cm², a spin-coated film was developed. **Fig. 30** shows the line and space test patterns which have 2.0 μm lines and 0.75 μm spaces (abbreviated as 2.0 μm in the figure), 1.5 μm lines and 0.75 μm spaces (1.5 μm), 1.0 μm lines and 0.75 μm spaces (1.0 μm), and 0.50 μm lines and 0.75 μm spaces (0.50 μm). Gels were observed in exposed areas but not in unexposed areas. Therefore, this film appears to act as a negative working resist. Following exposure to 135 mJ/cm², the lowest intensity, a test pattern of 0.50 μm lines and 0.75 μm spaces showed webbing and meandering of the lines. Other patterns show clear image lines without webbing or meandering.

Sensitivity of negative working resists is defined as $D_g^{0.5}$, which represents the intensity of light-forming a normalized half-thickness of a film. Contrast of a negative working resist is defined as follows [82]:

$$\gamma = [2 \log (D_g^{0.5} / D_g^0)]^{-1} \quad (12)$$

Here, D_g^0 represents the intensity of a light-forming gel that forms a gel point. From the exposure response curve, deep UV evaluation was made. The resultant lithographic characteristics of PVS-4 are shown in **Table 16**. Favorable values of lithographic characteristics of common negative working resists exposed to a deep UV light have been reported as follows [82, 85, 86]: $D_g^{0.5}$ (sensitivity) of 30 mJ/cm², resolution of 0.4 μm, and γ (contrast) of 3-5. The resultant PVS resist thus appears to possess favorable lithographic characteristics.

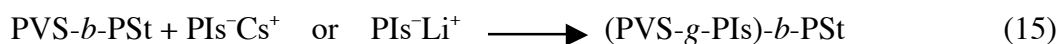
After exposure to an electron-beam, PVS films were developed in a mixture of xylene/methanol = 8/1. **Fig. 31** shows line and space test patterns of 1.0 μm lines and 1.0

μm spaces (abbreviated as 1.0 μm in the figure), 1.5 μm lines and 1.0 μm spaces (1.5 μm), 2.0 μm lines and 1.0 μm spaces (2.0 μm), and 2.5 μm lines and 1.0 μm spaces (2.5 μm). Gels were observed in the exposed areas. Webbing and meandering of lines were not observed in these films. Thus, these test patterns show PVS to act as a negative working resist to an electron beam. As shown in **Fig. 32**, exposure response curves of PVS-1 differed not so significantly, according to the developer used. In contrast, exposure response curves of PVS-4 ($M_n = 13.6 \times 10^4$) for all developers are located at lower energy levels than those of PVS-1 ($M_n = 2.5_0 \times 10^4$). Lithographic characteristics are summarized in Table 16.

As with many negative electron resists, an increase in molecular weight results in an increase in sensitivity, however gradually decreasing the contrast [85, 87, 88]. On the other hand, the contrast of PVS did not decrease with increasing molecular weight, possibly due to a narrow MWD of both PVS films. These contrast values are higher than those of common resists prepared radically. Favorable lithographic characteristics of common negative working resists exposed to an electron beam have been reported as follows [85, 88, 89]: $D_g^{0.5}$ (sensitivity) of 1×10^{-6} C/cm², resolution of 0.3 μm , and γ (contrast) of 3-6. The resultant PVS-4 thus appears to have favorable lithographic characteristics. In conclusion, PVS containing a silylvinyl group as a side chain was found to act as a negative working resist by exposing it to a deep UV light and an electron beam.

**3. 1. 3. Preparation of
[poly(4-vinylphenyl)dimethylvinylsilane-graft-polyisoprene]-block-polystyrene,
(PVS-g-PIs)-b-PSt**

Using VS as the "B" monomer, a model block-graft copolymer of [poly(4-vinylphenyl)dimethylvinylsilane-*graft*-polyisoprene]-*block*-polystyrene, (PVS-*g*-PIs)-*b*-PSt, was prepared through the following synthetic route [80]:



In Eq. (13), PVS-*b*-PSt block copolymer as a backbone was prepared. In Eq. (14), isoprene (Is) was polymerized for 8 h to yield living polyisoprene carbanions, such as the $\text{PIs}^- \text{Cs}^+$ in a THF/Cumyl Cs/ -78°C system and $\text{PIs}^- \text{Li}^+$ in a Bz/*sec*-BuLi/room temperature system. In Eq. (15), a THF solution of $\text{PIs}^- \text{Cs}^+$ was added to a THF solution of PVS-*b*-PSt, or each of the two Bz solutions of $\text{PIs}^- \text{Li}^+$ for the corresponding two grafts was added to a Bz solution of PVS-*b*-PSt. Experimental details of a "grafting onto" process (a backbone coupling) are described in **Table 17**. After 24 h, the backbone coupling was terminated by pouring a polymerization solution into excess methanol. PIs that did not react with PVS-*b*-PSt was removed from the products of (PVS-*g*-PIs)-*b*-PSt.

Fig. 33 shows three GPC chromatograms of (PVS-*g*-PIs)-*b*-PSt. Taking into account the results of the GPC examination and the sedimentation patterns (Beckman, Spinco Model E), the product of each of the three samples was found to contain (PVS-*g*-PIs)-*b*-PSt that had a narrow MWD, but no graft and no backbone.

3. 1. 4. Molecular characteristics of (PVS-*g*-PIs)-*b*-PSt

In the case of a regular star-branched polymer coil, a mean-square radius of gyration $\langle S^2 \rangle$ can be derived as [90],

$$\lim_{n \rightarrow \infty} \langle S^2 \rangle_{\text{branch}} = (nb^2 / 6) (3f - 2) / f^2 \quad (16)$$

Therefore,

$$g = \langle S^2 \rangle_{\text{branch}} / \langle S^2 \rangle_{\text{linear}} = (3f - 2) / f^2 \quad (17)$$

where n and b are a degree of polymerization of the polymer and a bond length; $\langle S^2 \rangle_{\text{branch}}$ and $\langle S^2 \rangle_{\text{linear}}$ are the mean-square radii of gyration for a branched polymer chain and a linear polymer chain; and f is the number of branches, respectively. The g value estimated from Eq. (17) may be considered as a measure of branching. In the case of comb-shaped polymers, g is given by a complex equation [91]. Furthermore, in the case of the block-graft copolymer wherein graft chains are different from a backbone chain and the graft points have a localized distribution on the backbone chain, g may be derived from a more complex equation. Although the g value has not been derived in the form of an exact equation, the mean-square radius of gyration of a block-graft copolymer should depend on the molecular weight and the number of graft molecules. Thus, the molecular weights of the block-graft copolymers could not be determined by GPC measurement and a conventional light scattering [92-94]. Based on osmometry, classical molecular characterizations must be achieved.

By comparison of the NMR signals of (PVS- g -PIs)- b -PSt with those of PVS- b -PSt, the molar ratio of the Is unit (a graft content) to the St units ($(A_{\text{Is}}/A_{\text{St}})_{\text{NMR}}$) is estimated. Thus, the number average molecular weight of a block-graft copolymer ($M_n^{\text{block-graft}}_{\text{NMR}}$) is calculated as follows:

$$M_n^{\text{block-graft}}_{\text{NMR}} = M_n^{\text{block}}_{\text{OSM}} + M_n^{\text{PSt}}_{\text{OSM}} (A_{\text{Is}}/A_{\text{St}})_{\text{NMR}} (M_{\text{Is}}/M_{\text{St}}) \quad (18)$$

where $M_n^{\text{block}}_{\text{OSM}}$ and $M_n^{\text{PSt}}_{\text{OSM}}$ are, respectively, the number average molecular weights of PVS- b -PSt and PSt in PVS- b -PSt, as determined by osmometry. M_{Is} and M_{St} are the molecular weights of Is and St. As shown in **Table 18**, the $M_n^{\text{block-graft}}_{\text{NMR}}$ value coincided with the $M_n^{\text{block-graft}}_{\text{OSM}}$ value determined by osmometry.

The number of grafts, N^{graft} , per backbone can be defined as,

$$N^{\text{graft}} = (M_n^{\text{block-graft}}_{\text{OSM}} - M_n^{\text{block}}_{\text{OSM}}) / M_n^{\text{graft}}_{\text{OSM}} \quad (19)$$

When preparing three grafts of PIs, three PIs precursors were obtained. The $M_n^{\text{graft}}_{\text{OSM}}$ values of the three PIs precursors were measured by membrane osmometry and/or vapor pressure osmometry. The thus-estimated N^{graft} values of the three block-graft copolymers are shown in Table 18.

The degree of polymerization of PVS in PVS-*b*-PSt is equal to the number of possible chemical links between the backbone and grafts. This characteristic number is termed DP^{VS} . When a backbone coupling was performed, the molar quantity of PIs⁻ carbanions was set at more than 4.4 times larger than that of DP^{VS} . However, the ratio of N^{graft} to DP^{VS} did not approach 100%, but approximately 30%, as shown in Table 18. Approximately 30% of the silylvinyl groups of PVS react with living carbanions of PIs⁻, and the remaining silylvinyl groups are sterically hindered by grafts. The $N^{\text{graft}}/DP^{\text{VS}}$ value was found to increase slightly with decreasing molecular weight of PIs as a graft. On the other hand, since the reaction of a silylvinyl group of VS with a PIs⁻ carbanion generates a negative charge in the vicinity of the backbone, an electrostatic repulsion between negative charges of the backbone and the PIs⁻ carbanions might be produced. However, the $N^{\text{graft}}/DP^{\text{VS}}$ value of SGI-1 prepared in THF is smaller than that of SGI-2 prepared in Bz. The observed result was contrary to the expected result arising from the electrostatic repulsion. Therefore, the most part of the non-quantitative coupling [16, 95] should be due to the steric hindrance and not the electrostatic repulsion. The mutual repulsion between the grafts due to steric hindrance should be uniform, because the backbone and grafts have narrow MWDs. Therefore, the spacing and its distribution of graft points on a PVS block of the backbone appear to be uniform and narrow, respectively. In other words, the $N^{\text{graft}}/DP^{\text{VS}}$ value is expected to be attributable to the spacing of graft points.

3. 1. 5. Morphology

The three samples of (PVS-*g*-PIs)-*b*-PSt cast from the respective benzene solutions into thin films. The resultant films were dried under a vacuum at 40°C for 3 days. To further promote the formation of equilibrium morphologies, the films should be annealed, however the annealing was not carried out at the present study. **Fig. 34** shows electron micrographs of the three films. The black and white regions in electron micrographs correspond to the PIs phase (graft chains) and PSt/PVS phase (backbone chains), respectively, wherein the PSt/PVS phase is suspected to be a mixed phase of PSt and PVS [96]. The three samples formed clear microphase-separated (MS) structures. The morphology of the SGI-2 film does not comply with a rule proposed by Molau [1, 7]; namely, the film forms neither globular domains nor a clear continuous phase, but a curious amoebae-like domain. Similar morphology of ABC-type three component block copolymers having a PIs block with a high 1, 4 content as a component has been reported by Kotaka et al. [97] and Fujimoto et al. [98].

Ensuing, this prompts us to comment on the amoebae-like morphology of SGI-2. The PIs chains of SGI-2 prepared by a *sec*-BuLi/Bz system have the geometrical microstructures with a high *cis*-1, 4 content [99]. A PIs chain with a high *cis*-1, 4 content has a dipole moment that is aligned in the direction parallel to the chain contour. The PIs chain exhibits a dielectric relaxation due to fluctuation of the end-to-end distance, which is referred to as "a dielectric normal mode process" [100-103]. According to the dipole-dipole repulsion between the PIs chains, the end-to-end vectors of the PIs chains should be randomly aligned in the solid state so as to minimize a potential energy. A regular molecular alignment such

as a spherical structure appears to be an unfavorable choice for PIs with a high *cis*-1, 4 content, though a detailed effect has not been clearly understood at present.

The SGI-1 film has a PIs content of 47 wt%. A linear block copolymer that has one composition in an amount of 47 wt% is expected to form a lamellar structure. However, the SGI-1 film showed a spherical structure of PSt/PVS, wherein PIs formed a continuous phase. The SGI-3 film contains PIs in an amount of 14 wt%. A linear block copolymer that has one composition in an amount of 14 wt% is expected to form a spherical structure of PIs, while PSt/PVS forms a continuous phase. However, the SGI-3 film showed a lamellar structure. From the viewpoint of morphological behavior, the PIs (graft) content dependence of the block-graft copolymers was found to shift to the higher PIs content side compared to that of the linear block copolymers.

Let us consider a process of a solvent's casting from a dilute polymer solution. When a concentration of the polymer solution attains a critical concentration [73, 104, 105], thereby inducing the formation of the MS structure, the morphology should be determined by an apparent volume fraction of one component containing the solvent. The apparent volume fraction of PIs (grafts) to PVS-*b*-PSt (backbones) at the critical concentration should be much larger than the corresponding real volume fraction. One of the causes behind this is thought to be that the graft chain extends rather than the corresponding unperturbed polymer chain [106-108], due to the graft chains becoming crowded near the PVS chain. Therefore, the block-graft copolymer is believed to form a characteristic MS structure that is distinct from that of the linear block copolymer [1, 7].

The MS structures of block copolymers with nonlinear architectures have been the focus of a considerable amount of recent work. One of the representative works is a series of miktoarm star block copolymers ($A_m B_n$) [109, 110] and model graft copolymers [111-113]

prepared using anionic polymerization and controlled chlorosilane chemistry. Gido and co-workers have reported that the MS structures shifted to those of higher volume fractions of the higher arm number component, as compared with those of linear block copolymers. This behavior is qualitatively the same as that of the present study. Milner has quantitatively calculated a shift of the morphological transition lines as a function of the volume fraction of component B (ϕ_B) and a molecular asymmetry parameter (ε) [114-116].

$$\varepsilon = (n_A/n_B) (l_A/l_B)^{1/2} \quad (20)$$

Here, n_A and n_B are the numbers of arms of A_mB_n , and $l_i = (V_i/R_i^2) = (v_i/b_i^2)$. V_i and R_i are the volume and radius of gyration of one arm of polymer i , while v_i is the segmental volume and b_i is the statistical segment length of component i . All shifts of the MS structures experimentally observed by Gido et al. from that of linear block copolymers could be explained qualitatively by the Milner's model, but a part of them could not be explained quantitatively. These discrepancies are going to be elucidated.

(PVS-*g*-PIs)-*b*-PSt can be considered as an asymmetric miktoarm star block copolymer of $(PIs)_n(PSt)_1$ although the molecular architectures of (PVS-*g*-PIs)-*b*-PSt are strictly different from that of Milner's model. Using $v_{PIs} = 0.132\text{nm}^3$ and $b_{PIs} = 0.68\text{nm}$ for PI_s, and $v_{PSt} = 0.176\text{nm}^3$ and $b_{PSt} = 0.69\text{nm}$ for PSt, an $(l_{PIs}/l_{PSt})^{1/2}$ of 0.878 is calculated [109]. Hence, asymmetry parameters of ε are 8.8 for SGI-1 ($n_A=10.0$, $n_B=1.0$), 9.6 for SGI-2 ($n_A=10.9$, $n_B=1.0$) and 11.0 for SGI-3 ($n_A=12.5$, $n_B=1.0$). **Fig. 35** shows the result of mapping the morphological results of the three samples onto the theoretical phase diagram calculated by Milner. The shifts of the MS structures from those of the corresponding linear block copolymers can be explained qualitatively by the asymmetric factor. However, a part of them could not be explained quantitatively. One of our desired goals is to understand the

morphological behavior of the block-graft copolymers. It is also desired to know the theoretical phase diagram of the block-graft copolymers.

3. 2. Poly(*p*-hydroxystyrene), PHSt

In order to prepare block-graft copolymers *via* anionic living polymerization, two approaches have been proposed: specifically, a "grafting onto" process (a backbone coupling) and a "grafting from" process (a backbone initiation) [16]. The backbone coupling is exemplified by a reaction of living PIs⁻ with the PVS-*b*-PSt backbone that bears the silylvinyl functional groups. This approach allows a precise control of the number and length of grafts. However, after the backbone coupling, the remaining PIs that did not react with the backbone must be removed from the products by repeated dissolution and precipitation. Preferably, the fractionation should be excluded. A "grafting from" process (a backbone initiation) will be described in the present section. For carrying out a "grafting from" process, *p*-hydroxystyrene (HSt) was employed as the B monomer that can provide the intermolecular chemical links between the backbone and grafts [117].

3. 2. 1. Polymerization of *p*-*tert*-butoxystyrene, BSt

HSt could not be polymerized by an anionic living mechanism because the propagating carbanionic species readily reacts with a labile proton of the hydroxyl group to terminate the polymerization. The hydroxyl group should be protected during anionic polymerization, and the protecting group can be readily and completely removed after the polymerization. A *tert*-butyldimethylsilyl group, -Si(CH₃)₂(*t*-C₄H₉), seems to be an inappropriate protective group for anionic polymerization of vinyl phenol [58, 118]. Therefore, *p*-*tert*-butoxystyrene (BSt) was prepared according to the previous methods [119].

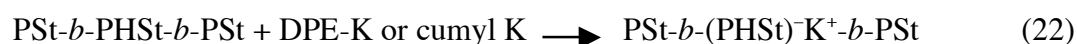
When an attempt was made to anionically polymerize BSt by *n*-BuLi in THF at -78°C , the polymer conversion was 100%. The M_n^{OSM} value was discovered to be the same as the M_k value. Also, the GPC chromatogram showed a single sharp peak and the M_w/M_n value was less than 1.0₅. Thus, when satisfactorily purified, BSt was found to be polymerized without difficulty under a *n*-BuLi/THF/ -78°C system to yield poly(*p*-*tert*-butoxystyrene) (PBSt) with a desired molecular weight and a narrow MWD.

Two approaches for preparing the block copolymers must be studied. As shown in **Table 19**, BSt was polymerized to yield PBSt and the resultant PBSt living end was allowed to initiate a newly added butadiene (Bu). St was polymerized to yield PSt and the resultant PSt living end was allowed to initiate a newly added BSt. In preparations of both PBSt-*b*-PBu and PSt-*b*-PBSt block copolymers, the respective M_n values of the two block copolymers moderately agreed with the corresponding M_k values. As shown in **Fig. 36**, each sample showed a single sharp GPC chromatogram. These results indicate that the PBSt living end could be capable of initiating Bu, and that BSt could be initiated by the PSt living end. Therefore, a PSt-*b*-PBSt-*b*-PSt triblock copolymer can be prepared by a sequential block copolymerization.

The *tert*-butyl group was removed from PBSt in PBSt-*b*-PBu and PSt-*b*-PBSt block copolymers by hydrogen bromide (HBr) in a mixture of Bz/acetone under reflux for 1 h to prepare the corresponding block copolymers of PHSt-*b*-PBu and PSt-*b*-PHSt. Spectroscopic evidence supports the preparation of the resultant block copolymers having a PHSt block. As shown in Fig. 36, all four samples showed single sharp GPC peaks having the M_w/M_n values of less than 1.0₄.

3. 2. 2. Preparation of polystyrene-block-[poly(*p*-hydroxystyrene)-graft-poly(ethylene oxide)]-block-polystyrene, PSt-*b*-(PHSt-*g*-PEO)-*b*-PSt

Using BSt as the “B” monomer, a model block-graft copolymer of polystyrene-*block*-[poly(*p*-hydroxystyrene)-*graft*-poly(ethylene oxide)]-*block*-polystyrene, PSt-*b*-(PHSt-*g*-PEO)-*b*-PSt was prepared through the following synthetic route [117]:



In Eq. (21), a PSt-*b*-PBSt-*b*-PSt block copolymer serving as a backbone was prepared. The polymerization conditions and results are described in **Table 20**. As shown in **Fig. 37**, the GPC chromatogram showed a single sharp peak ($M_w/M_n = 1.0_8$). The *tert*-butyl group was removed from PBSt in PSt-*b*-PBSt-*b*-PSt by HBr to yield PSt-*b*-PHSt-*b*-PSt. The resultant backbone of PSt-*b*-PHSt-*b*-PSt showed a single sharp GPC peak. In Eq. (22), a hydroxyl group of PSt-*b*-PHSt-*b*-PSt was allowed to react with Cumyl K in THF or with dimeric potassium dianions of 1, 1-diphenylethylene (DPE-K) in THF under the experimental conditions described in **Table 21**. Both the solutions changed their tone from colorless to deep red. Finally, two macromolecular initiators of PSt-*b*-(PHSt)⁻K⁺-*b*-PSt were prepared.

In Eq. (23), EO was added to each of the PSt-*b*-(PHSt)⁻K⁺-*b*-PSt solutions. The newly formed potassium alkoxide of PSt-*b*-(PHSt)⁻K⁺-*b*-PSt and the remaining initiator of DPE K or Cumyl K are capable of initiating the additionally introduced EO. The solutions gradually changed their tone from deep red to light brown and then became colorless. After 60 h, the "grafting from" process (a backbone initiation) was stopped. The product contained a mixture of PSt-*b*-(PHSt-*g*-PEO)-*b*-PSt and poly(ethylene oxide) (homo-PEO). Homo-PEO was removed from the mixtures by repeating dissolution and precipitation with hot methanol.

3. 2. 3. Molecular characteristics of *PSt-b-(PHSt-g-PEO)-b-PSt*

(a) *Block-graft copolymers, $M_n^{\text{block-graft}}$*

We can expect the kinetic molecular weight of *PSt-b-(PHSt-g-PEO)-b-PSt*, $M_k^{\text{block-graft}}$ to be as follows:

$$M_k^{\text{block-graft}} = M_n^{\text{block}}_{\text{OSM}} [(W^{\text{block}} + W^{\text{graft}}) / W^{\text{block}}] \quad (24)$$

where $M_n^{\text{block}}_{\text{OSM}}$ is the number average molecular weight of *PSt-b-PHSt-b-PSt* serving as the backbone; W^{block} is the weight of the backbone used in the “grafting from” process; and W^{graft} is the weight of grafts produced from the (PHSt)⁻K⁺ initiators. The molecular weight of *PSt-b-(PHSt-g-PEO)-b-PSt*, $M_n^{\text{block-graft}}_{\text{CONV}}$, was simply determined from the weight of the final product, $W^{\text{block-graft}}$, by the following equation.

$$M_n^{\text{block-graft}}_{\text{CONV}} = M_n^{\text{block}}_{\text{OSM}} (W^{\text{block-graft}} / W^{\text{block}}) \quad (25)$$

In addition, the molecular weight of *PSt-b-(PHSt-g-PEO)-b-PSt*, $M_n^{\text{block-graft}}_{\text{OSM}}$ was determined by osmometry.

By comparison of the ¹H-NMR signal of *PSt-b-(PHSt-g-PEO)-b-PSt* with that of *PSt-b-PHSt-b-PSt*, a molar ratio of the EO unit (a graft content) to the St unit for *PSt-b-(PHSt-g-PEO)-b-PSt*, $(A_{\text{EO}}/A_{\text{St}})_{\text{NMR}}$ was estimated. Thus, the number average molecular weight of *PSt-b-(PHSt-g-PEO)-b-PSt*, $M_n^{\text{block-graft}}_{\text{NMR}}$ was calculated as follows.

$$M_n^{\text{block-graft}}_{\text{NMR}} = M_n^{\text{block}}_{\text{OSM}} + M_n^{\text{PSt}}_{\text{OSM}} (A_{\text{EO}}/A_{\text{St}})_{\text{NMR}} (M_{\text{EO}}/M_{\text{St}}) \quad (26)$$

where $M_n^{\text{PSt}}_{\text{OSM}}$ is the number average molecular weights of a PSt block in the backbone; and M_{EO} and M_{St} are the respective molecular weights of EO and St. As shown in **Table 22**, the three values of $M_n^{\text{block-graft}}_{\text{CONV}}$, $M_n^{\text{block-graft}}_{\text{OSM}}$, and, $M_n^{\text{block-graft}}_{\text{NMR}}$ for each of the two samples coincided with each other. The resultant of each $M_n^{\text{block-graft}}$ value of the two samples was smaller than the corresponding $M_k^{\text{block-graft}}$ value. These results suggest that the metallation of

PHSt to (PHSt)⁻K⁺ by DPE-K or Cumyl K could not be performed in a 100% conversion even after long reaction times.

The sedimentation patterns of the two block-graft copolymers were also examined. As shown in **Fig. 38**, each pattern showed a single sharp peak. Taking into account the results of the GPC examination and the sedimentation patterns, the product of each of the two samples was found to contain PSt-*b*-(PHSt-*g*-PEO)-*b*-PSt block-graft copolymer that has a narrow MWD, no backbone, and no homo-PEO.

(b) Grafts, M_n^{graft}

When preparing SGE-2, two different initiators of PSt-*b*-(PHSt)⁻K⁺-*b*-PSt and Cumyl K existed in the solution of a “grafting from” process. Hence, homo-PEO was simultaneously prepared by the remaining Cumyl K. Homo-PEO showed a sharp GPC peak, corresponding to the M_w/M_n value of less than 1.1₀. A number average molecular weight of the resultant homo-PEO, M_n^{PEO} v_{PO} for SGE-2 was determined by vapor pressure osmometry. A kinetic molecular weight of the graft, M_k^{graft} , can be calculated by Eq. (27):

$$M_k^{graft} = W^{EO} / I^{total} \quad (27)$$

where W^{EO} is the weight of EO and I^{total} is the molar quantity of initiator introduced to the backbone solution.

The newly produced PSt-*b*-(PHSt)⁻K⁺-*b*-PSt macromolecular initiators have potassium alkoxide serving as grafting points and the remaining initiators of DPE-K and cumyl K have alkyl potassium. Although the initiation mechanisms of the potassium alkoxide and the alkyl potassium should be different from each other, the propagation mechanisms of them remains the same. Therefore, the polymerization results of EO by the potassium alkoxide and the alkyl potassium were expected to be the same as each other because of a long time

period required for propagation. From these considerations, we shall assume that the molecular weight of the graft, M_n^{graft} , is equal to that of homo-PEO; namely, $M_n^{\text{graft}} = M_n^{\text{PEO}}_{\text{VPO}}$ for SGE-2 and $M_n^{\text{graft}} = M_k^{\text{graft}}$ for SGE-1.

(c) Metallation efficiency, f_{metal}

The degree of polymerization of a PHSt block in PSt-*b*-PHSt-*b*-PSt is equal to the number of possible chemical links between the backbone and grafts. This characteristic number is termed N_k^{graft} . Metallation efficiency (f_{metal}) that characterizes scheme (28) can be defined as [120],

$$f_{\text{metal}} = (I_{\text{total}} - I_{\text{PEO}}) / (W^{\text{block}}/M_n^{\text{block}}) N_k^{\text{graft}} \quad (28)$$

where, I_{total} and I_{PEO} are the molar quantities of initiators for being introduced to the polymerization solution and for preparing homo-PEO, respectively. I_{PEO} can be determined from $W^{\text{PEO}}/M_n^{\text{PEO}}_{\text{VPO}}$, where W^{PEO} is the weight of homo-PEO prepared by the remaining initiator. W^{block} is the weight of PSt-*b*-PHSt-*b*-PSt used in the “grafting from” process. As shown in Table 22, the resultant f_{metal} values were found to be not 100%, but approximately 50% for SGE-1 and 28% for SGE-2. The nonquantitative metallation appears to be caused by electrostatic repulsion between negative charges of the initiator and the resultant (PHSt)⁻K⁺. The hydroxyl groups of PHSt are located in close proximity so that a potassium ion may induce a formation of a chelation and/or a complex in the adjacent hydroxyl group, or a hydroxyl group and potassium alkoxide may coexist at the equilibrium.

The difference in the f_{metal} values between SGE-1 and SGE-2 can be explained by a shielding effect and the equilibrium between the hydroxyl group and potassium alkoxide.

(d) Number of grafts, N^{graft}

The number of grafts, $N_{\text{OSM}}^{\text{graft}}$ and $N_{\text{ini}}^{\text{graft}}$ can be defined as

$$N_{\text{OSM}}^{\text{graft}} = (M_{\text{n}}^{\text{block-graft}}_{\text{OSM}} - M_{\text{n}}^{\text{block}}_{\text{OSM}}) / M_{\text{k}}^{\text{graft}} \quad (29)$$

$$N_{\text{ini}}^{\text{graft}} = N_{\text{k}}^{\text{graft}} f_{\text{metal}} \quad (30)$$

As shown in Table 22, the thus-estimated $N_{\text{OSM}}^{\text{graft}}$ and $N_{\text{ini}}^{\text{graft}}$ values of the two samples were smaller than the corresponding $N_{\text{k}}^{\text{graft}}$ value. Thus, $N_{\text{OSM}}^{\text{graft}}/N_{\text{k}}^{\text{graft}}$ and f_{metal} are expected to be attributable to the spacing (a frequency) of graft points on a backbone [94].

In the case of a “grafting onto” process (chapter 3. 1. 4), where PIs^- reacts with PSt-*b*-PVS to yield PSt-*b*-(PVS-*g*-PIs), the spacing of graft points on a backbone could be estimated to be 26%–32%. Moreover, the nonquantitative coupling was due to the steric hindrance. In the case of a “grafting from” process shown in the present chapter, the nonquantitative metallation result being 28%–50% appears to be reasonable due to the electrostatic repulsion. In conclusion, the anionic living technique appears to be unfavorable for preparing the graft copolymers with a quantitative metallation of 100%. On the other hand, the formation of the peptide bond between the carboxylic acids of OP and the amino groups of PAS (chapter 2. 2. 4) seems to quantitatively proceed and to yield the graft copolymers with a DOG value of 100%. Although the length of the graft should be important for discussing the coupling reaction, a coupling reaction using DCC appears to be more suitable for preparing the graft copolymers by a “grafting onto” process compared to the anionic living mechanism.

3. 2. 4. Morphology

Fig. 39 shows transmission electron micrographs of two samples of PSt-*b*-(PHSt-*g*-PEO)-*b*-PSt cast from the respective benzene solutions. The films were dried under a vacuum at 40°C for 3 days. However, the further annealing to promote the

formation of equilibrium morphologies was not carried out at the present study. The black and white regions in the electron micrographs correspond to the PEO phase serving as grafts and the PSt/PHSt phase serving as a backbone, respectively. Here, the PSt/PHSt phase is suspected to be a mixed phase of PSt and PHSt [96].

From DSC measurements, the two block-graft copolymers were found amorphous polymers, even though they have PEO as grafts. The degree of crystallinity, X_C , of PEO has been known to depend on its molecular weight and molecular architecture, wherein PEO is a homo polymer or a block of a linear block copolymer [121–123]. The PEO chain of $M_n=6000$ has been reported to have $X_C = 95\%$ for homo PEO and $X_C = 45\%$ for PEO-*b*-PSt-*b*-PEO block copolymer. Additionally, the PEO chain of $M_n = 3400$ has been reported to have $X_C = 92\%$ for homo PEO and $X_C = 30\%$ for PEO-*b*-PSt-*b*-PEO. Considering this, homo-PEO seems to be a floating chain whose two ends are not attached to a PSt block, while the PEO chain in PEO-*b*-PSt-*b*-PEO seems to be a cilium-chain having only one end attached to a PSt block. This confined PEO chain should disturb the crystallization of the PEO chain, and hence induce a decrease in the X_C value of the block copolymer [121-123]. From a viewpoint of the confined PEO chain, the molecular structure of the PEO chain in PSt-*b*-(PHSt-*g*-PEO)-*b*-PSt is thought to be the same as that in PEO-*b*-PSt-*b*-PEO. However, the PEO chains should be crowded near the PHSt backbone for PSt-*b*-(PHSt-*g*-PEO)-*b*-PSt. This finding is responsible for $X_C = 0\%$ of the two films of the block-graft copolymers.

Recently, a number of crystalline/amorphous diblock copolymers have been studied on the MS structure and crystallite of the crystalline segment [7, 124]. The crystalline characteristics such as melting temperatures, degrees of crystallization and crystalline lamellar thickness should be affected by annealing temperatures and annealing times.

However, these annealing effects were not considered in the present morphological result. Despite this, the samples have a remarkable feature of having $X_c = 0\%$, even if one block is a crystalline polymer of PEO.

As shown in **Fig. 39**, each of the two samples formed a clear lamellar structure, which can be observed in all points of the films. The SGE-1 and SGE-2 films had a PEO content of 28.6 wt% and 28.9 wt%, respectively. A linear block copolymer that has one component in an amount of 29 wt% is expected to form a spherical structure or a cylindrical structure of PEO, wherein PSt/PHSt forms a continuous phase. From the viewpoint of morphological behavior, the PEO (graft) content dependence of the block-graft copolymers was found to shift further to the higher PEO content side compared to that of the linear block copolymers. This morphological behavior did not depend on the molecular weight of PEO in the range of 3400 to 6000. The same morphological feature was observed in (PVS-*g*-PIs)-*b*-PSt prepared by a “grafting onto” process.

The lamellar thickness of the PSt phase and PEO phase could be determined from the transmission electron micrographs. Unperturbed root-mean-square of the end-to-end distances, $\langle R^2 \rangle_0^{1/2}$, for PSt and PEO chains can be calculated by the following [125]; $\langle R^2 \rangle^{1/2} = bn^{1/2}$, where b is a Kuhn's segment length and n is a degree of polymerization. As shown in **Table 23**, in each of the two films observed, lamellar thickness of the PSt phase is most likely the same as the corresponding calculated lamellar thickness. In contrast, in each of the two films observed, lamellar thickness of the PEO phase was found to be approximately two times larger than the corresponding calculated lamellar thickness. This finding corresponds to the speculation that the graft chain extends in contrast to the corresponding unperturbed polymer chain because the graft chains become crowded near the PHSt chain.

Therefore, the block-graft copolymers are believed to contain PEO that becomes amorphous and not crystalline.

Morphological shifts of the experimentally observed MS structure from those predicted from linear block copolymers should be discussed on a basis of the phase diagram calculated by Milner [114-116], in a similar manner as chapter 3. 1. 5. PSt-*b*-(PHSt-*g*-PEO)-*b*-PSt can be considered as an asymmetric miktoarm star block copolymer of (PEO)_n(PSt)₁ [109, 110]. Since the v_{PEO} and b_{PEO} values are not known, the $(l_{\text{PIS}}/l_{\text{PSt}})^{1/2}$ value could not be estimated. However, this value seems almost to be one [109, 126], which in turn creates the asymmetry parameters as follows: ϵ is close to 10.3 for SGE-1 ($n_{\text{A}}=20.6, n_{\text{B}}=2.0$) and 5.9 for SGI-2 ($n_{\text{A}}=11.8, n_{\text{B}}=2.0$). Fig. 35 shows the result of mapping the morphological results of the two samples onto the theoretical phase diagram calculated by Milner. The shifts of the MS structures from those of linear block copolymers can be explained by the asymmetric factor. It is also desired to know the theoretical phase diagram of the block-graft copolymers for discussing in detail.

4. Concluding remarks: anionic living polymerization

When carrying out anionic living polymerization of common monomers such as styrene and methacrylate, well-established techniques can be used to prepare well-defined polymers having desired molecular weights and narrow MWDs. However, when carrying out anionic living polymerization of new monomers that contain a vinyl group and another functional group, particular attention should be given to the removing impurities from the monomers prior to polymerization and suppressing side reactions by the living ends during anionic polymerization.

Although each of the three tAS contains a styryl group and tertiary amino group, the latter has no labile proton which causes extermination of the styryl living ends. Therefore, for an example, using three tAS as a general approach to anionically polymerize new monomers with no labile proton was described from a viewpoint of the three conditions and four experimental proofs.

As IBA and HSt have labile protons, they could not be anionically polymerized. To prepare well-defined PIBA and PHSt, ISBA and BSt having a trimethylsilyl group and a tertiary butoxy group as protecting groups, respectively, have to be anionically polymerized to yield the corresponding PISBA and PBSt, while subsequent deprotection should be performed. In these two protecting groups, the trimethylsilyl group of PISBA can be promptly and completely deprotected to yield PIBA. This finding corresponds to the fact that ISBA tends to contain a slight amount of IBA as impurity. When removing a slight amount of IBA from ISBA prior to polymerization, it is important to select a useful purging reagent that is steadily reactive to IBA but entirely unreactive to ISBA. In contrast, the *tert*-butyl group of PBSt can be strenuously deprotected to yield PHSt. This finding corresponds to the fact that BSt seems stable to the purging reagents and propagating carbanionic species. BSt, as well as common monomers, can be anionically polymerized itself with ease. Therefore, the anionic polymerization of BSt was not described in detail, although the anionic reactivity of BSt was discussed by performing block copolymerization.

As the silylvinyl group of VS could not be protected at the present time, a chemoselective polymerization of a styryl group has to be performed in order to prepare a well-defined PVS. For this subject, the influence of initiators, solvents, and polymerization times on anionic polymerization should be studied in detail. A systematic approach to

depress the two side reactions and performance of the chemoselective polymerization were described.

References

- [1] Ciferri A, editor. Supermolecular polymers. New York: Marcel Dekker; 2000.
- [2] Alexandridis P, Lindman B, editors. Amphiphilic block copolymers. New York: Elsevier; 2000.
- [3] Hedric LL. Dendrimer-like star block and amphiphilic copolymers by combination of ring opening and atom transfer radical polymerization. *Macromolecules* 1998; 31: 8691-705.
- [4] Yang XM, Peter RD, Nealey PF, Solak HH, Cerrina F. Guided self-assembly of symmetric diblock copolymer film on chemically nanopatterned substrates. *Macromolecules* 2000; 33: 9575-82.
- [5] Radzilowski LH, Carragber BO, Stupp SI. Three dimensional self-assembly of rodcoil copolymer nanostructures. *Macromolecule* 1997; 30: 2110-19.
- [6] Kobayashi S, Shoda S, Uyama H. In: Kobayashi S, editors. *Catalysis in precision polymerization*. New York: Wiley; 1997.
- [7] Hamley IW. *The Physics of Block Copolymers*. Oxford: Oxford Univ Press; 1998.
- [8] Pitsikalis M, Pispas S, Mays JW, Hadjichristidis N. Nonlinear block copolymer architectures. *Adv Polym Sci* 135, Berlin: Springer; 1998. p. 1-137.
- [9] Hadjichristidis N. Asymmetric star polymers: Synthesis and properties. *Adv Polym Sci* 142, Berlin: Springer; 1999. p. 71-127.

- [10] Kotaka T, editor. Polymer alloy. Tokyo: Tokyo Kagaku Dohjin; 1993.
- [11] Ishizu K, Uchida S. Synthesis and microphase-separated structures of star-block copolymers. *Prog Polym Sci* 1999; 24:1439-80.
- [12] Kennedy P. Synthesis, characterization and properties of octa-arm polyisobutylene-based star polymers. *Adv Polym Sci* 146, Berlin: Springer; 1999. p. 1-38.
- [13] Mishra M, Kobayashi S, editors. Star and hyperbranched polymers. Plastic engineering series 53, New York: Marcel Dekker; 1999.
- [14] Mishra M, organizer. Macromolecular design and application *via* macromonomers, macroinitiators and macroiniferters. *ACS Polym Prep* 37, Washington DC: ACS; 1996. p. 402-23.
- [15] Se K. Synthesis of the star polymers having the rod-like arms. IUPAC International Symp on Ionic Polym, Prep, Kyoto: IUPAC; 1999. p. 80.
- [16] Se K, Watanabe O, Isono Y, Fujimoto T. Synthesis and characterization of model block-graft copolymers *via* anionic polymerization: Introduction of poly(isoprene) and poly(ethylene oxide) as graft chains. *Makromol Chem, Macromol Symp* 1989; 25: 249-61.
- [17] Szwarc M. Carbanions, living polymers and electron transfer processes. New York: Interscience Publ, Wiley; 1968.
- [18] Quirk RP, editor. Application of anionic polymerization research. ACS symposium series 696, Washington, DC: ACS; 1996.
- [19] Hirao A, Loykulnant S, Ishizone T. Recent advance in living anionic polymerization of functionalized styrene derivatives. *Prog Polym Sci* 2002; 27: 1399-471.
- [20] Deng H, Kanaoka S, Sawamoto M, Higashimura T. Synthesis of star-shaped

- poly(*p*-alkoxystyrenes) by living cationic polymerization. *Macromolecules* 1996; 29: 1772-7.
- [21] Faust R, Shaffer TD, editors. Cationic polymerization. ACS symposium series 665, Washington, DC: ACS; 1997.
- [22] Coessens V, Pintauer T, Matyjaszewski K. Functional polymers by atom transfer radical polymerization. *Progr Polym Sci* 2001; 26: 337-77.
- [23] Matyjaszewski K, editor. Controlled radical polymerization. ACS symposium series 685, Washington, DC: ACS; 1998.
- [24] Se K, Kijima M, Fujimoto T. Anionic polymerization of tertiary aminostyrenes and characterization of polymers. *Polymer J* 1988; 20: 791-9.
- [25] Se K. Anionic living polymerization of *tert*-aminostyrenes and application of the polymers. *Polym Adv Tech* 2002; 13: in press.
- [26] Nakamaha S. Synthesis of functionalized polymers by living anionic polymerization. In: Hatada K, Kitayama T, Vogl T, editors. *Macromolecular design of polymeric materials*. Plastic engineering series 40, Marcel Dekker: New York; 1997. p. 85-94.
- [27] Hirao A, Nakahama S. Anionic living polymerization of monomers with functional silyl groups. *Prog Polym Sci* 1992; 17: 283-317.
- [28] Ishizone T, Kato H, Yamazaki D, Hirao A, Nakahama S. Anionic polymerization of monomers containing functional groups. 14. Anionic polymerization of aryl 4-vinylbenzoates. *Macromol Chem Phys* 2000; 201: 1077-87.
- [29] Se K, Kudoh S. Anionic polymerization of secondary aminostyrene and characterization of the polymer. *J Appl Polym Sci* 1999; 71: 2039-48.
- [30] Se K, Kijima M, Ohtomo R, Fujimoto T. Quaternization of poly(tertiary aminostyrene)s and characterization of the quaternized polymers. *J Polym Sci, Part*

- A: Polym Chem 1997; 35: 1219-26.
- [31] Kijima M, Se K, Fujimoto T. Photochemical isomerization of *p*, *p'*-bis(chloromethyl azobenzene) incorporated in poly(tertiary aminostyrenes) by crosslinkage. Polymer 1992; 33: 2402-07.
- [32] Se K, Kijima M, Fujimoto T. Photochemical isomerization of azobenzene incorporated in poly(*N,N*-dimethyl-4-vinylphenethylamine-*block*-styrene) diblock copolymer by cross linkage. Polymer 1997; 38: 5755-60.
- [33] Se K, Suzuki M, Matsuo T, Umeda T, Ueno M. Preparation of poly(*p*-isopropenylphenethyl)poly(α -methylstyrene) macromonomer and anionic polymerization of the macromonomer. Kobunshi Ronbunshu (Jpn J Polym Sci Technol) 1992; 49: 817-23.
- [34] Se K, Teramoto M. Anionic synthesis of star-block copolymers with macroinitiators prepared from macromonomer and characterization of the polymers (Jpn J Polym Sci Technol) 1997; 54: 930-8.
- [35] Szwarc M. Living polymers and mechanism of anionic polymerization. Adv Polym Sci 49. Berlin: Springer; 1983. p. 1-177.
- [36] Patai S, editor. The chemistry of the amino group. New York: Interscience Publ; 1968.
- [37] Higo Y, Chosi H, Fujimoto T, Nagasawa M. Preparation and characterization of a poly(strong base) with narrow molecular weight distribution; poly(4-vinylbenzyltrimethylammonium chloride). Polym J 1980; 12: 729-34.
- [38] Sperling LH. Cross-linked polymers and rubber elasticity. In: Introduction to physical polymer science, 3rd ed. New York: Wiley; 2001. p. 363-431.
- [39] Barar DG, Staller KP, Peppas NA. Friedel-Craft crosslinking methods for polystyrene

- modification. IV. Macromolecular structure of crosslinked particles. J Polym Sci, Part A: Polym Chem 1983; 21: 1013-24.
- [40] Van Krevelen DW, Hoftyzer PJ. Properties of polymers. Amsterdam: Elsevier; 1972.
- [41] Grulke EA. Solubility parameter values. In: Brandrup J, Immergut EH, editors. Polymer handbook, 3rd ed. Wiley: New York; 1989. VII 519-59.
- [42] Yamaguchi T, Nakazumi H, Irie M. Photochromic reactions of two azobenzene chromophors in a chiral cyclohexane moiety. Bull Chem Soc Jpn 72; 1999: 1623-27.
- [43] Nuyken O, Scheren C, Baidl A, Brenner AR, Dahn U, Gartner R, Kaiser-Rohrich S, Kollfrath R, Matusche P, Voit B. Azo-group-containing polymers for use in communications technologies. Progr Polym Sci 1997; 22: 98-183.
- [44] Irie M, Ikeda T. Photoresponsive polymers. In: Takemoto K, Ottenbrite RM, Kamachi M, editors. Functional monomers and polymers, 2nd ed. New York: Marcel Dekker; 1997. p. 65-116.
- [45] Yoshiyuki K, Machida S, Horie K. Local free volume and structural relaxation structures with photoisomerization of azobenzene and persistent spectral hole burning poly(alkyl methacrylate)s at low temperature. J Polym Sci, Part B: Polym Phys 2000; 38: 3098-105.
- [46] Se K, Kijima M. Photochemical isomerization of *p*, *p'*-bis(chloromethyl) azobenzene incorporated in poly(*N,N*-dimethyl-4-vinylphenethylamine)-*block*-polystyrene. Rept Prog Polym Phys Jpn 1994; 37: 545-8.
- [47] Se K, Berry GC. Frank elastic constants and Leslie-Ericksen viscosity coefficients of nematic solutions of rodlike polymers. Mol Cryst Liq Cryst 1987; 153: 133-42.
- [48] Berry GC, Se K, Srinivasarao M. Rheological, rheo-optical and light scattering studies of nematic solutions of poly(1,4-phenylene-2, 6-benzobisthiazole). In:

- Zachariades AE, Porter RS, editors. High modulus polymers. Plastic engineering series 17, New York: Marcel Dekker; 1989. p. 195-224.
- [49] Smets G. Photochromic phenomena in the solid phase. Adv Polym Sci 50. Berlin: Springer; 1983. p. 17-44.
- [50] Deblauwe V, Smets G. Photochromisms of spirofluorenylindolizines. J Poly Sci, Part B: Polym Phys 1989; 27: 671-80.
- [51] Yu WC, Sung CSP, Robertson RE. Site-specific labeling and distribution of free volume in glassy polystyrene. Macromolecules 1988; 21: 355-64.
- [52] Munakata Y, Tsutsui T, Saito S. The matrix effect on the thermal reactions of spirooxazine in polymer matrices. Polymer J 1990; 22: 843-48.
- [53] Tomioka H, Sato H. Preparation of polyion complexes consisting of spiroopyrans and photochromism of their spin-coated films. Nihon-kagakukaishi (J Chem Soc Jpn) 1992; 1083-90.
- [54] Klafter J, Bulumen A. Models for dynamically controlled relaxation. Chem Phys Lett 1985; 119: 377-82.
- [55] Matsuda A, Baba A. In: Izumi N, Ogawa K, Katou S, Shiokawa J, Shiba T, editors. Kiki bunnseki no tebiki (Jpn A Handbook of Instrumental Analysis), 2nd ed. Tokyo: Kagakudojin; 1996.
- [56] Ishizone T, Nakao A, Nakahawa S. Living anionic polymerization of styrenes substituted with electron-withdrawing groups. Koubunshi Ronbunshu (Jpn J Polym Sci Techn) 1997; 12: 829-42.
- [57] Yamaguchi K, Hirano A, Suzuki K, Takenaka K, Nakahama S, Yamazaki N. Anionic living polymerization of *p*-*N*, *N*-bis(trimethylsilyl)-aminostyrene. Synthesis of linear poly(*p*-aminostyrene) with a narrow molecular weight distribution. J Polym

- Sci, Polym Lett Ed 1983; 21: 395-401.
- [58] Ito H. Preparation of lithographic resist polymers by anionic polymerization. In: Quirk RP, editor. Application of anionic polymerization research. ACS symposium series 696, Washington, DC: ACS; 1996. p. 218-34.
- [59] Se K, Ohtomo R. Grafting of oligopeptide on poly(aminostyrene)s and characterization of the Polymers. J Appl Polym Sci 2000; 77: 1558-67.
- [60] Hoffman AS. A commentary on the advantages and limitations of synthetic polymer-biomolecular conjugates. In: Okano T, editor. Biorelated polymers and gels. Boston: Academic press; 1998. p. 231-48.
- [61] Tsuruta T. Contemporary topics in polymeric materials for biomedical applications. Adv. Polym. Sci 126, Berlin: Springer; 1996. p. 1-51.
- [62] Peptide Institute Inc: address; 4-1-2 Ina, Minoh-Shi, Osaka 562-8686, Japan.
<http://www.peptide.co.jp/>
- [63] Suoda KK, Gong H, Trinkaus-Randall V. Collagen expression and orientation in ocular tissues. Progr Polym Sci 1998; 23: 329-74.
- [64] Bodanszky M, Bodanszky A. The practice of peptide synthesis. New York: Springer; 1984.
- [65] Klee D, Hocker H. Polymers for biomedical applications: Improvement of the interface compatibility. Adv. Polym. Sci 149, Berlin: Springer; 2000. p. 1-57.
- [66] Jin HL, Hai BL, Andrade JD. Blood compatibility of polyethylene oxide surfaces. Progr Polym Sci 1995; 20: 1043-79.
- [67] Akashi M, Furuzone T, Kishida A, Maruyama I. A novel biomaterials: Aramid-silicone resin. In: Takemoto K, Ottenbrite RM, Kamachi M, editors. Functional monomers and polymers, 2nd ed. New York: Marcel Dekker; 1997. p.

267-308.

- [68] Beugeling T, Does LVD, Rejda BV, Bantjes A. Antithrombogenic polymers synthesized from polyisoprenes. In: Williams D, editor. Biocompatibility of implant materials. London: Sector Publishing Ltd; 1976. p. 187-92.
- [69] Miyake H, Miyaki Y, Se K, Fujimoto T. Non-thrombogenic behaviors of charge-mosaic membranes prepared from pentablock copolymers. *Jinnkoh Zouki (Jpn J Artificial Organ)* 1984; 13: 1243-49.
- [70] Miyaki Y, Nagamatsu H, Iwata M, Ohkoshi K, Se K, Fujimoto T. Artificial Membrane from multiblock copolymers. III. Preparation and characterization of charge-mosaic membranes. *Macromolecules* 1984; 17: 2231-36.
- [71] Nakajima A, Hayashi H, Satou H. Molecular design, structure and physical properties of nonthrombogenic polymeric materials. In: Asahara T, editor. *Iyou Koubunnshi Zairyuu (Jpn Medical Polymers)*. Tokyo: Gakujyutsu Publ Center; 1981. p. 123-30.
- [72] Kataoka K, Ito H, Amano H, Nagasaki Y, Kato M, Tsuruta T, Suzuki K, Okano T, Sakurai Y. Minimized platelet interaction with poly(2-hydroxyethylmethacrylate-*block*-4-bis(trimethylsilyl)methylstyrene) hydrogel showing anomalously high free water content. *J Biomater Sci, Polym Ed* 1998; 9: 112-29.
- [73] Hasegawa H, Tanaka H, Yamasaki Y, Hashimoto T. Bicontinuous microdomain morphology of block copolymers. 1. Tetrapod-network structure of polystyrene-polyisoprene diblock polymers. *Macromolecules* 1987; 20: 1651-62.
- [74] Mogi Y, Nomura M, Kotsuji H, Onishi K, Matsushita Y, Noda I. Superlattice structures in morphologies of the ABC triblock copolymers. *Macromolecules* 1994;

27: 6755-60.

- [75] Roovers J. Relaxation by constraint release in combs and star-combs. *Macromolecules* 1987; 20: 2300-06.
- [76] Ito K. Polymeric design by macromonomer technique. *Progr Polym Sci* 1998; 23: 581-620.
- [77] Rempp P, Franta E. *Makromol Chem, Macromol Symp* 91; 1995: 51-63.
- [78] Se K, Matsumura K, Kazama T, Fujimoto T. Preparation and characterization of poly(4-vinylphenyldimethylvinylsilane) *via* anionic living polymerization. *Polymer J* 1997; 29: 434-41.
- [79] Se K, Matsumura K, Kazama T, Fujimoto T. Lithographic characterization of poly(4-vinylphenyldimethylvinylsilane) having a narrow molecular weight distribution. *Polymer J* 1997; 29: 387-90.
- [80] Se K, Yamazaki H, Shibamoto T, Takano A, Fujimoto T. Model block-graft copolymers *via* anionic living polymerization: preparation and characterization of [poly(4-vinylphenyldimethylvinylsilane)-*graft*-polyisoprene)]-*block*-polystyrene. *Macromolecules* 1997; 30: 1570-76.
- [81] Hasegawa E. Recent research developments of super-high resolution resists. In: Yoshida T, editor. *Catch-ball between polymer science and physics. Polymer frontier series 3*, Tokyo: The Soc Polym Sci Jpn; 2002. p. 51-81.
- [82] Thompson LF, Willson CG, Tagawa S. *Polymers for microelectronics. ACS symposium series 537*, Washington, DC: ACS; 1994.
- [83] Itaya K, Shibayama K, Fujimoto T. High resolution electron beam negative resist with very narrow molecular weight distributions. *J Electrochem Soc* 1982; 129: 663-5.

- [84] Endo M, Tani Y, Sasago M, Nomura N. Azide-styrene resin negative deep UV resist for KrF excimer laser lithography. *J Electrochem Soc* 1989; 136: 2615-18.
- [85] Cai SX, Wybourne MN, Keana FW. Superiority of bis(perfluorophenyl) azides over nonfluorinated analogues as cross-linkers in polystyrene-based deep-UV resists. In: Thompson LF, Willson CG, Tagawa S, editors. *Polymers for microelectronics*. ACS symposium series 537, Washington, DC: ACS; 1994 , p. 348-55.
- [86] Iwasa S, Maeda K, Hasegawa E. Chemically amplified negative resists based on alicyclic acrylate polymers for 193-nm lithography. *J Photopolym Sci Tech* 1999; 12: 487-92.
- [87] Sharma VK, Affrossman S, Pethrick RA. Poly(α -methylstyrene) and α -methylstyrene-maleic anhydride copolymer: An electron beam lithographic study. *Polymer* 1984; 25: 1087-89.
- [88] Shimada H, Onodera M, Shimomura S, Hirose K, Ohmi T. Residual-surfactan-free photoresist development process. *J Electrochem Soc* 1992; 139: 1721-30.
- [89] Kihara N, Ushirogouchi T, Tada T, Naito T, Saito A, Nakase M. Chemically amplified resist using self-solubility acceleration effect. *J Electrochem Soc* 1994; 141: 3162-66.
- [90] Berry GC, Orofino TA. Branched polymers. III. Dimensions of chain with small excluded volume. *J Chem Phys* 1964; 40: 1614-21.
- [91] Roovers J. Dilute solution properties of regular star polymers. In: Mishra M, Kobayashi S, editors. *Star and hyperbranched polymers*. Plastic engineering series 53, New York: Marcel Dekker; 1999. p. 285-341.
- [92] Se K. Molecular characterization of star block copolymers. *Kobunshi Kakou (Jpn J Polym Process)* 1998; 47: 207-14.

- [93] Se K., Sakakibara T., Ogawa E. Molecular weight determination of star polymers and star block copolymers using GPC equipped with low-angle laser light-scattering. *Polymer* 2002; 43:5447-53.
- [94] Teramachi S, Sato S, Shimura H, Watanabe S, Tsukahara Y. Chemical composition distribution of poly(methyl methacrylate)-*graft*-polystyrene prepared by a macromonomer technique. Effect of graft length. *Macromolecules* 1995; 28; 6183-87.
- [95] Roovers JE, Bywater S. Preparation and characterization of four-branched star polystyrene. *Macromolecules* 1972; 5: 384-8.
- [96] Takano A, Okada M, Nose T, Fujimoto T. Synthesis and characterization of star-shaped polymer with one labeled arm. *Macromolecules* 1992; 25: 3596-8.
- [97] Arai K, Kotaka T, Kitano Y, Yoshimura K. Poly(styrene-*b*-butadiene-*b*-4-vinylpyridine) three-block polymers: Synthesis, characterization, morphology, and mechanical properties. *Macromolecules* 1980; 13: 1670-8.
- [98] Matsushita Y, Yamada K, Hattori T, Fujimoto T, Sawada Y, Nagasawa M, Matsui C. Morphologies of ABC-type triblock copolymers with different composition. *Macromolecules* 1983; 16: 10-3.
- [99] Sato H, Ono A, Tanaka Y. Distribution of isomeric structures in polyisoprenes. *Polymer* 1977; 18: 580-6.
- [100] Se K, Takayanagi O, Adachi K. Dielectric study of miscibility in weakly segregated polymer blends. *Macromolecules* 1997; 30: 4877-81.
- [101] Se K, Yamamoto Y. Dielectric study of miscibility in *cis*-polyisoprene/vinyl-polyisoprene polymer blends: Molecular weight dependence.

- Rept Prog Polym Phys Jpn 1999; 41: 498-501.
- [102] Se K, Shirasaki Y. Dielectric study of miscibility in *cis*-polyisoprene/vinyl-polyisoprene polymer blends. Rept Prog Polym Phys Jpn 1998; 40: 483-6.
- [103] Hirai T, Fujimura N, Urakawa K, Adachi K, Donkai M, Se K. Dielectric relaxation of poly(*n*-hexylisocyanate) in concentrated solutions of polybutadiene. Polymer 2002; 43: 1133-8.
- [104] Helfand E, Wassermann ZR. Block copolymer theory. B. Cylindrical domains. Macromolecules 1980; 13: 994-998.
- [105] Se K, Uesaka T. Determination of the χ parameter and the spinodal curve for polystyrene/polyisoprene pair using thermal jump. Rept Prog Polym Phys Jpn 1996; 39: 421-4.
- [106] Hashimoto T, Fujimura M, Kawai H. Domain-boundary structure of styrene-isoprene block copolymer films cast from solutions. 5. Molecular-weight dependence of spherical microdomains. Macromolecules 1980; 13: 1660-9.
- [107] Okumoto M, Terao K, Nakamura Y, Norisue T, Teramoto A. Excluded-volume effects in star polymer solutions: Four-arm star polystyrene in cyclohexane near the Θ temperature. Macromolecules 1997; 30: 7493-9.
- [108] Matsushita Y, Nomura M, Watanabe J, Noda I, Imai M. Alternating lamellar structure of triblock copolymers of ABC type. Macromolecules 1995; 28: 6007-13.
- [109] Yang L, Hong S, Gido SP, Velis G, Hadjichristidis N. I₃S Miktoarm star block copolymers: Packing constraints on morphology and discontinuous chevron tilt grain boundaries. Macromolecules 2001; 34: 9069-73.
- [110] Beyer FL, Gido SP, Uhrig D, Mays JW, Tan NB, Trevino S. Morphological

- behavior of A_2B_2 star block copolymers. *J Polym Sci, Part B: Polym Phys* 1999; 37: 3392-400.
- [111] Gido SP, Pochan D, Pispas S, Mays JW. Synthesis, characterization, and morphology of model graft copolymers with trifunctional branch points. *Macromolecules* 1996; 29: 7022-8.
- [112] Xenidou M, Beyer FL, Hadjichristidis N, Gido SP, Tan NB. Morphology of model graft copolymers with randomly placed trifunctional and tetrafunctional branch points. *Macromolecules* 1998; 31: 7659-67.
- [113] Beyer FL, Gido SP, Buschl C, Iatrou H, Uhrig D, Mays JW, Chang MY, Garetz BA, Balsara NP, Tan NB, Hadjichristidis N. Graft copolymers with regularly spaced, tetrafunctional branch points: Morphology and grain structure. *Macromolecules* 2000; 33: 2039-48.
- [114] Milner ST. Chain architecture and asymmetry in copolymer microphases. *Macromolecules* 1994; 27: 2333-5.
- [115] Olmsted PD, Milner ST. Strong-segregation theory of bicontinuous phases in block copolymers. *Phys Rev Lett* 1994; 72: 936-9.
- [116] Olmsted PD, Milner ST. Strong segregation theory of bicontinuous phases in block copolymers. *Macromolecules* 1998; 31: 4011-22.
- [117] Se K, Miyawaki K, Hirahara K, Takano A, Fujimoto T. Model block-graft copolymers *via* anionic living polymerization: preparation and characterization of polystyrene-*block*-[poly(*p*-hydroxystyrene)-*graft*-Poly(ethylene oxide)]-*block*-Polystyrene. *J Polym Sci, Part A: Polym Chem* 1998; 36: 3021-34.
- [118] Firestone MA, Park J, Minami N, Ratner MA, Marks T. Chromophore-functionalized glassy polymers with large second-order nonlinear

- optical responses: Synthesis, characterization, and architecture-processing response characteristics of poly(*p*-hydroxystyrene) functionalized with chiral chromophoric side chains. *Macromolecules* 1995; 28: 2247-59.
- [119] Conlon DA, Crivell JV, Lee JL, O'Brien MJ. Synthesis, characterization, and deblocking of poly(4-*tert*-butoxystyrene) and poly(4-*tert*-butoxy- α -methylstyrene). *Macromolecules* 1989; 22: 509-16.
- [120] Se K, Suzuki M. Initiation efficiency of anionic living polymerization of macromonomers. *Kobunshi Ronbunshuu (Jpn J Polym Sci Technol)* 2000; 57: 851-4.
- [121] Se K, Adachi K, Kotaka T. Dielectric relaxation in poly(ethylene oxide): Dependence on molecular weight. *Polym J* 1981; 13: 1009-17.
- [122] Se K, Adachi K, Kotaka T. Dielectric behavior of Poly(ethylene oxide)-polystyrene-poly(ethylene oxide) block copolymers. *Rept Prog Polym Phys Jpn* 1979; 22: 393-6.
- [123] Se K, Kotaka T. Thermal-depolarization-current study of poly(ethylene oxide) polystyrene-poly(ethylene oxide) block copolymers. *Rept Prog Polym Phys Jpn* 1979; 22: 397-8.
- [124] Hong S, Yang L, MacKnight J, Gido SP. Morphology of a crystalline/amorphous diblock copolymer: Poly((ethylene oxide)-*b*-butadiene). *Macromolecules* 2001; 34: 7009-16.
- [125] Shibayama M, Hasegawa H, Hashimoto T, Kawai H. Microdomain structure of an ABC-type triblock polymers of polystyrene-poly[(4-vinylbenzyl)dimethylamine]-polyisoprene cast from solutions. *Macromolecules* 1982; 15: 274-80.

[126] Mark DG, Frank SB. Conformational asymmetry in poly(vinylcyclohexane) containing diblock copolymers. *Macromolecules* 1994, 27; 3611-18.

Figure Captions

Fig. 1. Molecular structures of four useful monomers: tertiary aminostyrenes (tAS), *N*-isopropyl-*N*-trimethylsilyl-4-vinylbenzylamine (IBA), (4-vinylphenyl)dimethylvinylsilane (VS), and *p*-butoxystyrene (BSt).

- Fig. 2.** Molecular structures of poly(aminostyrene)s which have amino groups classified as primary, secondary and tertiary groups (R is an alkyl group). Each of these three amino groups is also classified as phenylamine, benzylamine and phenethylamine.
- Fig. 3.** GPC chromatograms of PDPA prepared by (a) a *n*-BuLi/THF system ($M_n = 8.4 \times 10^4$), (b) a Cumyl K/THF system ($M_n = 26 \times 10^4$), and (c) a Cumyl Cs/THF system ($M_n = 6.5 \times 10^4$). The carrier solvent is THF, the flow rate is 1.0 ml min^{-1} , the polymer concentration is 0.05 w/v%, and the RI detector is employed.
- Fig. 4.** Plots of $-\ln(1 - x)$ versus $[\text{LE}]t$ for PDPA, prepared by using a Cumyl K/THF system and a Cumyl Cs/THF system in the lower polymer conversion side.
- Fig. 5.** A neutralization curve of QPDBA treated with an anion-exchange resin. A point of neutralization is $\text{pH} = 7.4$, which is indicated as an arrow in the figure.
- Fig. 6.** Reaction time dependence of the degree of quaternization (DQ) of PDPA, PDPA, and PDPTA at 60°C . The inserted figure describes reaction time dependence of DQ of PDPA at 100°C .
- Fig. 7.** Temperature dependence of the degree of quaternization of PDPA, PDPA, and PDPTA for 6 h.
- Fig. 8.** Arrhenius' plots of apparent reaction rate constants, k_a , for quaternization of PDPA, PDPA, and PDPTA.

Fig. 9. A structural formula of the crosslinked film for poly(tertiary aminostyrene)s (PtAS) with *p, p'*-bis(chloromethyl)azobenzene (CAB).

Fig. 10. A plot of an apparent effective network concentration (ν_e) versus $Q_t^{-5/3}$ for PDBA(CAB)_Y films in THF at 25°C. An effective network concentration (ν_e) calculated by Small's method ($\mu = 0.34$) (---) or by Hoy's method ($\mu = 0.32$) (- - -) is also described.

Fig. 11. Changes in the absorption spectra of CAB with UV (300–380 nm) irradiation time in methanol: (a) $t = 0$; (b) $t = 45$; (c) $t = 60$; (d) $t = 90$; (e) $t = 150$; (f) $t = 600$ s.

Fig. 12. Changes in the absorption spectra of CAB with UV (300–380 nm) irradiation time for a PDBA(CAB)₁₅ film: (a) $t = 0$; (b) $t = 2$; (c) $t = 6$; (d) $t = 30$ min.

Fig. 13. Photochemical isomerization from *trans* to *cis* form of CAB at a fixed temperature in the following films: (PDPTA-*b*-PSt)(CAB)_{2.5} at 60°C (○), PDPTA(CAB)_{1.3} at 20°C (○), PDPTA(CAB)_{1.3} at 60°C (- - -) and PSt(CAB)_{1.5} at 20°C (●). Absorbance (A_t) was detected at 320 nm after irradiation with an ultraviolet light ($300 \text{ nm} < \lambda_1 < 380 \text{ nm}$) for time, t , which is plotted as an axis of the abscissa on the figure. The A_t/A_0 value represents a fraction of a *trans* form, which was not converted to a *cis* form of CAB.

Fig. 14. Typical plots of $-\ln[(C_t - C_e)/(C_0 - C_e)]$ versus t for the photochemical isomerization from *trans* to *cis* form of CAB in the following films: PSt(CAB)_{1.5} at 20°C (○), (PDPTA-*b*-PSt)(CAB)_{2.86} at 50°C (○) and 70°C (○), and (PDPTA-*b*-St)(CAB)_{2.74} at 80°C (○).

Fig. 15. A relationship between the parameter α and temperature, at which the photochemical isomerization from *trans* to *cis* form of CAB proceeded in the (PDPTA-*b*-PSt)(CAB)_Y films.

Fig. 16. Temperature dependence of the half-life period, $\tau_{1/2}$ (○), and a three fourths-life period, $\tau_{3/4}$ (●), for the photochemical isomerization from *trans* to *cis* form of CAB proceeded in the (PDPTA-*b*-PSt)(CAB)_Y films..

Fig. 17. Photochemical isomerization from *trans* to *cis* form of CAB and from *cis* to *trans* form of CAB in a (PDPTA-*b*-PSt)(CAB)_{1.5} film. The film was first irradiated with a UV light at 60°C (○) or 20°C (●) for 2 h. Next, each film was irradiated with a visible light at 20°C. The result of a reverse thermal isomerization is also described by storing the film in darkness at 20°C for 180 h (○). The film after irradiation with a UV light at 60°C for 2 h was finally irradiated with a visible light at 90°C (-○-).

Fig. 18. GPC chromatograms of PISBA prepared from ISBA (a) once, (b) twice, and (c) three times dried over BuMgBr in THF. The experimental conditions are as

follows: the carrier solvent of THF containing *N*-methylpyrrolidine (2 v/v%), the flow rate of 1.0 ml min⁻¹, the RI detector, and the polymer concentration of 0.05 w/v%.

Fig. 19. GPC chromatograms of (a) PISBA-*b*-PSt and (b) PSt-*b*-PISBA. The sequence of the addition of the two monomers was inverted in block copolymerization.

Fig. 20. ¹H-NMR spectra of PISBA (top) and the resultant PIBA (bottom) after the removal of a trimethylsilyl group. A sharp NMR signal of PISBA at 0 ppm was due to the trimethylsilyl group and was completely disappeared in PIBA, whereas a sharp NMR signal of PIBA at 1.0 ppm was newly observed and was assigned to the amino group.

Fig. 21. GPC chromatograms of (a) PISBA (—), $M_n = 1.7 \times 10^5$, and the resultant poly(*N*-isopropyl-4-vinylbenzylamine) (PIBA) (---), $M_n = 1.2 \times 10^5$ after removal of the trimethylsilyl group.

Fig. 22. A ¹³C-NMR spectrum of PPA-*g*-(Gly-Boc) prepared with [Boc-Gly] / [PA] = 1 at 0°C for 2 h. Signals are assigned in the figure.

Fig. 23. Reaction time dependence of the degree of grafting for PPA-*g*-(Gly-Boc) with [Boc-Gly] / [PA] = 1 at 0°C (○) and 45°C (●).

Fig. 24. Plots of the degree of grafting *versus* molar ratios of (a) Boc-Gly, (b) Z-Gly-Pro, and (c) Z-Gly-Pro-Leu-Gly-Pro, to the monomer unit for PPA fed in the reaction mixtures at 0°C for 2 h.

Fig. 25. Lee-White relative clotting times (L-WRCT) of polystyrene, PPA, PPA-*g*-(Gly-Boc), and PPA-*g*-(Pro-Gly-Leu-Pro-Gly-Z) having 100% of DOG. The L-WRCT values were determined from a Lee-White method using human whole blood.

Fig. 26. Two schematic structures of the model block-graft copolymers, where A, B, and C are a backbone chain without grafting sites, a backbone chain with grafting sites, and graft chains, respectively.

Fig. 27. GPC chromatograms of PVS prepared using *n*-BuLi, Cumyl K, and Cumyl Cs as initiators, THF as a solvent, and a polymerization time of 3 h.

Fig. 28. GPC chromatograms of PVS prepared using THF, Me-THF, and 1, 3-DX as solvents, Cumyl Cs as an initiator, and polymerization times as described in the figure.

Fig. 29. GPC chromatograms of PVS prepared at a polymerization time between 0.5 h and 2 h, using Cumyl Cs as an initiator, and a mixture of Ether/1, 3-DX = 1/2 (a left figure) or Ether/1, 3-DX = 1/1 (a right figure) as a solvent.

Fig. 30. Scanning electron micrographs of image lines from resists of PVS-4 exposed to a deep UV light of 270 nm. The developer is a mixture of xylene/methanol = 8/1. A number such as 2.0 μm appearing in this figure represents 2.0 μm lines, and all spaces between the lines are 0.75 μm . Intensities of a deep UV light are (a) 135 mJ/cm^2 (185 seconds), (b) 145 mJ/cm^2 (199 s), (c) 166 mJ/cm^2 (227 s), and 186 mJ/cm^2 (255 s).

Fig. 31. A scanning electron micrograph of image lines from a resist of PVS-4 exposed to an electron beam. A developer is a mixture of xylene/methanol = 8/1. A number such as 1.0 μm appearing in this figure represents 1.0 μm lines, and all spaces between the lines are 1.0 μm .

Fig. 32. Exposure response curves of PVS-1 and PVS-4 exposed to electron beams. Developers in the figure are *n*-heptane (C_7H_{16})/isopropyl acetate (IPA) = 1/1, ethyl acetate/isopropyl acetate (IPA) = 1/1, xylene/methanol (MeOH) = 8/1, tetrahydrofuran (THF)/methanol (MeOH) = 35/65, and methyl ethyl ketone (MEK).

Fig. 33. GPC chromatograms of (PVS-*g*-PIs)-*b*-PSt block-graft copolymers of (a) SGI-1, (b) SGI-2, and (c) SGI-3 samples, prepared *via* a backbone coupling (a “grafting onto” process).

Fig. 34. Transmission electron micrographs of (PVS-*g*-PIs)-*b*-PSt block-graft copolymer films of (a) SGI-1, (b) SGI-2, and (c) SGI-3, which were cast from the respective

benzene solutions and were subsequently stained with OsO₄. White and black regions correspond to PSt/PVS and PIs phases, respectively.

Fig. 35. Theoretical phase diagram of (A)_m(PSt)_n calculated by Milner, where the bicontinuous phases are omitted due to being complicated. The A polymer is PIs for three SGI films or PEO for two SGE films. Symbols represent the MS structures of Sph_{PSt} (spheres of PSt), Cyl_{PSt} (cylinders of PSt), Lam (lamella), Cyl_A (cylinders of A polymer), and Sph_A (spheres of A polymer). Boldly outlined symbols indicate samples characterized in this study.

Fig. 36. GPC chromatograms of (a) PSt-*b*-PBSt block copolymer (—) and the resultant PSt-*b*-PHSt block copolymer (- - -) after removal of the *tert*-butyl group, and (b) PBSt-*b*-PBu block copolymer (—) and the resultant PHSt-*b*-PBu block copolymer (- - -).

Fig. 37. GPC chromatograms of PSt-*b*-PBSt-*b*-PSt block copolymer (—) and the corresponding PSt-*b*-PHSt-*b*-PSt block copolymer (- - -) as a backbone chain deprotected by HBr.

Fig. 38. Sedimentation patterns of two PSt-*b*-(PHSt-*g*-PEO)-*b*-PSt block-graft copolymers of (a) SGE-1 and (b) SGI-2: a concentration of 0.25 g dl⁻¹ and a time of 21 min for SGE-1, and a concentration of 0.20 g dl⁻¹ and a time of 18 min for SGE-2, THF solvent, a temperature of 25°C, a speed of rotation of 59,780 rpm, and an angle of 70 degrees.

Fig. 39. Transmission electron micrographs of PSt-*b*-(PHSt-*g*-PEO)-*b*-PSt block-graft copolymer films of (a) SGE-1 and (b) SGE-2, which were cast from the respective benzene solutions and were subsequently stained with OsO₄ and RuO₄, respectively. White and black regions correspond to PSt/PHSt and PEO phases, respectively.

Table 1

Preparation of poly(*N,N*-dimethyl-4-vinylphenylamine), PDPA

Monomer mol l ⁻¹	Initiator		Solvent		Time h	Conv %	10 ⁻⁴ M _k ^a	10 ⁻⁴ M _n ^b	M _w /M _n ^b
	Name	m mol l ⁻¹	Name	ml					
0.25	<i>s</i> -BuLi	0.51 ₆	Benzene	220	15	80	5.6	2.8	1.3 ₂
0.22	<i>n</i> -BuLi	0.42 ₄	THF	210	24	100	7.6	8.4	1.2 ₂
0.22	Cumyl Cs	0.44 ₀	THF	170	24	40	3.0	3.6	1.0 ₉
0.34	Cumyl Cs	0.61 ₀	THF	120	48	75	6.0	6.5	1.0 ₆
0.32	Cumyl Cs	0.81 ₅	THF	110	48	85	4.9	5.8	1.0 ₈
0.25	Cumyl K	0.14 ₄	THF	220	24	100	25 _{.2}	26 _{.0}	1.0 ₄

^a Calculated from the amounts of monomer and initiator.^b Determined from GPC measurement.

Table 2

Preparation of poly(*N, N*-dimethyl-4-vinylbenzylamine), PDBA and poly(*N, N*-dimethyl-4-vinylphenethylamine), PDPTA.

Monomer		Initiator		Solvent		Time	Conv	$10^{-4}M_k^a$	$10^{-4}M_n^b$	M_w/M_n^b
Name	mol l ⁻¹	Name	m mol l ⁻¹	Name	ml	h	%			
DBA	0.22	<i>n</i> -BuLi	0.63 ₄	THF	120	24	100	5.4	4.1	1.3 ₈
DBA	0.20	Cumyl K	0.92 ₂	THF	200	24	100	3.4	3.5	1.0 ₉
DBA	0.27	Cumyl Cs	0.42 ₁	THF	200	3	100	10. ₄	11. ₁	1.0 ₅
DPTA	0.16	<i>n</i> -BuLi	0.62 ₂	THF	120	24	100	4.5	4.1	1.2 ₂
DPTA	0.17	Cumyl K	0.85 ₇	THF	200	24	100	3.5	3.0	1.0 ₈
DPTA	0.21	Cumyl Cs	0.51 ₄	THF	160	5	100	7.1	7.7	1.0 ₄

^a Calculated from the amounts of monomer and initiator.^b Determined from GPC measurement.

Table 3

Apparent rate constants of the anionic living polymerization for PDPA

$\frac{10^2 k_{ap}^{Cs}}{1 \text{ mol}^{-1} \text{ s}^{-1}}$	$k_{ap}^{Cs}/k_{ap}^{PSt-Na^a}$	$\frac{10^2 k_{ap}^K}{1 \text{ mol}^{-1} \text{ s}^{-1}}$	$k_{ap}^K/k_{ap}^{PSt-Na^a}$	k_{ap}^K/k_{ap}^{Cs}
1.5	1.7×10^{-5}	16	18×10^{-5}	10.1

^a k_{ap}^{PSt-Na} is an apparent rate constant of polymerization for polystyrene using a K ion in THF at 25°C: k_{ap}^{PSt-Na} is about $900 \text{ l mol}^{-1} \text{ s}^{-1}$.

Table 4

Kinetic characteristics of quaternization of three poly(tertiary aminostyrene)s, PtAS with *n*-butyl bromide

Polymer	$10^{-3} \Delta E^* / \text{J mol}^{-1}$	$A^* / \text{l mol}^{-1} \text{ min}^{-1}$
PDPA	25	3.4×10^3
PDBA	50	4.2×10^7
PDPTA	50	$1.3_0 \times 10^8$

Table 5

The degree of swelling in equilibrium with THF at 25°C for PDBA(CAB)_Y films

Polymer	$10^{-4}M_n^a$	Y^b	Q_r	$10^5\nu_e^c$	$10^5\nu_e^d / \text{mol cm}^{-3}$	
		%		mol cm^{-3}	Small	Hoy
PDBA	3.5	0.6	16.0	0.6	1.9	2.1
PDBA	3.5	1.0	11.0	3.6	3.7	4.1
PDBA	3.5	1.5	7.5	6.6	6.9	7.8
PDBA	3.5	1.7	6.0	7.8	10.0	11.0
PDBA	11.0	2.2	4.4	13.0	17.0	19.0
PDBA	11.0	4.0	3.1	24.0	30.0	33.0

^a Determined from GPC measurement.

^b The ratio of chloromethyl groups of CAB to tertiary amino groups in the polymer.

^c An apparent effective network concentration calculated from the amount of polymer and CAB in the films.

^d An effective network concentration calculated from the polymer-solvent interaction parameter (μ) estimated by Small's method ($\mu = 0.34$) and Hoy's method ($\mu = 0.32$), respectively.

Table 6

Experimental conditions^a and results for the preparation of poly(*N*, *N*-dimethyl-4-vinylphenethylamine)-*block*-polystyrene, PDPTA-*b*-PSt diblock copolymer

First monomer		Second monomer		Solv	Initi ^b	Conv	PSt cont	10 ⁻⁴ M _n		M _w /M _n ^d
DPTA	Time	St	Time	THF				Calc ^c	Obs ^d	
g	h	g	h	ml	m mol	%	%			
3.4	10	3.9	3.5	160	0.15 ₈	100	53	4.6	3.9	1.0 ₇

^a Polymerization was carried out at -78°C under a pressure of 10⁻⁶ mmHg.

^b Cumyl K.

^c Calculated from the amounts of monomer and initiator.

^d Determined from GPC measurement.

Table 7

Effects of purging reagents on anionic polymerization of *N*-isopropyl-*N*-trimethylsilyl-4-vinylbenzylamine, ISBA

Purging reagent	Monomer m mol	Initiator	Conv %	$10^{-4}M_k^a$	$10^{-4}M_n$		M_w/M_n^b	f^d
		n -BuLi m mol			GPC ^b	OSM ^c		
C ₈ BP-Na ^c	14	0.10	0	3.5				
BuMgBr ^f	6.0	0.11	0	1.3				
BuMgBr/THF/once ^g	11	0.22	Trace	1.2	4.0			
BuMgBr/THF/twice ^g	6.2	0.18	17	0.85	3.8			
BuMgBr/THF/thrice ^g	17	0.066	100	6.4	6.0	7.1	1.0 ₅	0.90
BuMgBr/THF/thrice ^g	21	0.035	100	15	16	17	1.0 ₃	0.89

^a Calculated from the amounts of monomer and initiator.^b Determined from the GPC measurement.^c Determined from membrane osmometry.^d Initiation efficiency of the initiator.^e Octylbenzophenone sodium.^f *sec*-Butylmagnesium bromide.^g A THF solution of ISBA was dried over BuMgBr once, twice, or thrice.

Table 8

Preparation of two block copolymers containing poly(*N*-isopropyl-*N*-trimethylsilyl-4-vinylbenzylamine), PISBA and PSt blocks using *n*-BuLi as an initiator in THF at -78°C

First monomer			Second monomer			Initiator	Solvent		PISBA			
Name	m mol	Time h	Name	m mol	Time h	<i>n</i> -BuLi m mol	THF ml	Conv %	Cont ^a %	$10^{-4}M_k^b$	$10^{-4}M_n^c$	M_w/M_n^c
ISBA	10	20	St	30	4	0.15	140	100	44	3.7	4.0	1.0 ₅
St	29	4	ISBA	11	20	0.16	145	100	47	3.6	3.7	1.2 ₅

^a Determined from a $^1\text{H-NMR}$ spectrum.

^b Calculated from the amounts of monomer and initiator.

^c Determined from GPC measurement.

Table 9

Aminostyrene derivatives discussed in this chapter

Monomer	Polymer	R ^a	β-carbon ^b / ppm
DPA ^c	PDPA	$\begin{array}{c} -N-CH_3 \\ \backslash -CH_3 \end{array}$	108
DBA ^d	PDBA	$\begin{array}{c} -CH_2-N-CH_3 \\ \backslash -CH_3 \end{array}$	110
ISBA ^e	PISBA	$\begin{array}{c} -CH_2-N-CH(CH_3)_2 \\ \backslash -Si(CH_3)_3 \end{array}$	110
SPA ^f	PSPA	$\begin{array}{c} -N-Si(CH_3)_3 \\ \backslash -Si(CH_3)_3 \end{array}$	110
St	PSt	-H	112

^a A *p*-substituent group of the styrene derivatives.

^b A carbon of CH₂ in CH₂ = CH-Phenyl-R, where R is a *p*-substituent group.

^c *N,N*-dimethyl-4-vinylphenylamine.

^d *N,N*-dimethyl-4-vinylbenzylamine.

^e *N*-isopropyl-*N*-trimethylsilyl-4-vinylbenzylamine.

^f *N,N*-bis(trimethylsilyl)phenylamine.

Table 10

Anionic polymerization of *N, N*-bis(trimethylsilyl)phenylamine, SPA and ISBA by *n*-BuLi in THF at -78°C

Monomer		Initi m mol	Solv ml	Polym time h	Conv %	Polymer with a protecting group			Polymer without a protecting group			
Name	m mol					$10^{-4}M_n$		M_w/M_n^c	Name	$10^{-4}M_n$	M_w/M_n^c	
SPA ^a	16	0.18	40	1	100	PSPA	2.3	2.4	1.0 ₄	PPA	1.1	1.0 ₅
ISBA ^a	17	0.066	57	24	100	PISBA	6.4	6.0	1.0 ₅	PIBA	4.9	1.0 ₅

^a SPA and ISBA were polymerized to yield PSPA and PISBA, respectively. Two trimethylsilyl groups of PSPA and a trimethylsilyl group of PISBA were deprotected to produce PPA and PIBA, respectively.

^b Calculated from the amounts of monomer and initiator.

^c Determined from GPC measurement.

Table 11

Contact angles of the films for a drop of water

Sample	Contact angle
PSt ^a	91
PPA	83
PPA- <i>g</i> -(Gly-Boc)	78
PPA- <i>g</i> -(Pro-Gly-Leu-Pro-Gly-Z)	73 ^b

^a PSt was measured as a reference.

^b After 10 minutes, the contact angle attained a constant value of 36 degrees.

Table 12

Anionic polymerization of (4-vinylphenyl)dimethylvinylsilane, VS with various initiators

Solvent	Initiator		Monomer	Polym time	$10^{-4}M_k^a$	Conv
	Name	m mol l ⁻¹	mol l ⁻¹	h		%
THF	<i>n</i> -BuLi	1.6 ₃	0.43 ₅	3.0	3.0 ₁	60
THF	Cumyl K	1.9 ₆	0.31 ₅	3.0	3.0 ₂	100
THF	Cumyl Cs	2.0 ₄	0.43 ₅	3.0	4.0 ₁	100

^a Calculated from the amounts of monomer and initiator.

Table 13

Anionic polymerization of VS in various solvents

Solvent	Initiator		Monomer	Polym time	$10^{-4}M_k^a$	$10^{-4}M_n^b$	Conv	M_w/M_n^c
	Name	m mol l ⁻¹	mol l ⁻¹	h			%	
Ether ^d	Cumyl K	5.0 ₅	0.23 ₁	2.0	0.86 ₀		Trace	
Me-THF ^e	Cumyl Cs	1.8 ₅	0.42 ₀	2.0	4.2 ₇	4.3 ₉	30	1.0 ₇
THF	Cumyl Cs	0.86 ₂	0.21 ₀	1.0	4.5 ₈		90	
1, 3-DX ^f	Cumyl Cs	1.1 ₈	0.25 ₃	0.5	4.0 ₃		100	
Ether/1, 3-DX= 1 / 2 ^g	Cumyl Cs	0.51 ₆	0.11 ₀	0.5	4.0 ₁		100	1.0 ₄

^a Calculated from the amounts of monomer and initiator.^b Determined by membrane osmometry.^c Determined from GPC measurement.^d Diethyl ether.^e 2-methyltetrahydrofuran.^f 4, 4-dimethyl-1, 3-dioxane.^g A 1:2 mixture of Ether/1, 3-DX (a volume fraction).

Table 14

Anionic polymerization of VS in a mixture of Ether/1, 3-DX for various polymerization times

Solvent	Initiator		Monomer	Polym time	$10^{-4}M_k^a$	Conv	M_w/M_n^b
	Name	m mol l ⁻¹	mol l ⁻¹	h		%	
Ether/1, 3-DX = 1 / 2 ^c	Cumyl Cs	0.23 ₂	0.12 ₉	0.5	10. ₅	100	1.0 ₃
Ether/1, 3-DX = 1 / 2 ^c	Cumyl Cs	0.53 ₅	0.11 ₀	1.0	3.8 ₇	100	1.0 ₇
Ether/1, 3-DX = 1 / 2 ^c	Cumyl Cs	0.55 ₉	0.10 ₈	2.0	3.6 ₃	100	1.1 ₁
Ether/1, 3-DX = 1 / 1 ^d	Cumyl Cs	0.29 ₂	0.09 ₈	0.5	6.3 ₁	100	1.0 ₄
Ether/1, 3-DX = 1 / 1 ^d	Cumyl Cs	0.72 ₆	0.11 ₄	1.0	2.9 ₅	100	1.0 ₅
Ether/1, 3-DX = 1 / 1 ^d	Cumyl Cs	0.67 ₆	0.12 ₈	2.0	3.5 ₆	100	1.0 ₉

^a Calculated from the amounts of monomer and initiator.

^b Determined from GPC measurement.

^c A 1:2 mixture of diethyl ether/4, 4-dimethyl-1, 3-dioxane (a volume fraction).

^d A 1:1 mixture of diethyl ether/4, 4-dimethyl-1, 3-dioxane (a volume fraction).

Table 15

Molecular characteristics of poly[(4-vinylphenyl)dimethylvinylsilane], PVS prepared under an optimum condition^a

Sample	Monomer g	Initiator m mol	$10^{-4}M_k^b$	Conv %	$10^{-4}M_n^c$	M_w/M_n^d
PVS-1	9.5 ₃	0.39 ₂	2.4 ₃	100	2.5 ₀	1.0 ₅
PVS-2	8.9 ₉	0.20 ₆	4.3 ₆	100	4.5 ₉	1.0 ₈
PVS-3	8.3 ₇	0.18 ₁	4.6 ₂	100	4.8 ₁	1.0 ₈
PVS-4	7.4 ₅	0.057 ₈	12. ₉	100	13. ₆	1.0 ₃

^a Anionic polymerization using Cumyl Cs as an initiator in a 1:2 mixture of Ether/1, 3-DX as a solvent for 30 min at -78°C .^b Calculated from the amounts of monomer and initiator.^c Determined by membrane osmometry.^d Determined from GPC measurement.

Table 16

Lithographic characteristics of PVS thin films spin-coated onto silicon wafers

Sample	$10^{-4}M_n^a$	Light	Sensitivity ^b	Contrast ^b
			$D_g^{0.5}$	γ
PVS-1	2.5 ₀	UV light ^c		
PVS-4	13.6	Deep UV light	19 mJ/cm ²	3.8
PVS-1	2.5 ₀	Electron beam	7.0 x 10 ⁻⁶ C/cm ²	2.8
PVS-4	13.6	Electron beam	2.1 x 10 ⁻⁶ C/cm ²	3.6

^a Determined by membrane osmometry.

^b Symbols for $D_g^{0.5}$ and γ are explained in Eq. (12).

^c No gel was observed in the exposed area.

Table 17

Preparation^a of [poly((4-vinylphenyl)dimethylvinylsilane)-*graft*-polyisoprene]-*block*-polystyrene, (PVS-*g*-PIs)-*b*-PSt block-*graft* copolymers by a “grafting onto” process

Sample code	Backbone ^b				Graft				A backbone coupling	
	Code	g	Solvent	ml	Code	g	Solvent	ml	[PIs] / [VS] ^f	Temp °C
SGI-1	B-1	1.5 ₀	THF	55	G-1 ^c	12.5	THF	250	4.4	-78
SGI-2	B-1	0.98	Bz	40	G-2 ^d	7.3	Bz	125	4.6	40
SGI-3	B-1	1.1 ₂	Bz	45	G-3 ^e	3.9	Bz	80	7.9	40

^a A backbone coupling (a ‘grafting onto’ process) was carried out for 24 h under 10⁻⁶ mmHg.

^b VS (1.0 g) and St (32.4 g) were sequentially polymerized by Cumyl Cs in THF (580 ml) for 20 min and 1 h, respectively at -78°C; the M_k value of 22.9 x 10⁴, the M_n value of 23.9 x 10⁴ by osmometry and the M_w/M_n value of 1.0₆ from GPC measurement.

^c Is (12.7 g) was polymerized by Cumyl Cs in THF (250 ml) for 8 h at -78°C; the M_k value of 2.1₁ x 10⁴, the M_n value of 2.1 x 10⁴ and the M_w/M_n value of 1.0₅

^d Is (21.5 g) was polymerized by *sec*-BuLi in Bz (370 ml) for 8 h at room temperature; the M_k value of 1.7₆ x 10⁴, the M_n value of 1.8 x 10⁴ and the M_w/M_n value of 1.0₆.

^e Is (11.5 g) was polymerized by *sec*-BuLi in Bz (240 ml) for 8 h at room temperature; the M_k value of 0.31₉ x 10⁴, the M_n value of 0.32 x 10⁴ and the M_w/M_n value of 1.1₀.

^f A molar ratio of living polyisoprene (graft chains) to VS unit (number of possible chemical links).

Table 18

Molecular characteristics of three (PVS-*g*-PIs)-*b*-PSt block-graft copolymers

Sample code	Backbone			Graft			Block-graft copolymer				
	$10^{-4}M_n$		DP ^{VS} ^a	$10^{-4}M_n$	N^{graft}	$N^{\text{graft}}/\text{DP}^{\text{VS}}$ ^b	$10^{-4}M_n^{\text{block-graft}}$ ^c		wt%		
	PVS	PSt		PIs			NMR	OSM	VS	St	Is
SGL-1	0.72	23. ₂	38. ₃	2.1	10. ₀	0.26 ₁	44. ₇	45. ₀	1.6	51. ₆	46. ₈
SGL-2	0.72	23. ₂	38. ₃	1.8	10. ₉	0.28 ₄	44. ₂	43. ₅	1.7	53. ₃	45. ₀
SGL-3	0.72	23. ₂	38. ₃	0.32	12. ₅	0.32 ₆	28. ₀	27. ₉	2.6	83. ₂	14. ₂

^a A degree of polymerization of a VS block in PVS-*b*-PSt used as a backbone.

^b A ratio of N^{graft} to DP^{VS}.

^c Number average molecular weights of $M_n^{\text{block-graft}}_{\text{NMR}}$ determined by NMR measurement, and $M_n^{\text{block-graft}}_{\text{OSM}}$ determined by membrane osmometry.

Table 19

Preparation and characterization of two block copolymers of poly(*p-tert*-butoxystyrene)-*block*-polybutadiene, PBSt-*b*-PBu and polystyrene-*block*-poly(*p-tert*-butoxystyrene), PSt-*b*-PBSt

Initiator		Solvent	First monomer		Second monomer		Temp °C	Block copolymer			
Name	m mol		Name	g	Name	g		Conv/%	$10^{-4}M_k$	$10^{-4}M_n^a$	M_w/M_n^a
<i>n</i> -BuLi	0.11 ₀	THF	BSt	6.8	Bu	2.0	-78	100	8.1	7.3	1.0 ₆
<i>n</i> -BuLi	0.11 ₂	THF	St	3.8	BSt	6.8	-78	100	9.5	8.9	1.0 ₄

^a Determined from GPC measurement.

Table 20

Preparation and characterization of polystyrene-*block*-poly(*p*-*tert*-butoxystyrene)-*block*-polystyrene, PSt-*b*-PBSt-*b*-PSt block copolymer as a backbone

Initiator		Solvent	Monomer / g			Temp °C	Time / min			10 ⁻⁴ M _k ^a				10 ⁻⁴ M _n ^b	M _w /M _n ^c
Name	m mol		St	BSt	St		St	BSt	St	St	BSt	St	Total		
<i>n</i> -BuLi	0.19 ₀	THF	16.2	1.2 ₈	16.2	-78	15	15	15	8.5 ₆	0.69	8.5 ₆	17.8	17.7	1.0 ₈

^a Calculated from the amounts of monomer and initiator.^b Determined by membrane osmometry.^c Determined from GPC measurement.

Table 21

Preparation of polystyrene-*block*-[poly(*p*-hydroxystyrene)-*graft*-poly(ethylene oxide)]-*block*-polystyrene, PSt-*b*-(PHSt-*g*-PEO)-*b*-PSt block-graft copolymers by a “grafting from” process

Backbone		Initiator			Solvent		Grafts	Metallation		Grafting	
Polymer	g	Name	m mol	[I]/[HSt] ^a	Name	ml	EO g	Temp °C	Time h	Temp °C	Time h
SGE-1	1.6 ₅	DPE-K	2.1 ₆	5.7	THF	250	7.6 ₀	60	1	40	60
SGE-2	0.70	Cumyl K	0.48 ₃	3.0	THF	110	3.0 ₄	60	1	40	60

^a A molar ratio of initiator to the hydroxyl group in the PHSt block.

Table 22

Molecular characteristics of two PSt-*b*-(PHSt-*g*-PEO)-*b*-PSt block-graft copolymers

Polymer	Backbone	Block-graft copolymer			Graft		Metallation		Number of grafts		
	$10^{-4}M_n^{\text{block}}$	$10^{-4}M_k^{\text{block-graft}}$	$10^{-4}M_n^{\text{block-graft}}$			$10^{-4}M_k^{\text{graft}}$	$10^{-4}M_n^{\text{PEO}}_{\text{VPO}}$	f_{metal}	N_k^{graft}	OSM	Ini
	Obs ^a	Eq. (24) ^b	CONV Eq. (25) ^b	OSM Obs ^a	NMR Eq. (26) ^b	Eq. (27) ^b	Obs ^a	Eq. (28) ^b	Obs ^a	Eq. (29) ^b	Eq. (30) ^b
SGE-1	17.5	31.8	25.2	24.5	25.0	0.35		0.49 ₆	41.5	20.6	21.1
SGE-2	17.5	42.5	26.5	24.6	25.0	0.63	0.60	0.28 ₄	41.5	11.8	11.2

^a Obs implies that the molecular weight (M_n) and number of grafts (N^{graft}) can be determined experimentally without special assumption.

^b Each of M_n and N^{graft} can be calculated from the corresponding equations defined in this review.

Table 23

Compositions and domain sizes of two PSt-*b*-(PHSt-*g*-PEO)-*b*-PSt block-graft copolymers cast from the respective benzene solutions

Polymer	Composition / wt %			Domain size / nm			
				Backbone (PSt)		Graft (PEO)	
	St	HSt	EO	Calc ^a	Obs ^b	Calc ^a	Obs ^b
SGE-1	69.9	1.5	28.6	19.6	17 – 20	6.1	10 – 13
SGE-2	69.6	1.5	28.9	19.6	19 – 21	8.1	15 – 20

^a Calc means an unperturbed root-mean-square of the end-to-end distance, $\langle R^2 \rangle_0^{1/2} = bn^{1/2}$ of the corresponding polymer chains. The n is a degree of polymerization of a PEO chain or a PSt chain in PSt-*b*-(PHSt-*g*-PEO)-*b*-PSt, as described in Table 22. The b is a Kuhn's segment length.

^b Obs could be determined from the transmission electron micrographs.

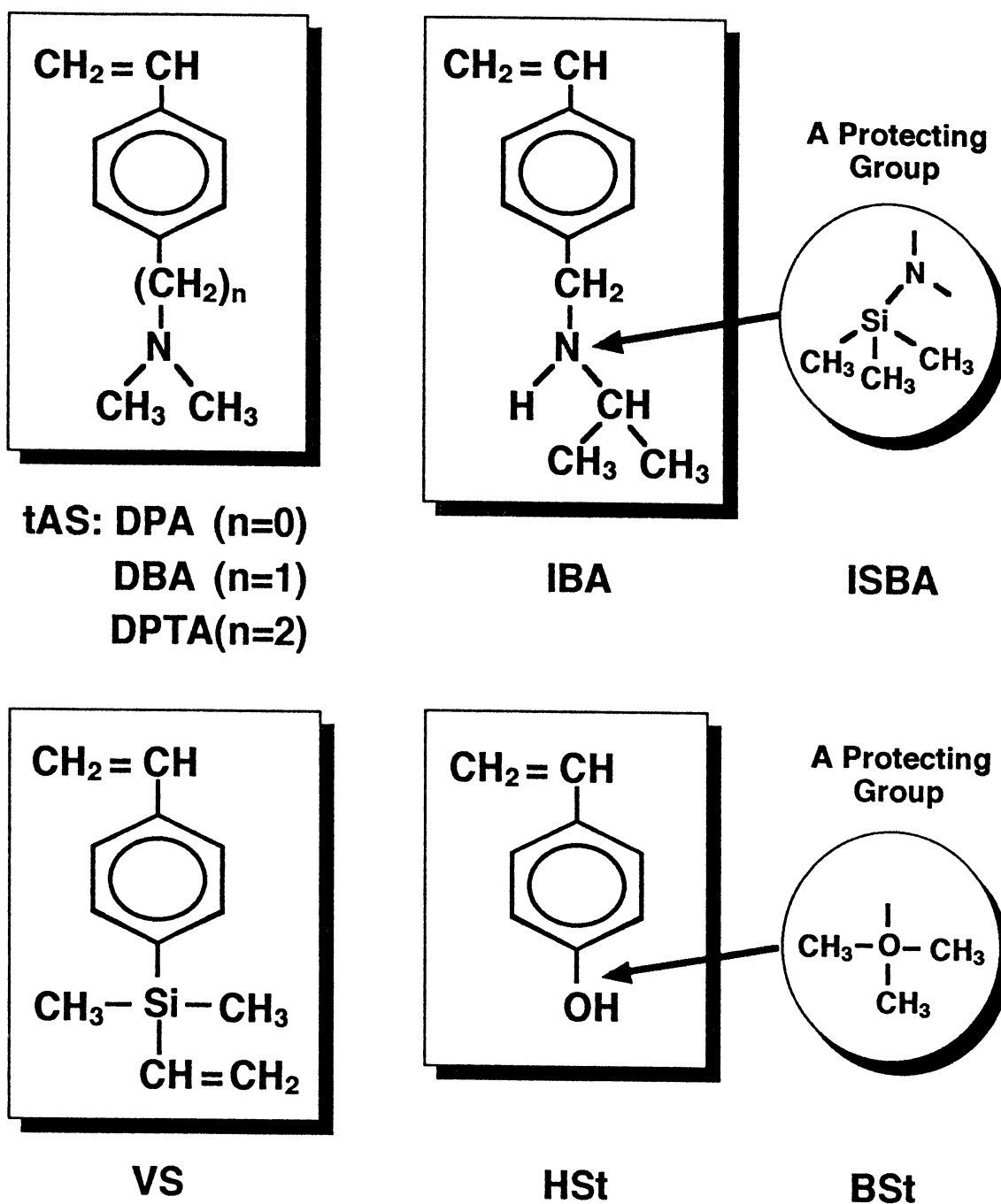


Fig. 1. Molecular structures of four useful monomers: tertiary aminostyrenes (tAS), *N*-isopropyl-*N*-trimethylsilyl-4-vinylbenzylamine (IBA), (4-vinylphenyl)dimethylvinylsilane (VS), and *p*-butoxystyrene (BSt).

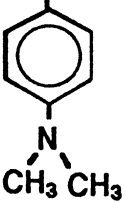
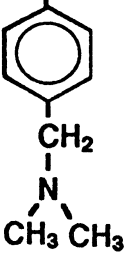
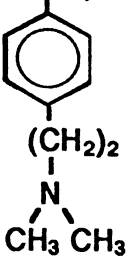
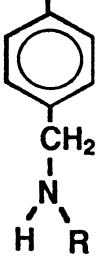
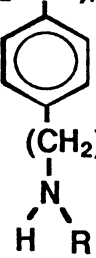
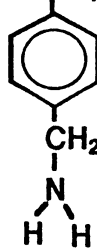
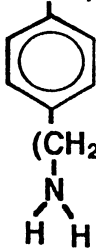
	Phenyl	Benzyl	Phenethyl
Tertiary	$-(\text{CH}_2-\text{CH})_n-$  PDPA	$-(\text{CH}_2-\text{CH})_n-$  PDPA	$-(\text{CH}_2-\text{CH})_n-$  PDPA
Secondary	$-(\text{CH}_2-\text{CH})_n-$  	$-(\text{CH}_2-\text{CH})_n-$  PIBA	$-(\text{CH}_2-\text{CH})_n-$ 
Primary	$-(\text{CH}_2-\text{CH})_n-$  PPA	$-(\text{CH}_2-\text{CH})_n-$  	$-(\text{CH}_2-\text{CH})_n-$ 

Fig. 2. Molecular structures of poly(aminostyrene)s which have amino groups classified as primary, secondary and tertiary groups (R is an alkyl group). Each of these three amino groups is also classified as phenylamine, benzylamine and phenethylamine.

PDPA

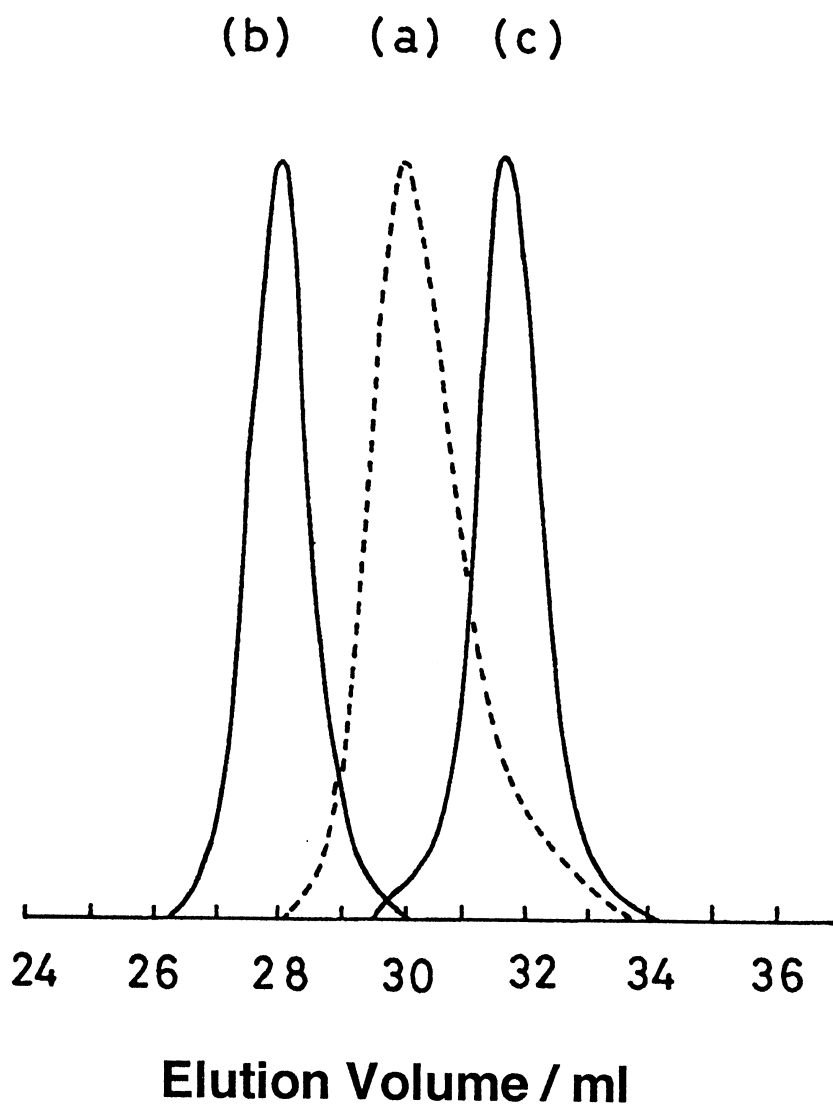


Fig. 3. GPC chromatograms of PDPA prepared by (a) a *n*-BuLi/THF system ($M_n = 8.4 \times 10^4$), (b) a Cumyl K/THF system ($M_n = 26 \times 10^4$), and (c) a Cumyl Cs/THF system ($M_n = 6.5 \times 10^4$). The carrier solvent is THF, the flow rate is 1.0 ml min^{-1} , the polymer concentration is 0.05 w/v%, and the RI detector is employed.

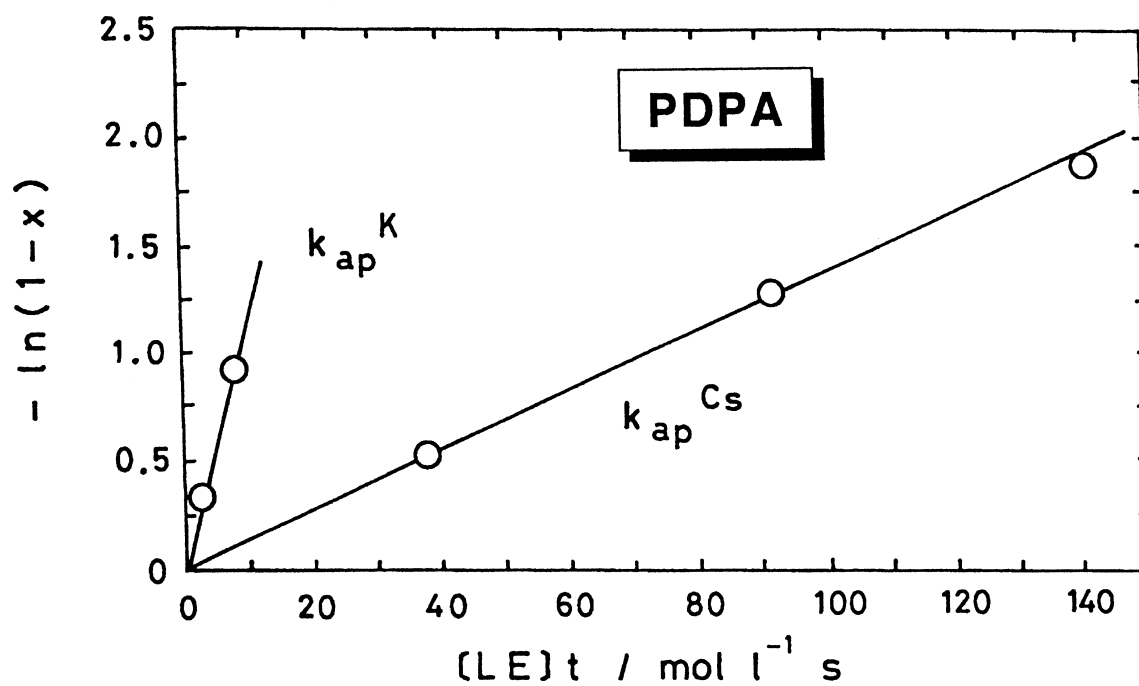


Fig. 4. Plots of $-\ln(1-x)$ versus $[LE]t$ for PDPA, prepared by using a Cumyl K/THF system and a Cumyl Cs/THF system in the lower polymer conversion side.

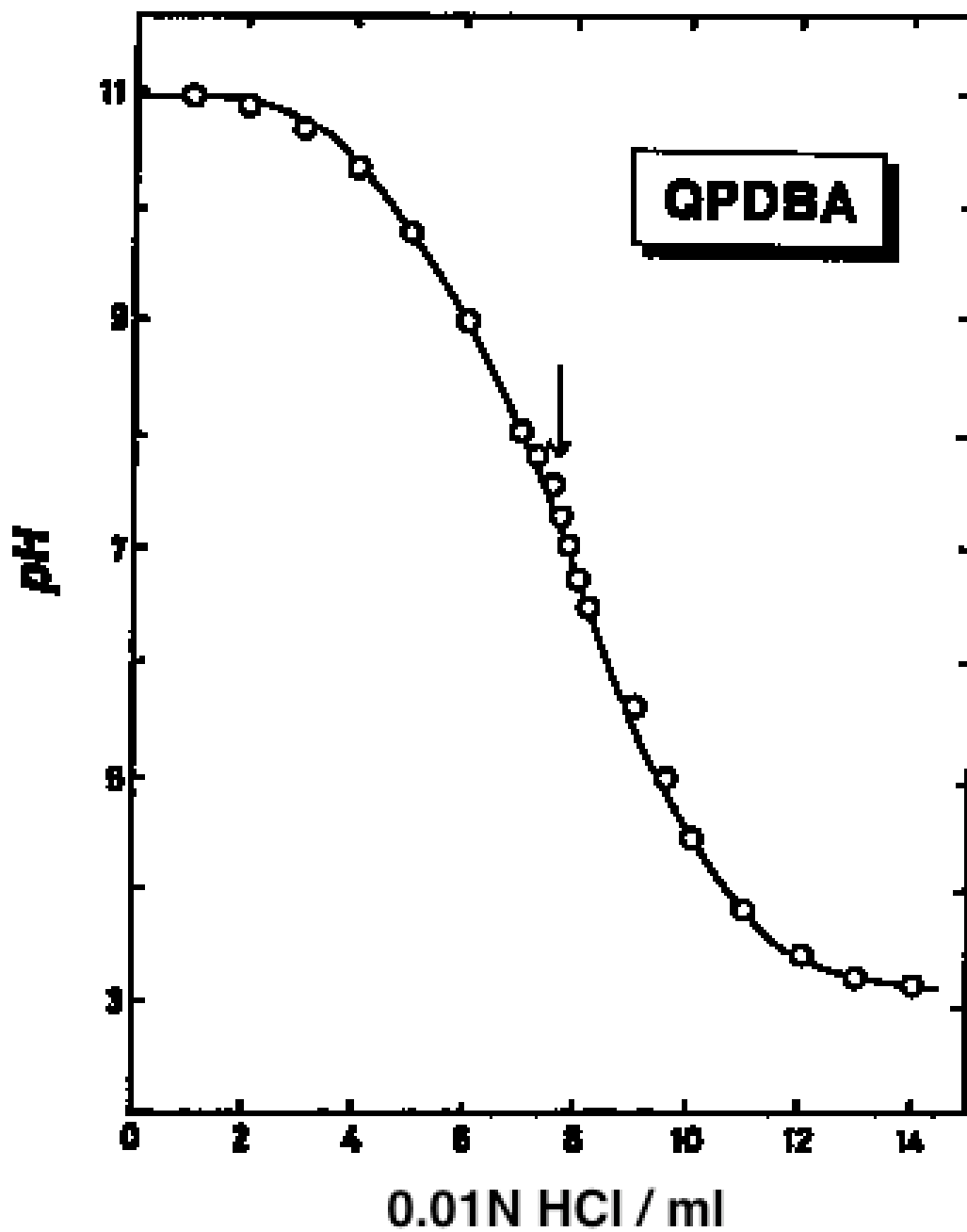


Fig. 5. A neutralization curve of QPDBA treated with an anion-exchange resin. A point of neutralization is $\text{pH} = 7.4$, which is indicated as an arrow in the figure.

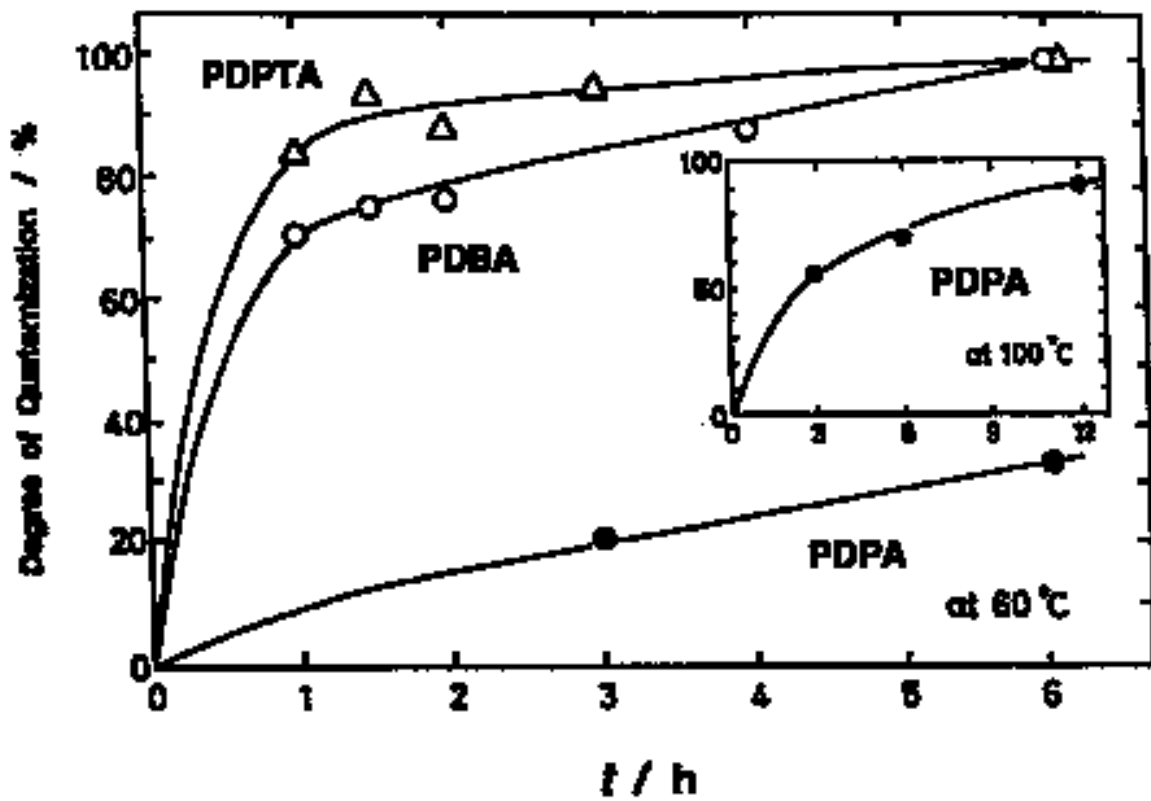


Fig. 6. Reaction time dependence of the degree of quaternization (DQ) of PDPA, PDBA, and PDPTA at 60°C. The inserted figure describes reaction time dependence of DQ of PDPA at 100°C.

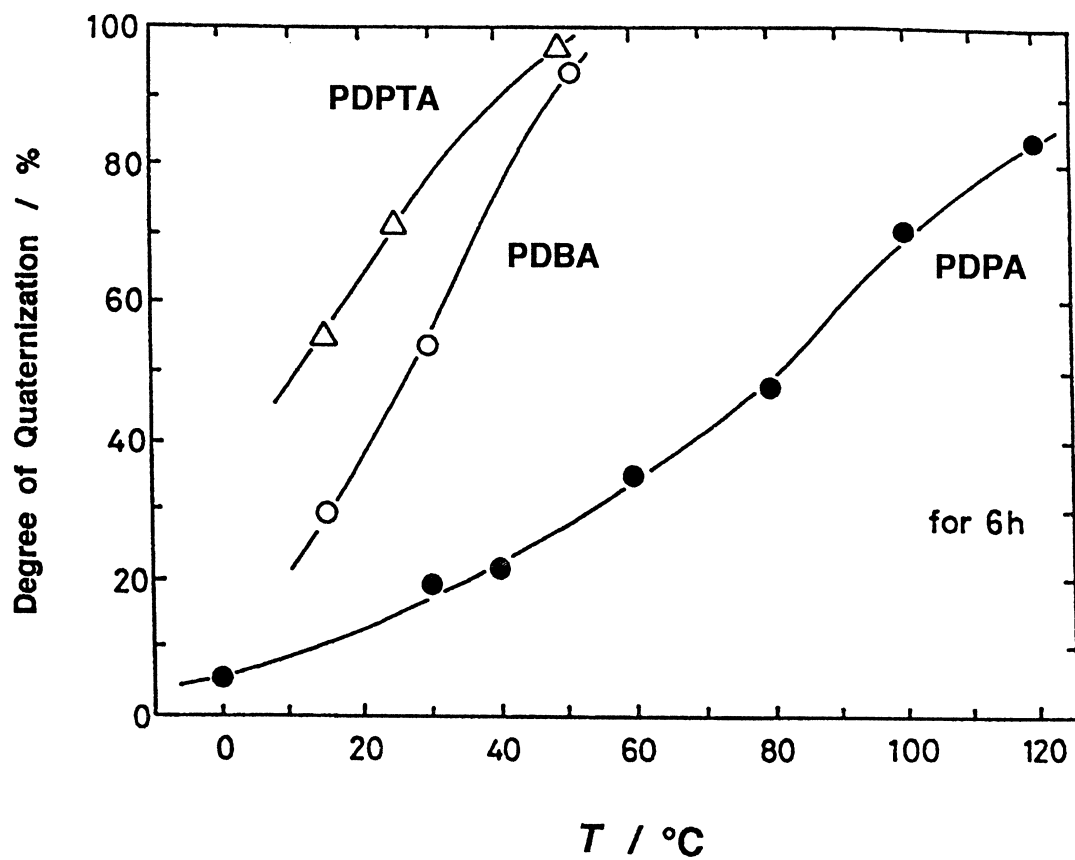


Fig. 7. Temperature dependence of the degree of quaternization of PDPA, PDDBA, and PDPTA for 6 h.

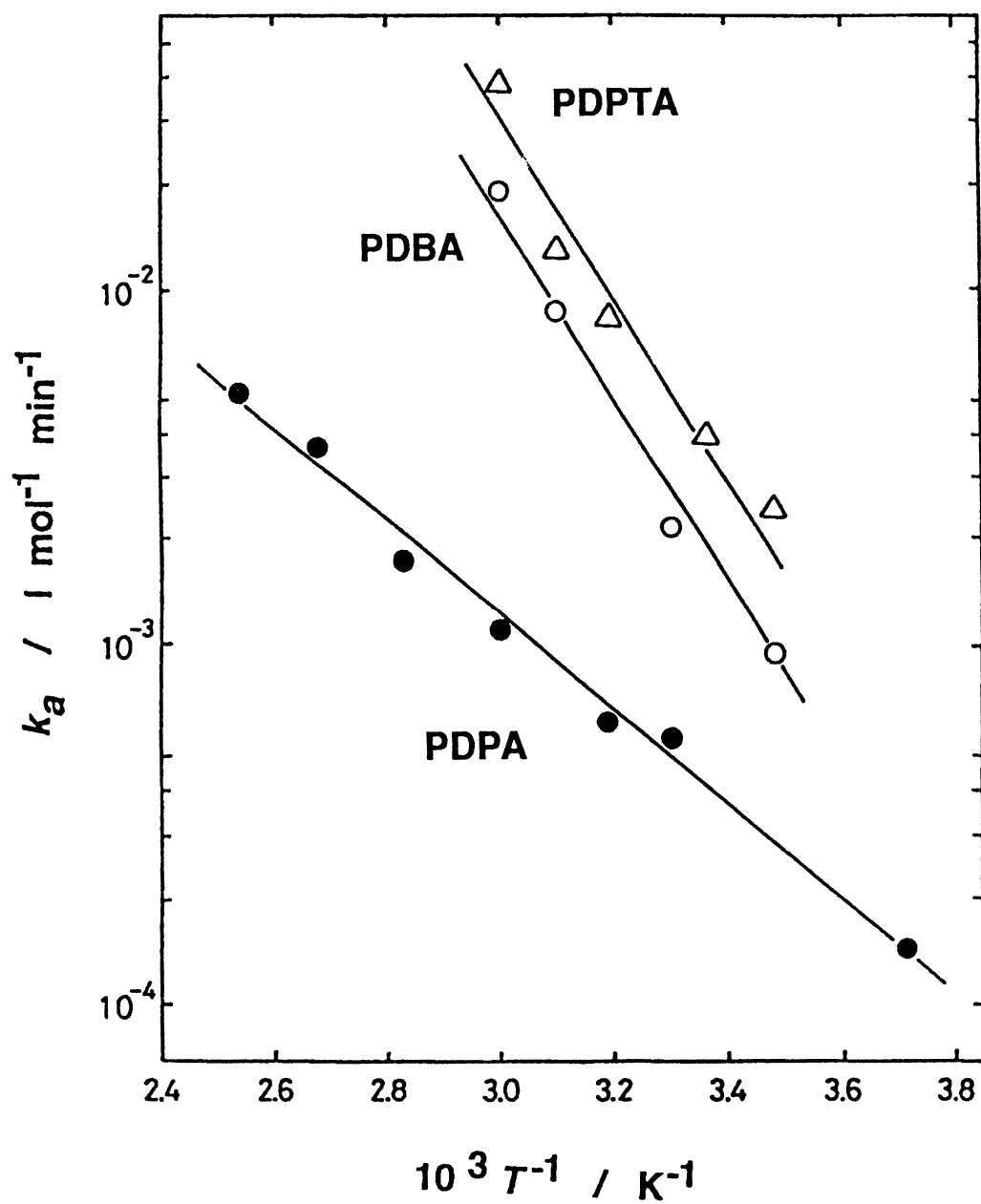


Fig. 8. Arrhenius' plots of apparent reaction rate constants, k_a , for quaternization of PDPA, PDBA, and PDPTA.

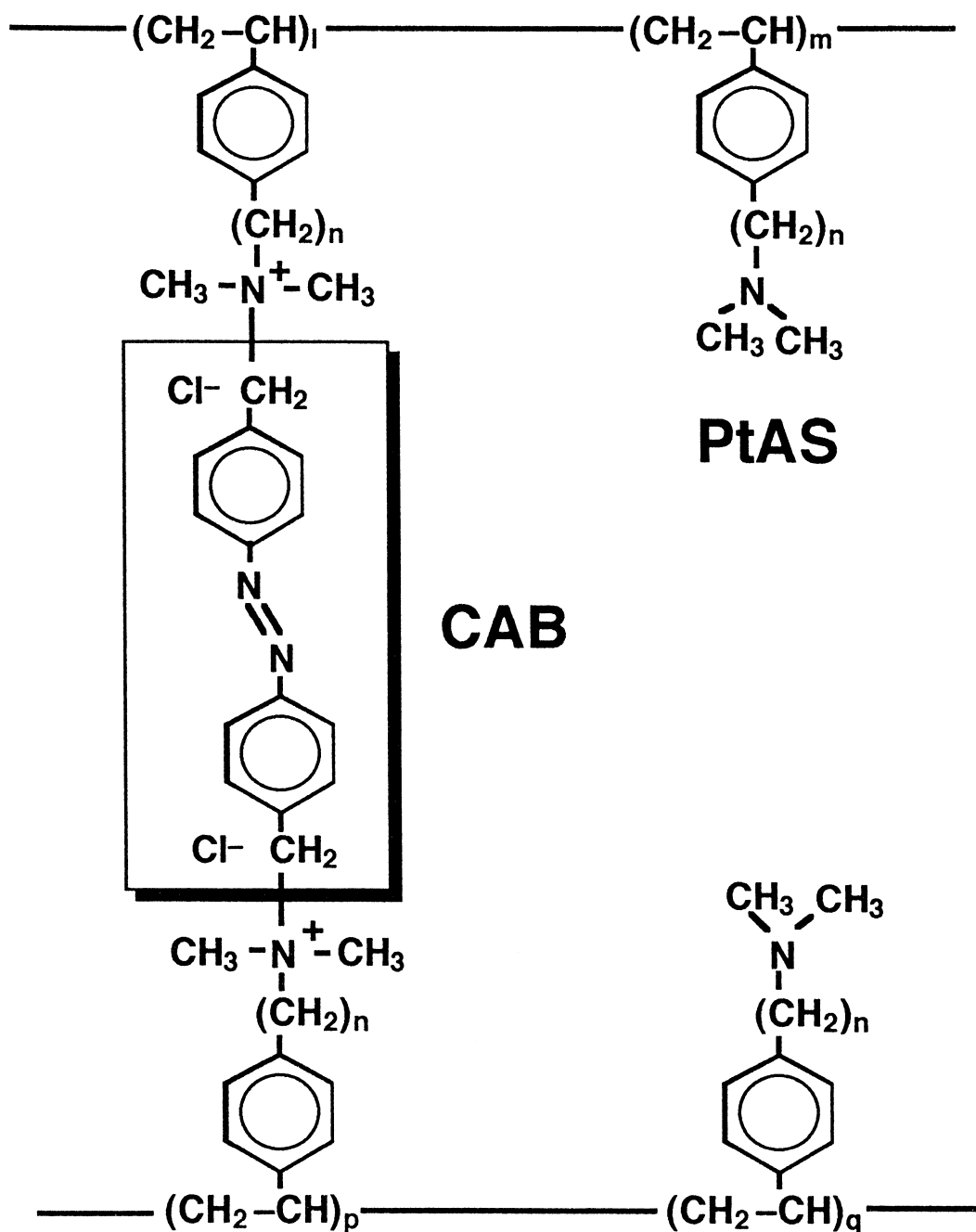


Fig. 9. A structural formula of the crosslinked film for poly(tertiary aminostyrene)s (PtAS) with *p,p'*-bis(chloromethyl)azobenzene (CAB).

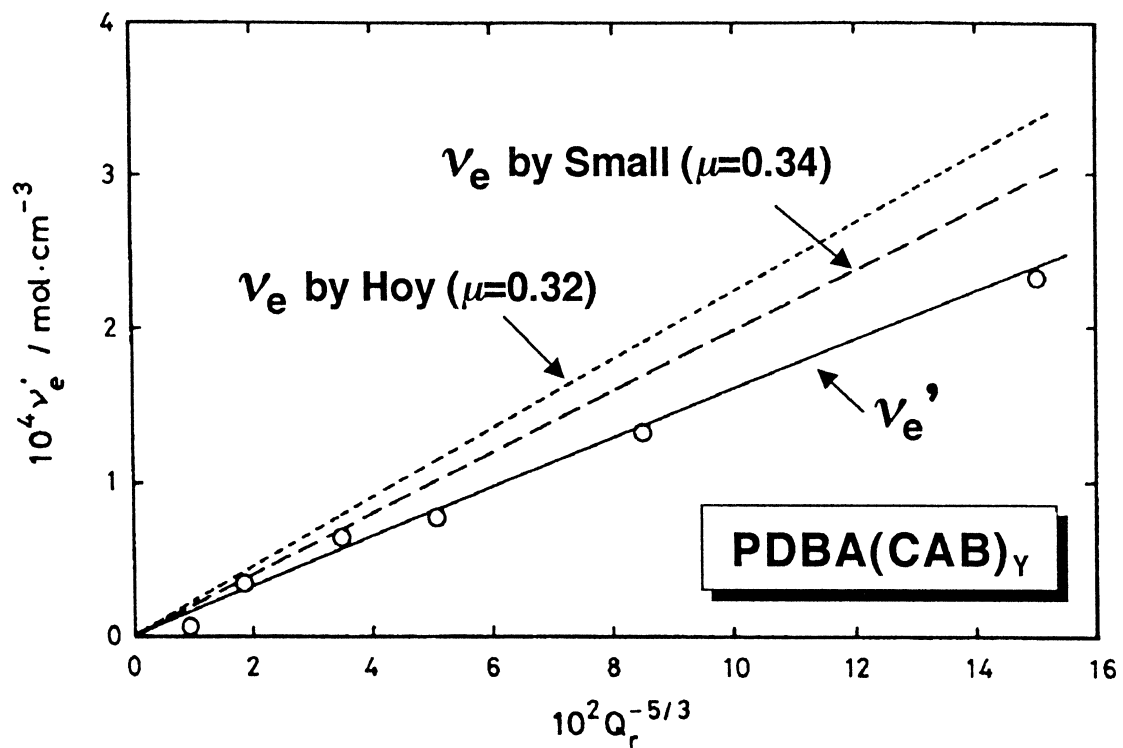


Fig. 10. A plot of an apparent effective network concentration (v_e') versus $Q_r^{-5/3}$ for PDBA(CAB)_Y films in THF at 25°C. An effective network concentration (v_e) calculated by Small's method ($\mu = 0.34$) (---) or by Hoy's method ($\mu = 0.32$) (- - - -) is also described.

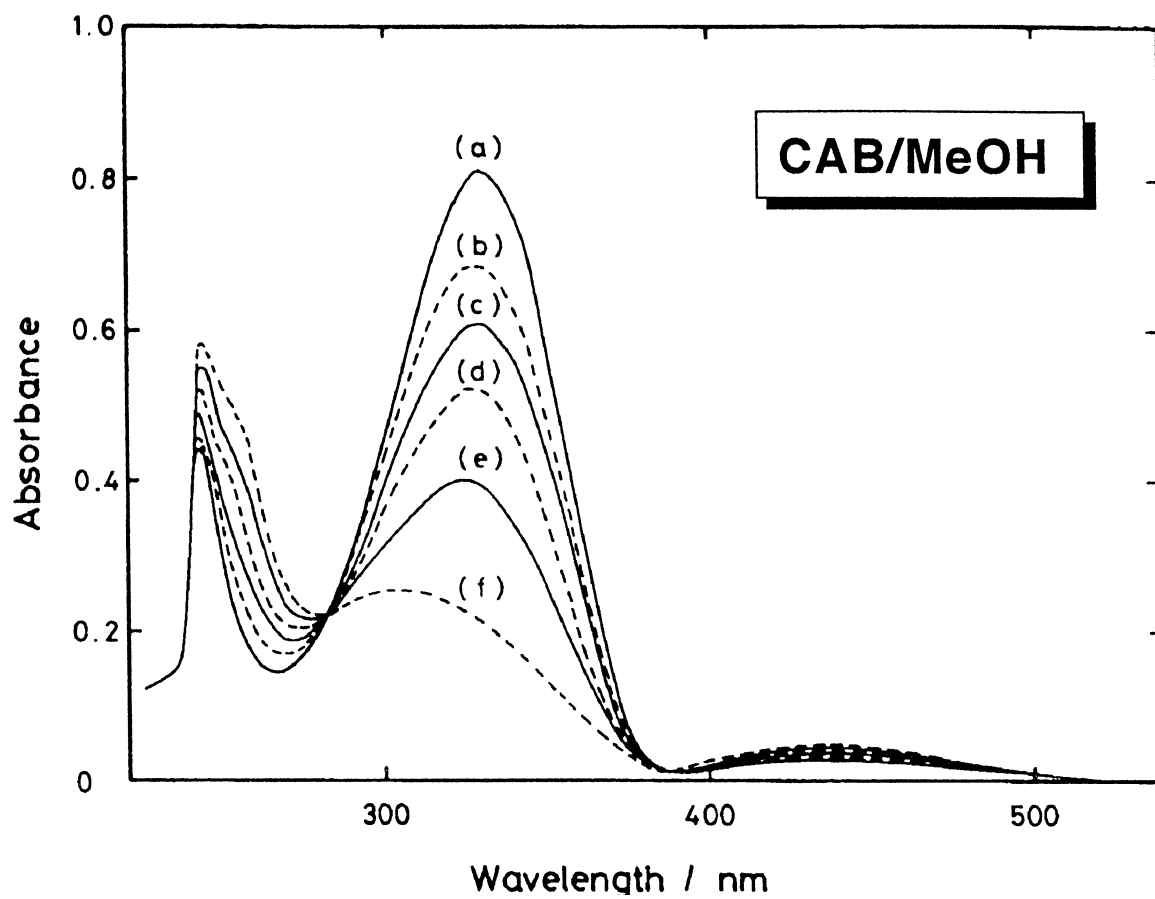


Fig. 11. Changes in the absorption spectra of CAB with UV (300–380 nm) irradiation time in methanol: (a) $t = 0$; (b) $t = 45$; (c) $t = 60$; (d) $t = 90$; (e) $t = 150$; (f) $t = 600$ s.

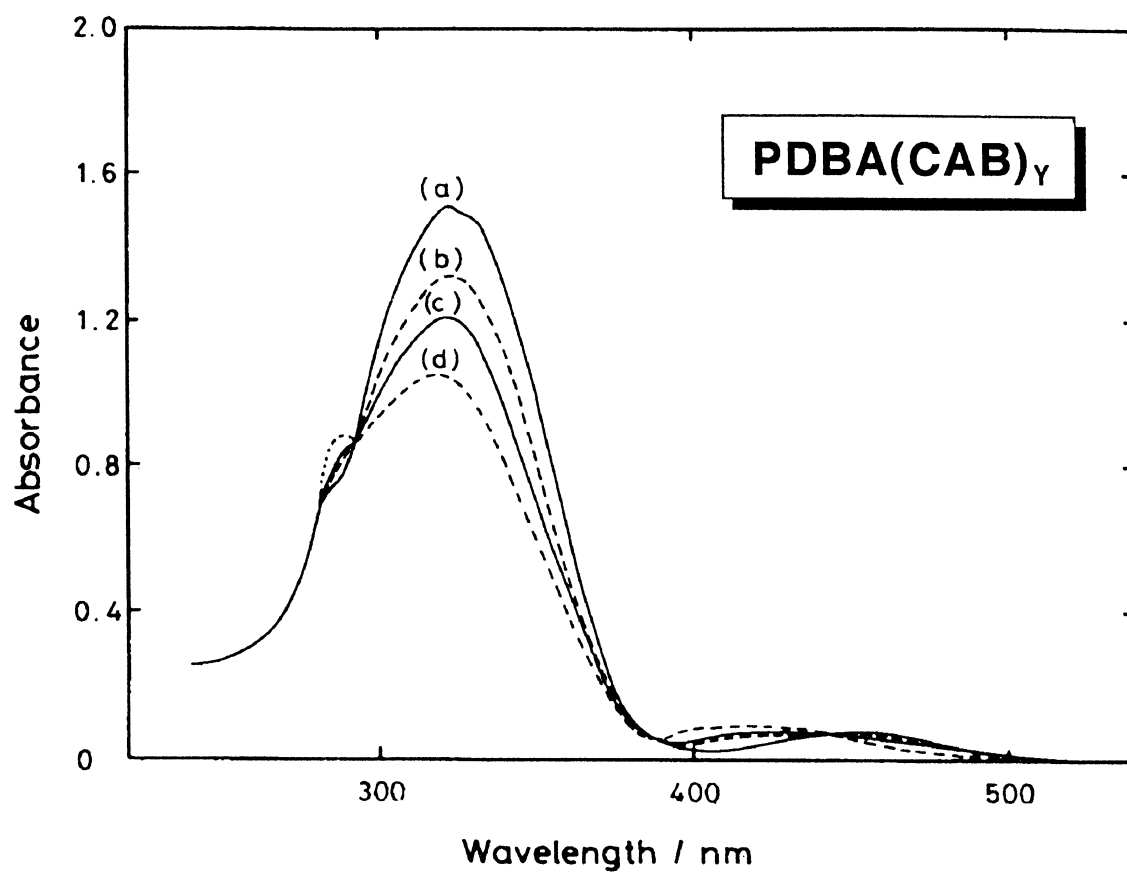


Fig. 12. Changes in the absorption spectra of CAB with UV (300–380 nm) irradiation time for a PDBA(CAB)₁₅ film: (a) $t = 0$; (b) $t = 2$; (c) $t = 6$; (d) $t = 30$ min.

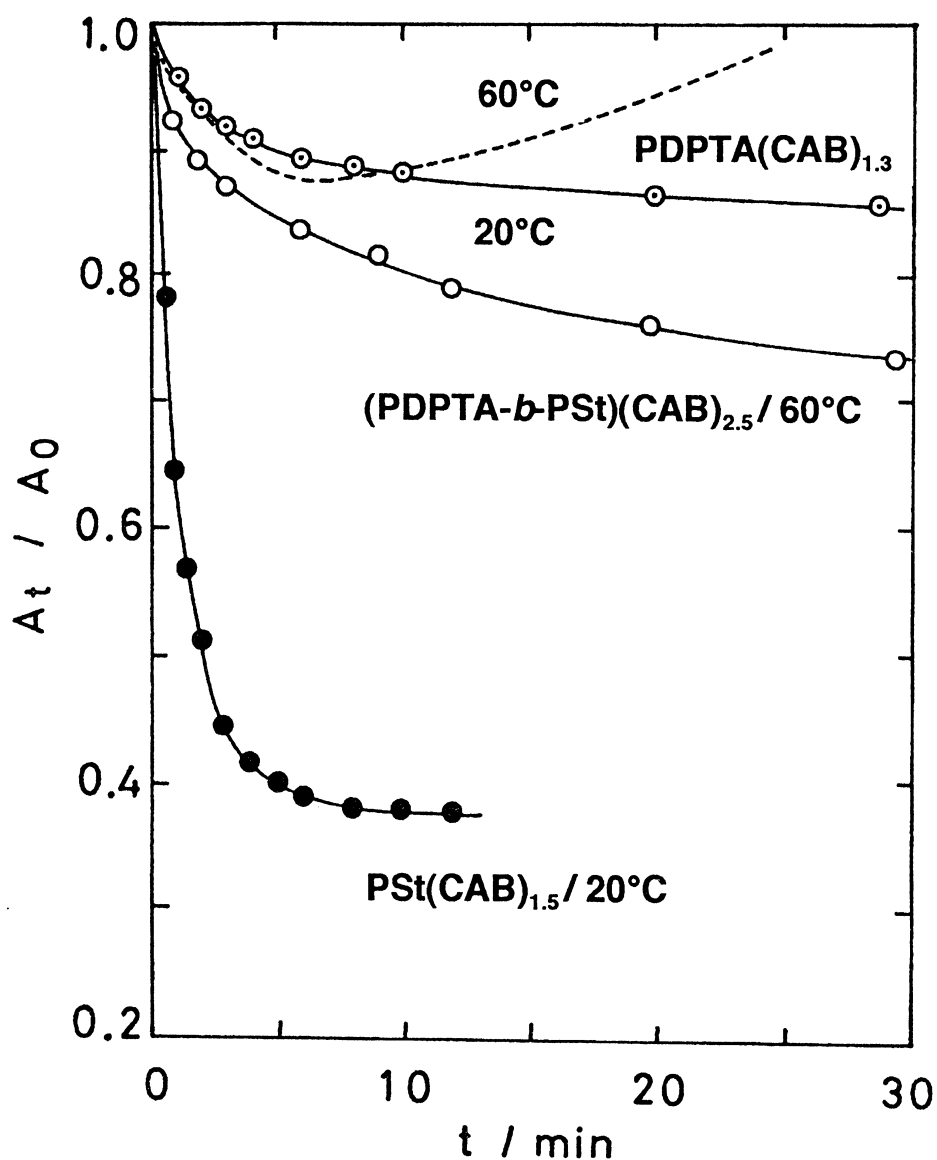


Fig. 13. Photochemical isomerization from *trans* to *cis* form of CAB at a fixed temperature in the following films: (PDPTA-*b*-PSt)(CAB)_{2.5} at 60°C (○), PDPTA(CAB)_{1.3} at 20°C (○), PDPTA(CAB)_{1.3} at 60°C (- - -) and PSt(CAB)_{1.5} at 20°C (●). Absorbance (A_t) was detected at 320 nm after irradiation with an ultraviolet light ($300 \text{ nm} < \lambda_1 < 380 \text{ nm}$) for time, t , which is plotted as an axis of the abscissa on the figure. The A_t/A_0 value represents a fraction of a *trans* form, which was not converted to a *cis* form of CAB.

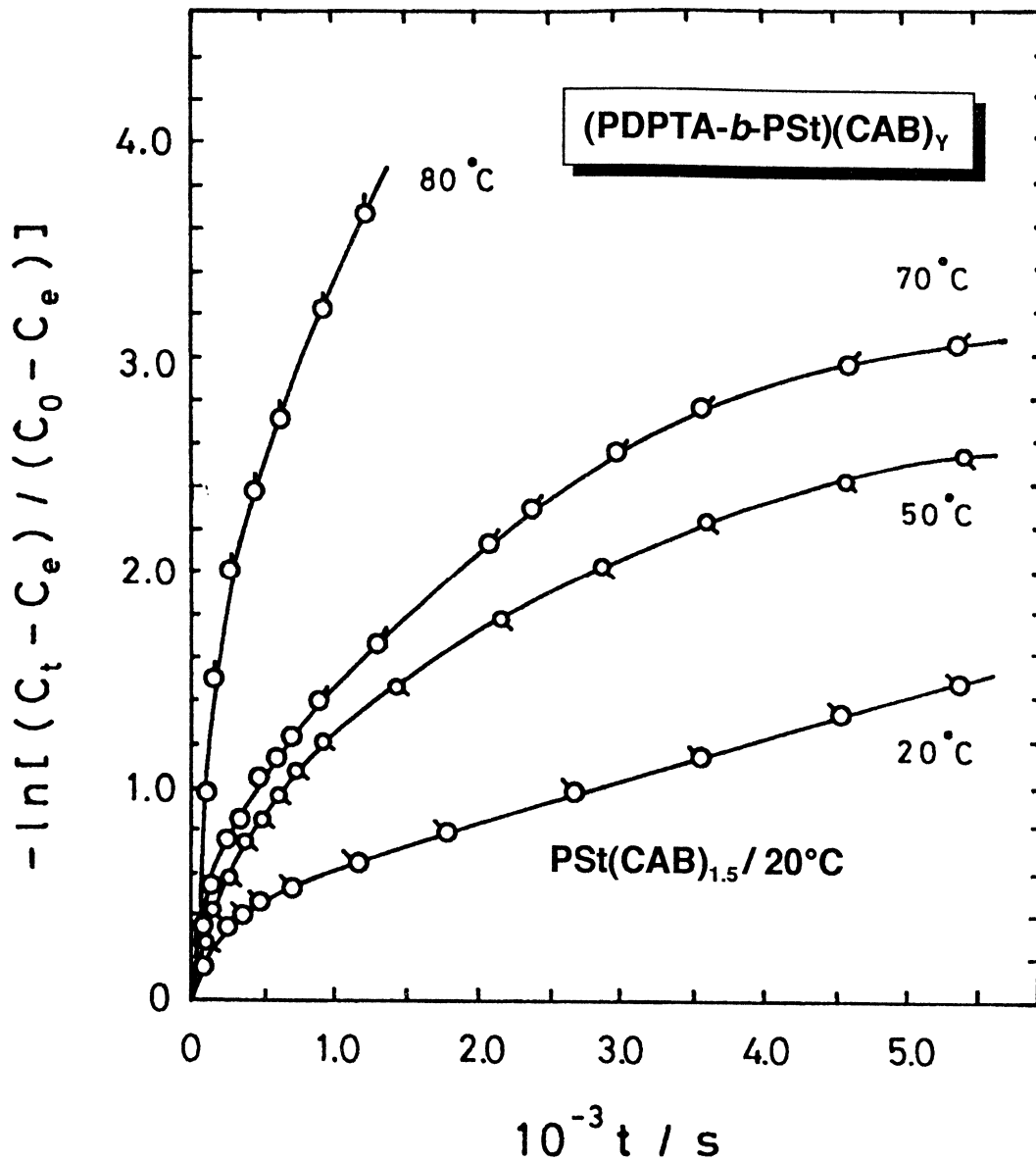


Fig. 14. Typical plots of $-\ln[(C_t - C_e)/(C_0 - C_e)]$ versus t for the photochemical isomerization from *trans* to *cis* form of CAB in the following films: PSt(CAB)_{1.5} at 20°C (○), (PDPTA-*b*-PSt)(CAB)_{2.86} at 50°C (○) and 70°C (○), and (PDPTA-*b*-St)(CAB)_{2.74} at 80°C (○).

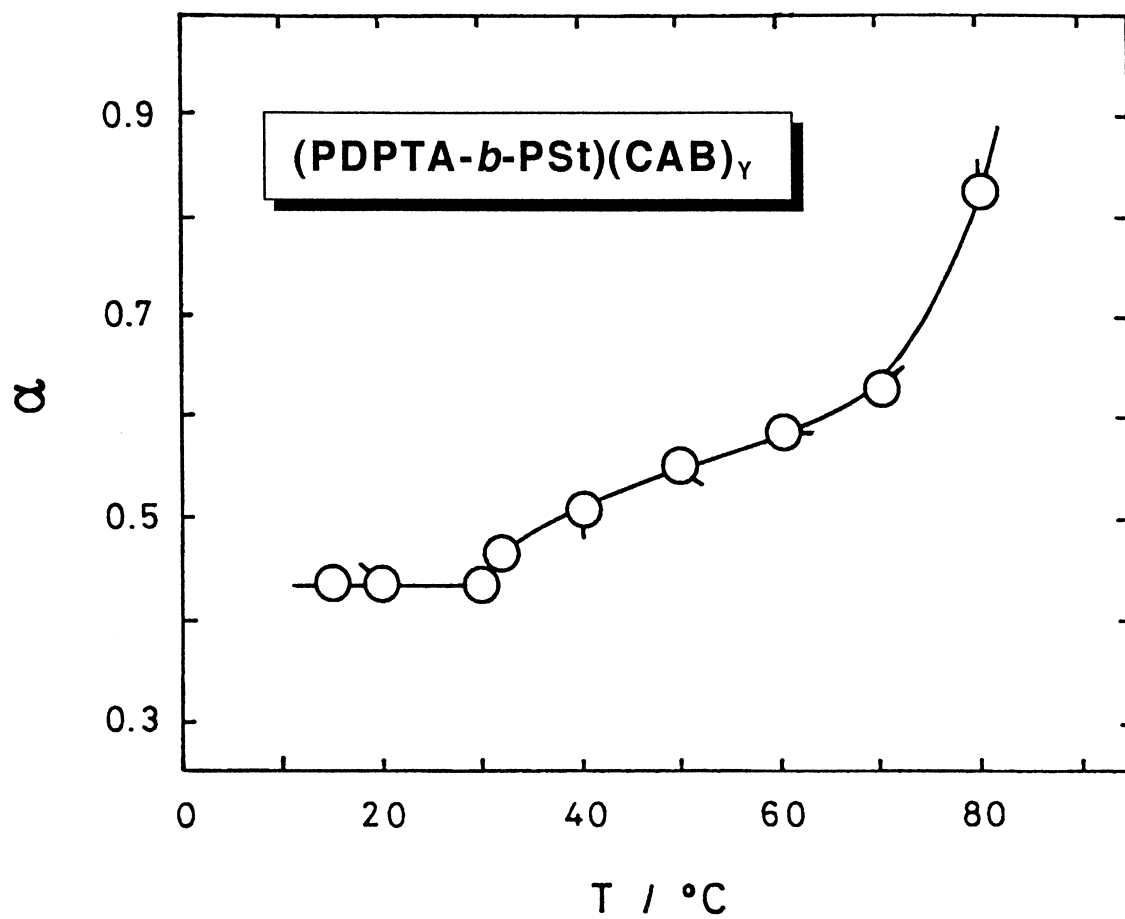


Fig. 15. A relationship between the parameter α and temperature, at which the photochemical isomerization from *trans* to *cis* form of CAB proceeded in the $(\text{PDPTA-}b\text{-PSt})(\text{CAB})_y$ films.

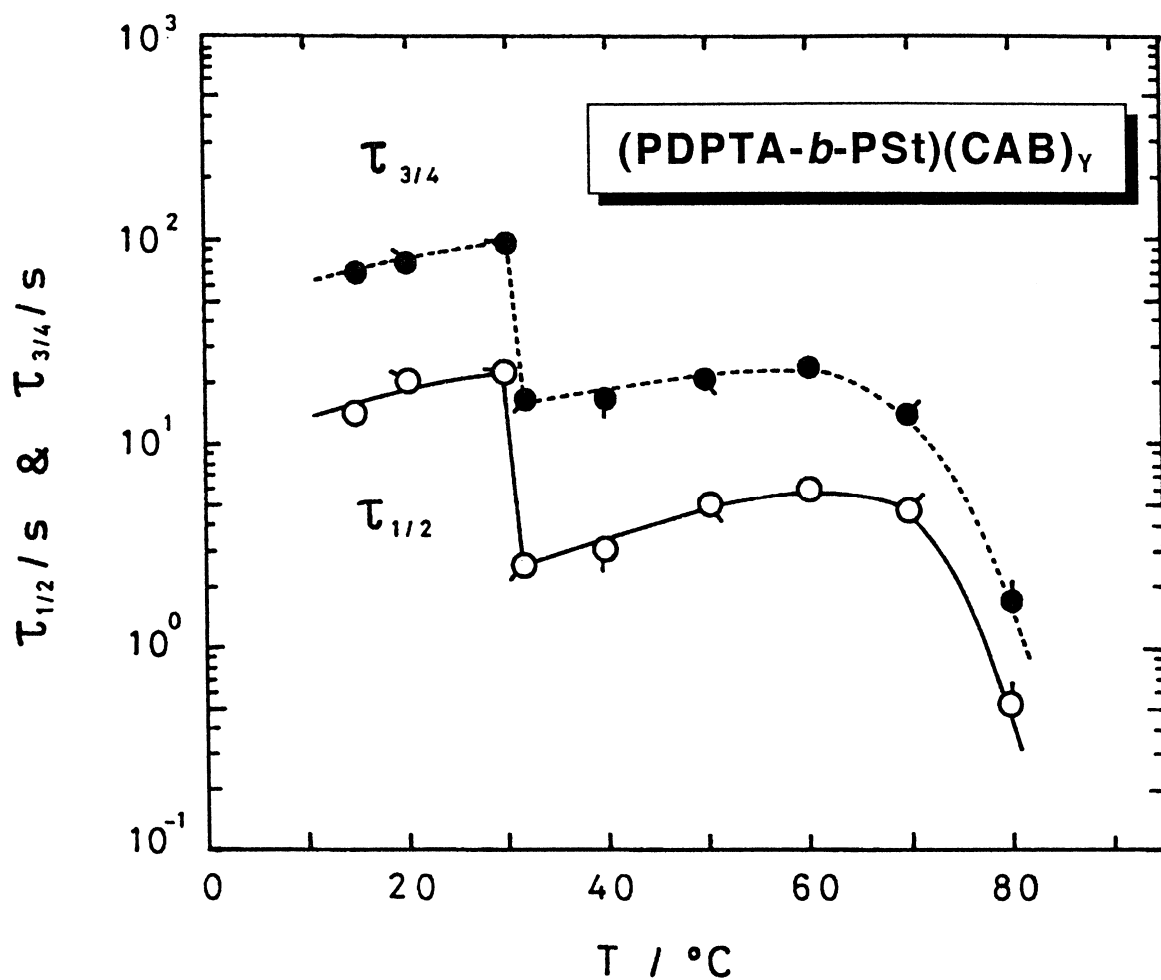


Fig. 16. Temperature dependence of the half-life period, $\tau_{1/2}$ (○), and a three fourths-life period, $\tau_{3/4}$ (●), for the photochemical isomerization from *trans* to *cis* form of CAB proceeded in the (PDPTA-*b*-PSt)(CAB)_γ films..

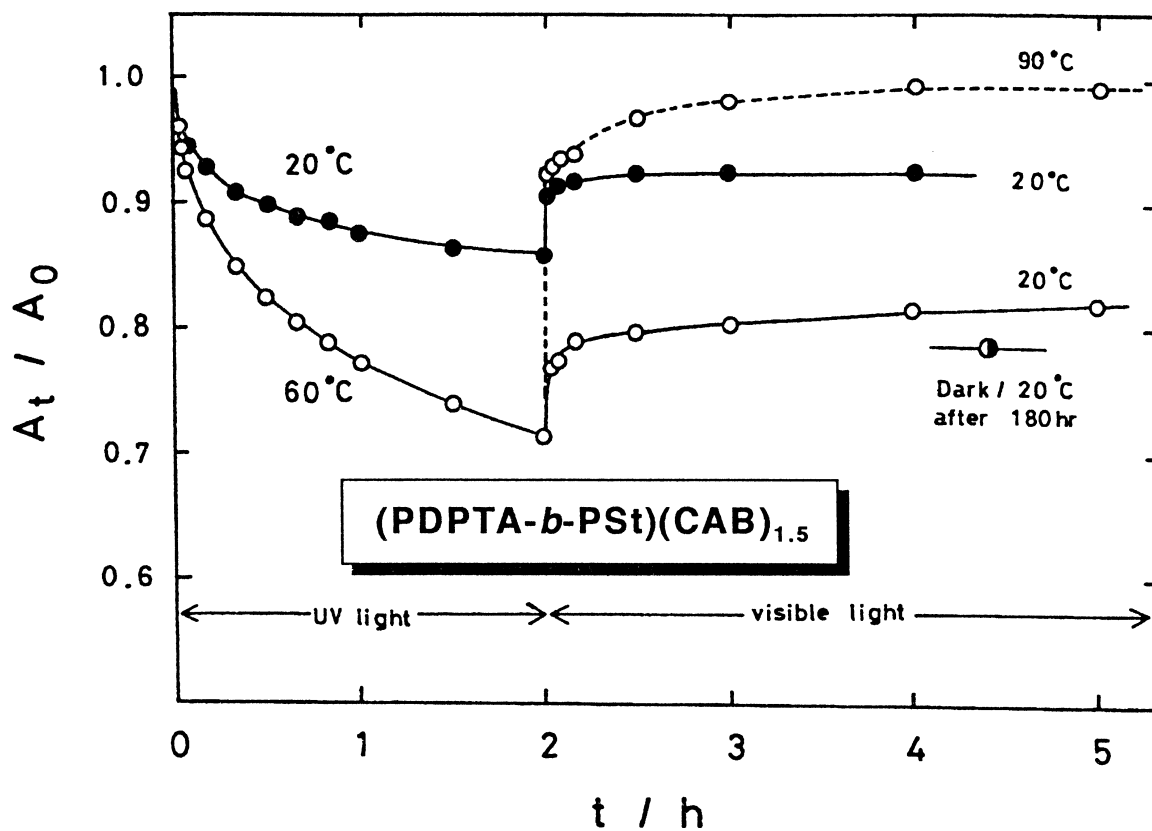


Fig. 17. Photochemical isomerization from *trans* to *cis* form of CAB and from *cis* to *trans* form of CAB in a $(PDPTA-b-PSt)(CAB)_{1.5}$ film. The film was first irradiated with a UV light at 60°C (○) or 20°C (●) for 2 h. Next, each film was irradiated with a visible light at 20°C. The result of a reverse thermal isomerization is also described by storing the film in darkness at 20°C for 180 h (○). The film after irradiation with a UV light at 60°C for 2 h was finally irradiated with a visible light at 90°C(- ○ -).

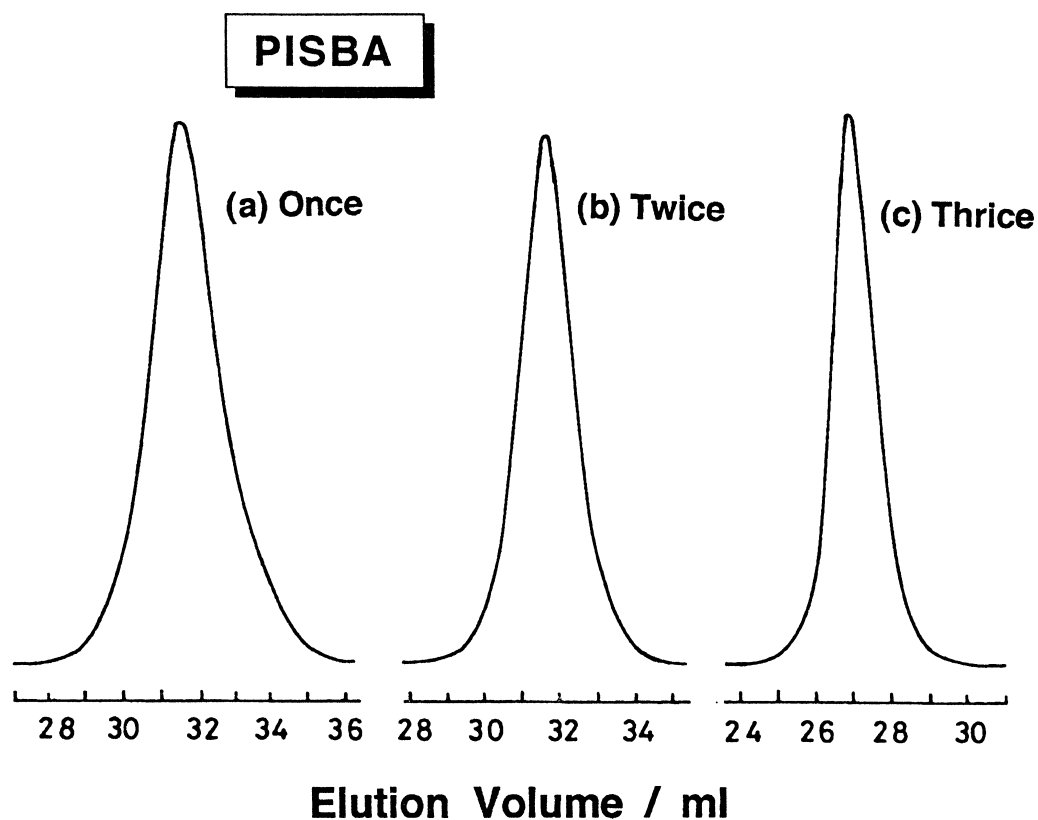


Fig. 18. GPC chromatograms of PISBA prepared from ISBA (a) once, (b) twice, and (c) three times dried over BuMgBr in THF. The experimental conditions are as follows: the carrier solvent of THF containing *N*-methylpyrrolidine (2 v/v%), the flow rate of 1.0 ml min⁻¹, the RI detector, and the polymer concentration of 0.05 w/v%.

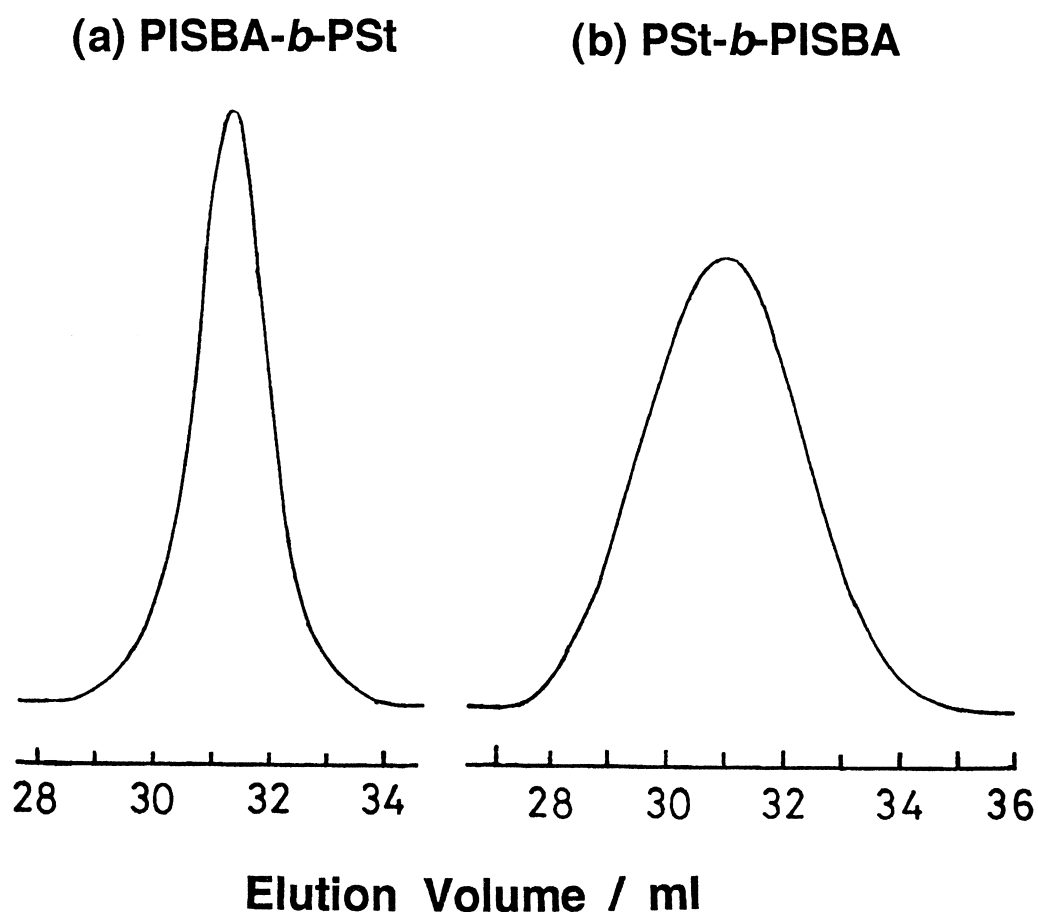


Fig. 19. GPC chromatograms of (a) PISBA-*b*-PSt and (b) PSt-*b*-PISBA. The sequence of the addition of the two monomers was inverted in block copolymerization.

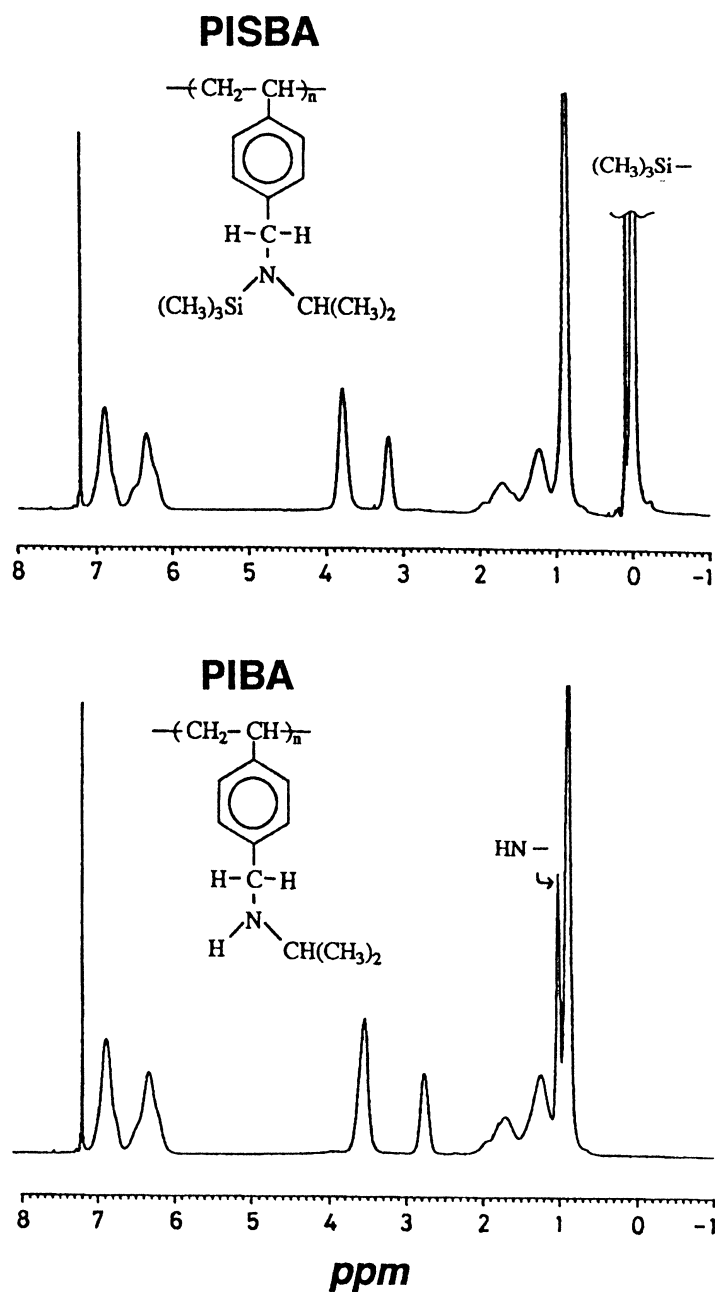


Fig. 20. $^1\text{H-NMR}$ spectra of PISBA (top) and the resultant PIBA (bottom) after the removal of a trimethylsilyl group. A sharp NMR signal of PISBA at 0 ppm was due to the trimethylsilyl group and was completely disappeared in PIBA, whereas a sharp NMR signal of PIBA at 1.0 ppm was newly observed and was assigned to the amino group.

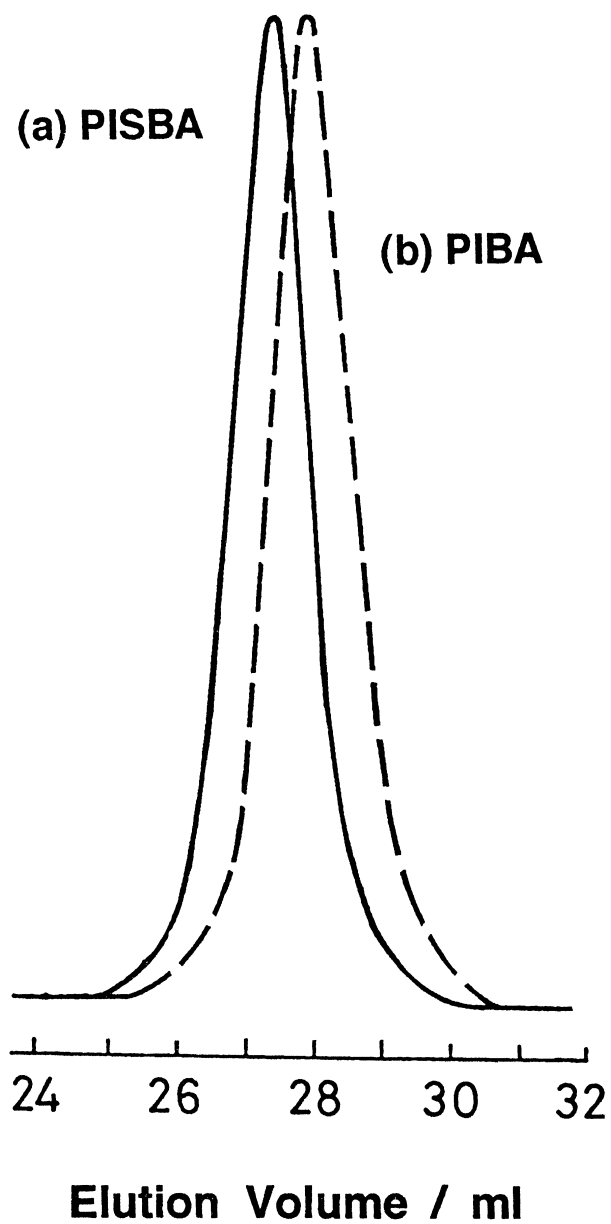


Fig. 21. GPC chromatograms of (a) PISBA (—), $M_n = 1.7 \times 10^5$, and the resultant poly(*N*-isopropyl-4-vinylbenzylamine) (PIBA) (---), $M_n = 1.2 \times 10^5$ after removal of the trimethylsilyl group.

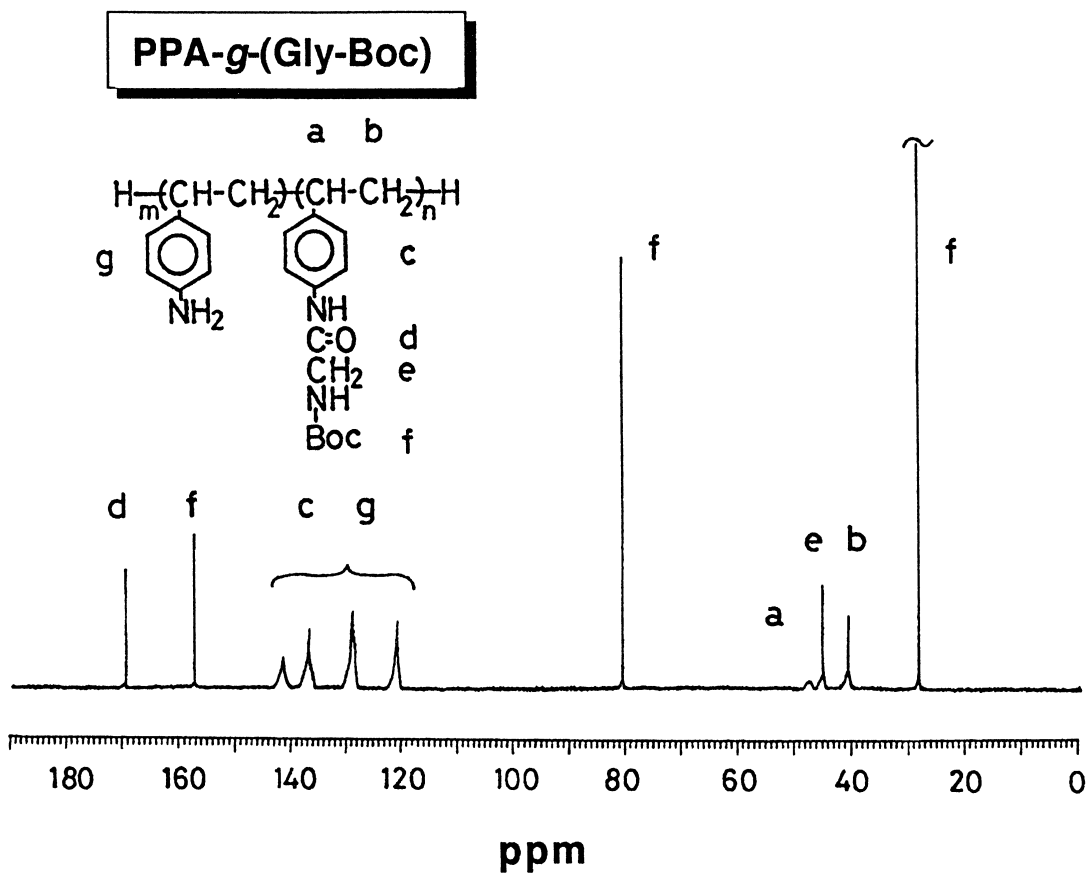


Fig. 22. A ¹³C-NMR spectrum of PPA-g-(Gly-Boc) prepared with [Boc-Gly] / [PA] = 1 at 0°C for 2 h. Signals are assigned in the figure.

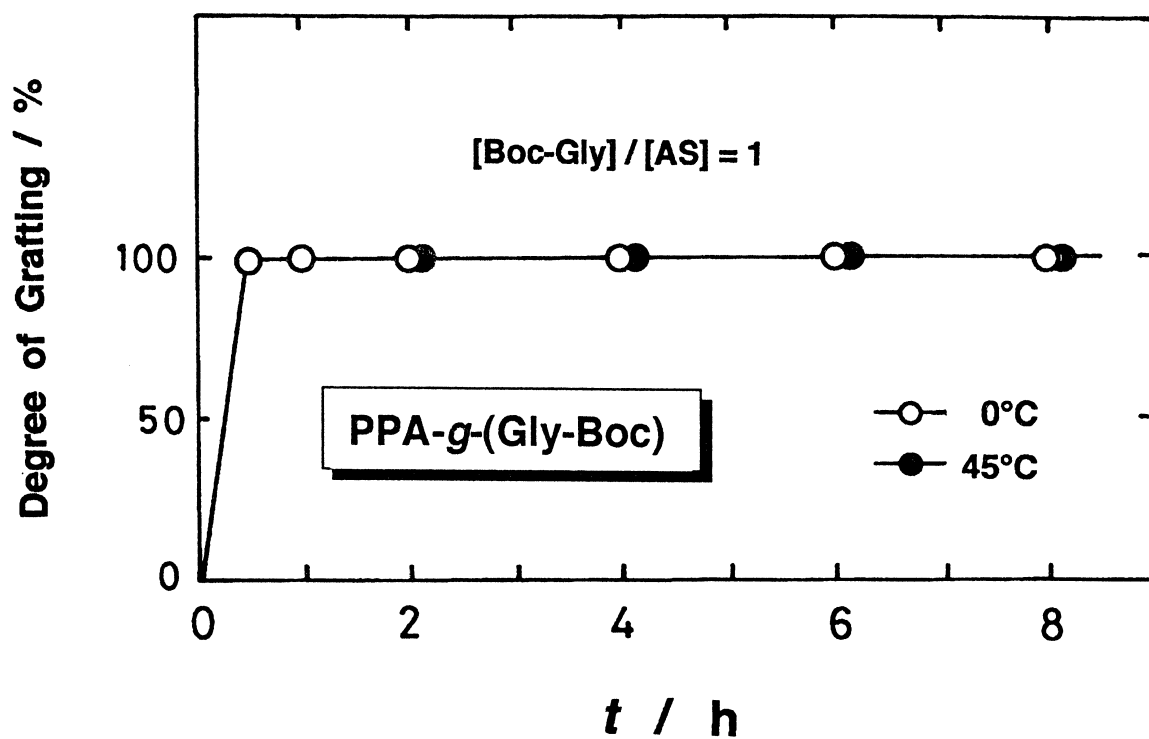


Fig. 23. Reaction time dependence of the degree of grafting for PPA-g-(Gly-Boc) with [Boc-Gly] / [PA] = 1 at 0°C (○) and 45°C (●).

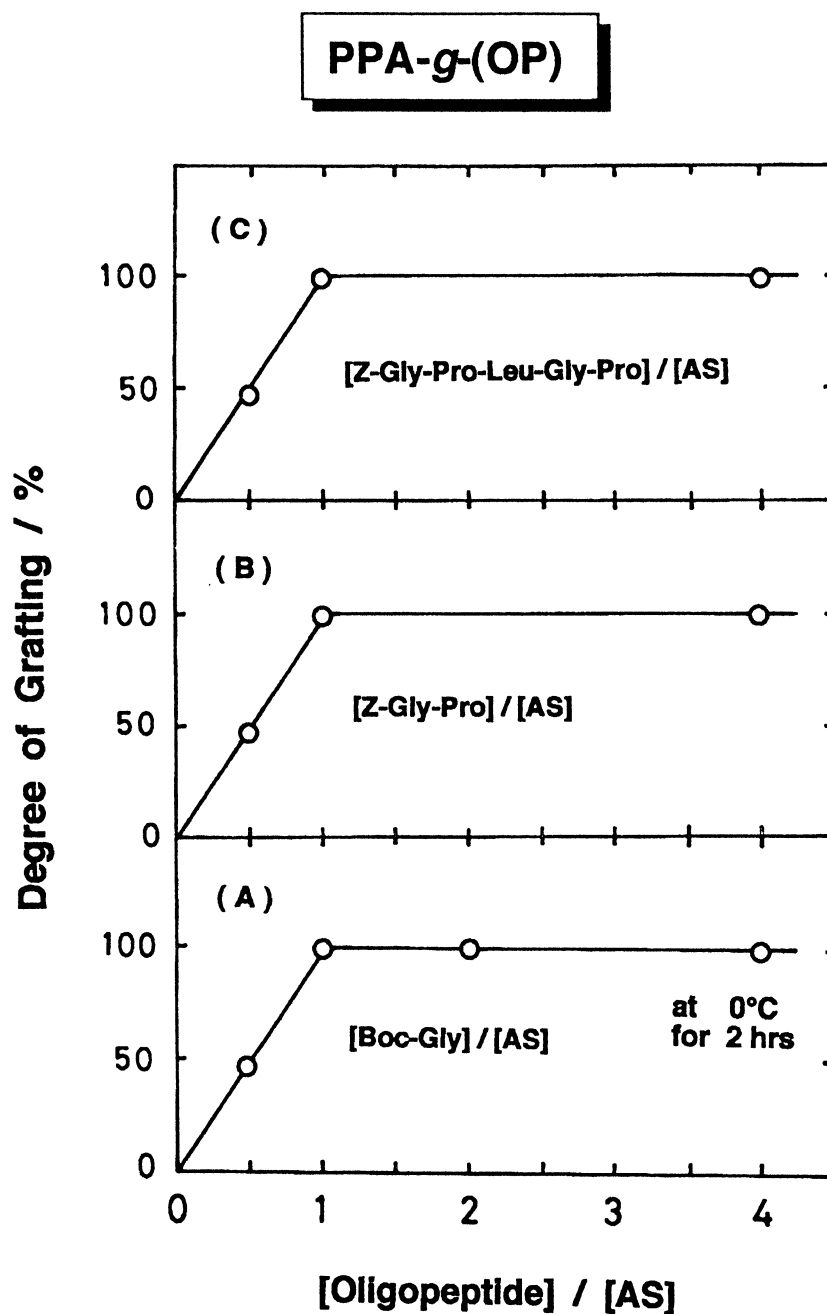


Fig. 24. Plots of the degree of grafting *versus* molar ratios of (a) Boc-Gly, (b) Z-Gly-Pro, and (c) Z-Gly-Pro-Leu-Gly-Pro, to the monomer unit for PPA fed in the reaction mixtures at 0°C for 2 h.

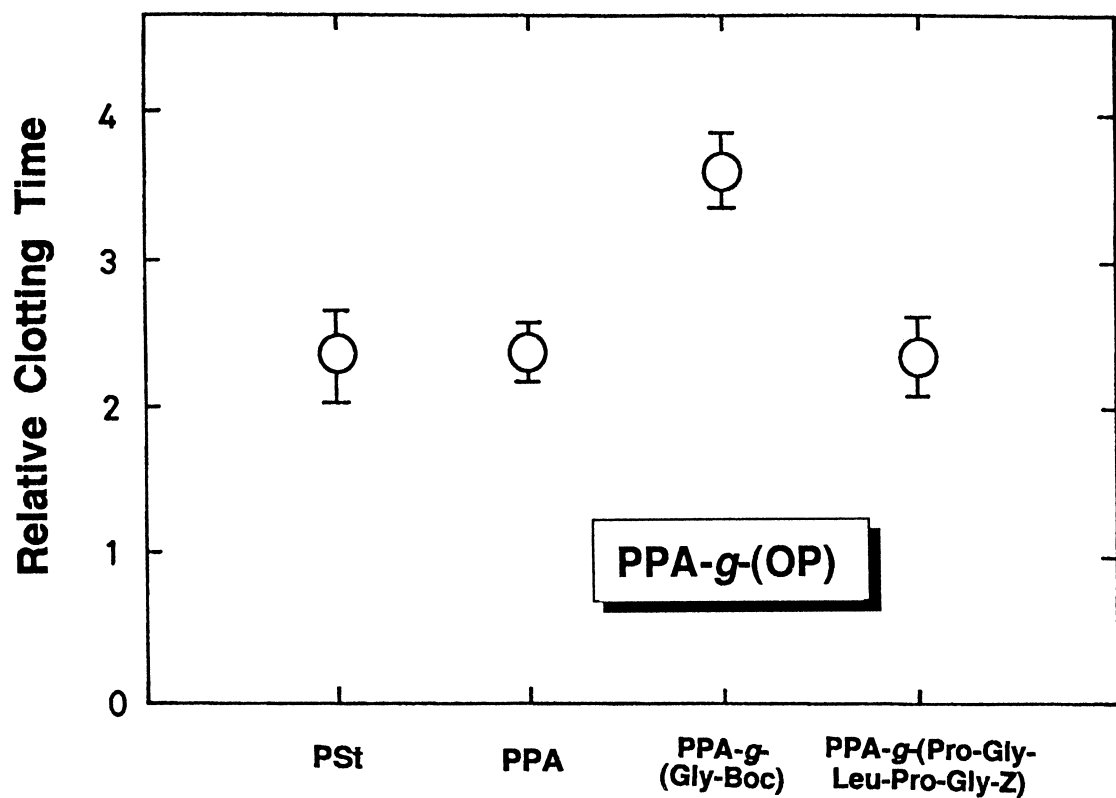


Fig. 25. Lee-White relative clotting times (L-WRCT) of polystyrene, PPA, PPA-g-(Gly-Boc), and PPA-g-(Pro-Gly-Leu-Pro-Gly-Z) having 100% of DOG. The L-WRCT values were determined from a Lee-White method using human whole blood.

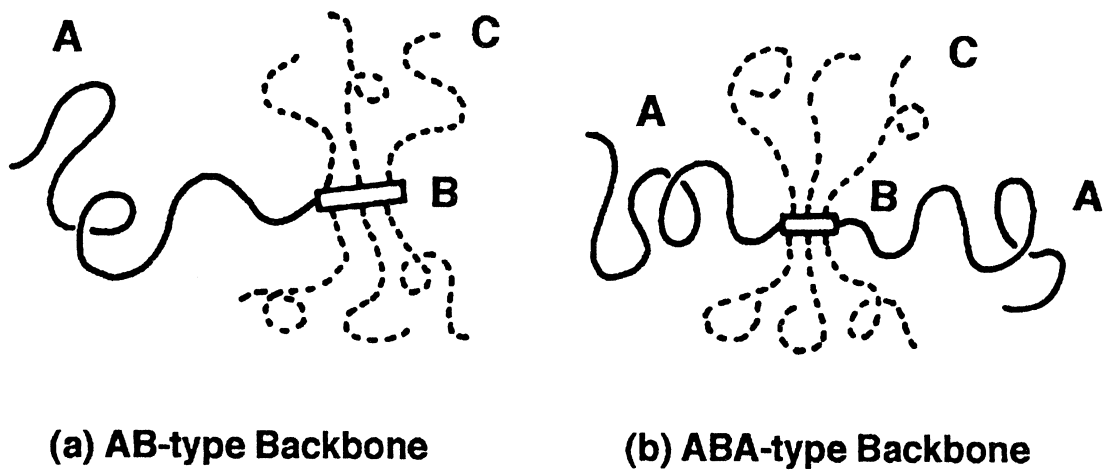


Fig. 26. Two schematic structures of the model block-graft copolymers, where A, B, and C are a backbone chain without grafting sites, a backbone chain with grafting sites, and graft chains, respectively.

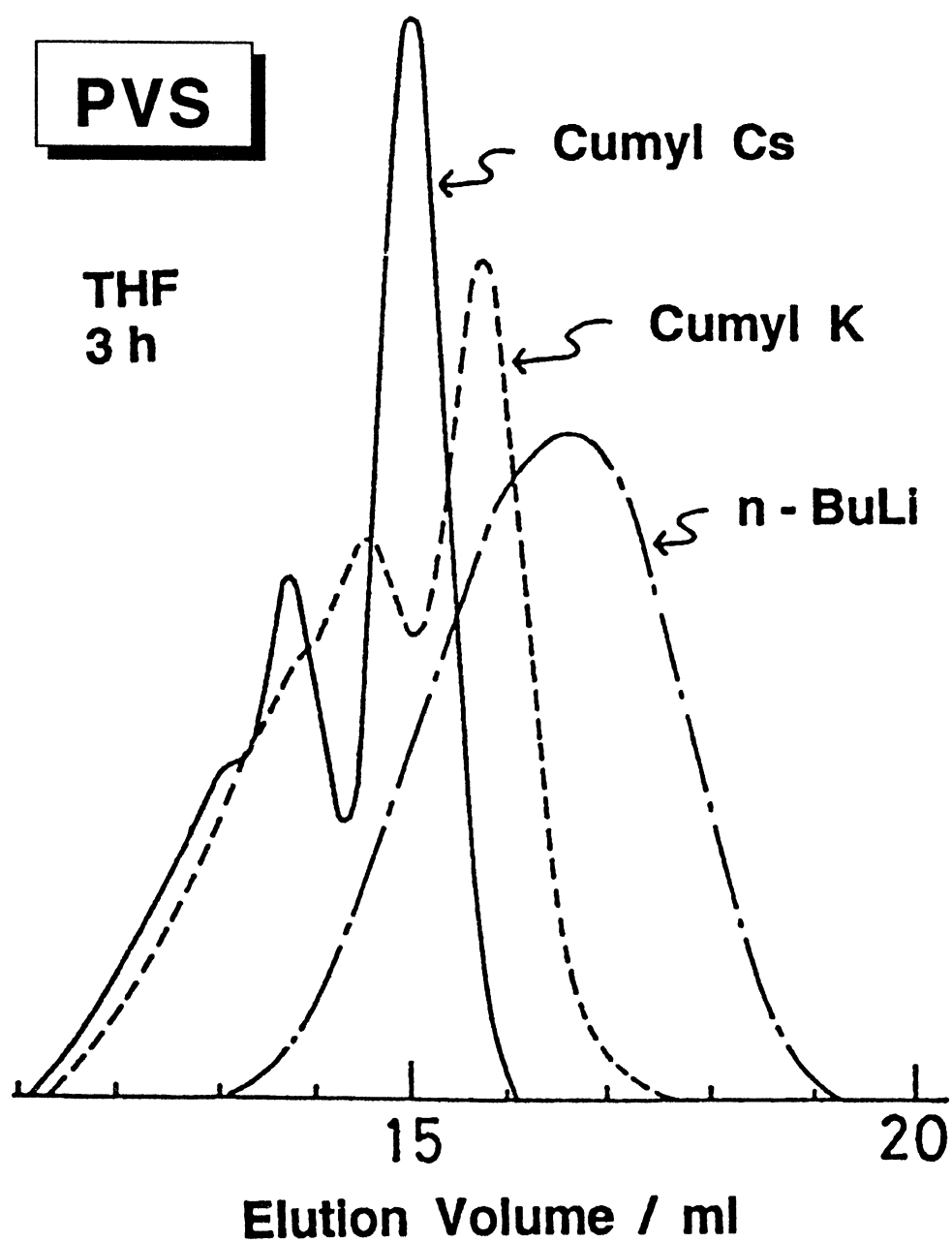


Fig. 27. GPC chromatograms of PVS prepared using *n*-BuLi, Cumyl K, and Cumyl Cs as initiators, THF as a solvent, and a polymerization time of 3 h.

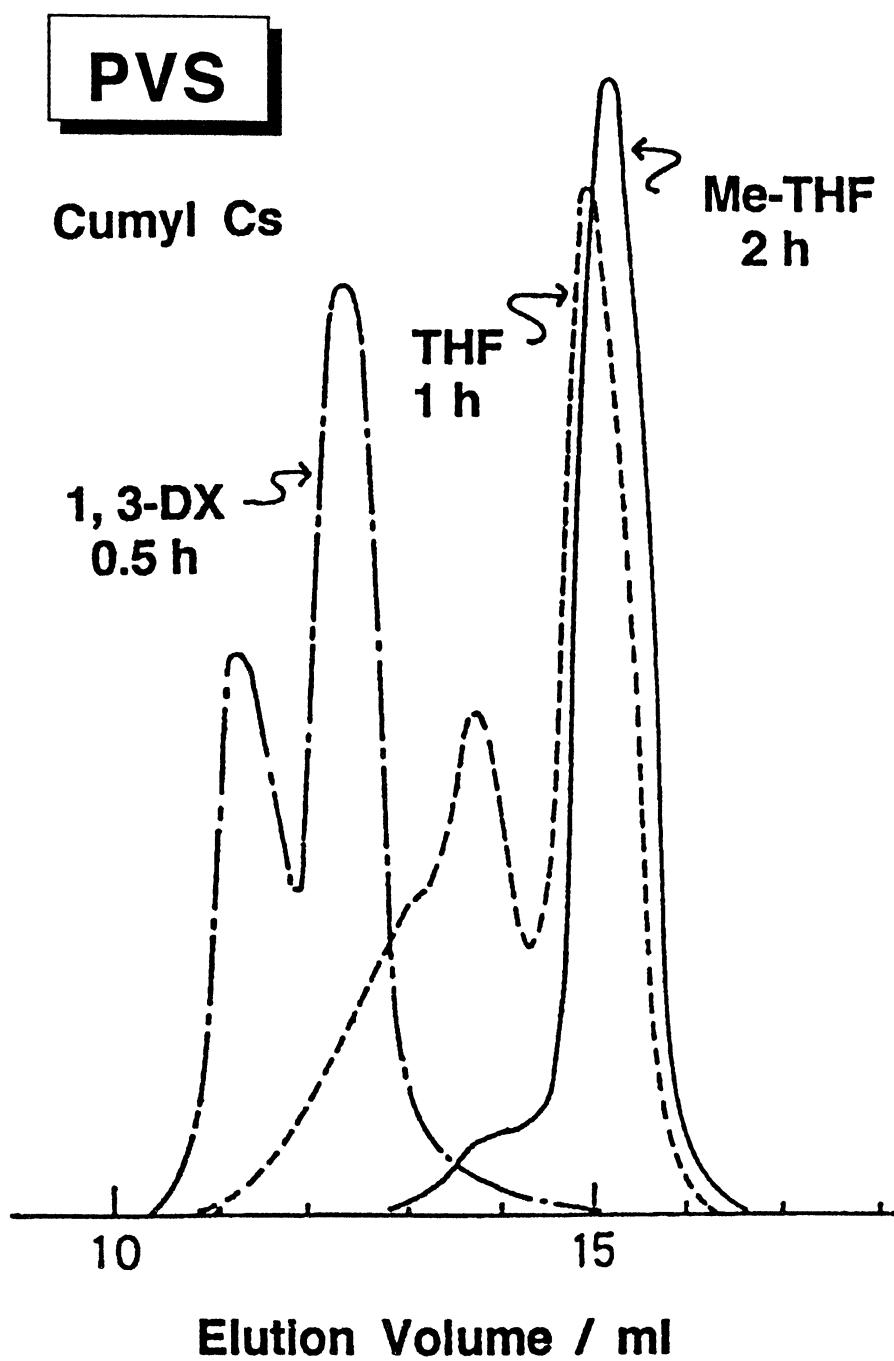
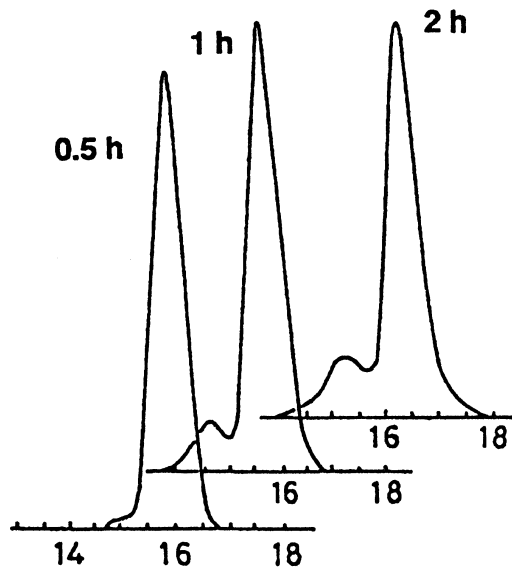


Fig. 28. GPC chromatograms of PVS prepared using THF, Me-THF, and 1, 3-DX as solvents, Cumyl Cs as an initiator, and polymerization times as described in the figure.

PVS

Ether / 1, 3-DX = 1 / 2

Cumyl Cs



Ether / 1, 3-DX = 1 / 1

Cumyl Cs

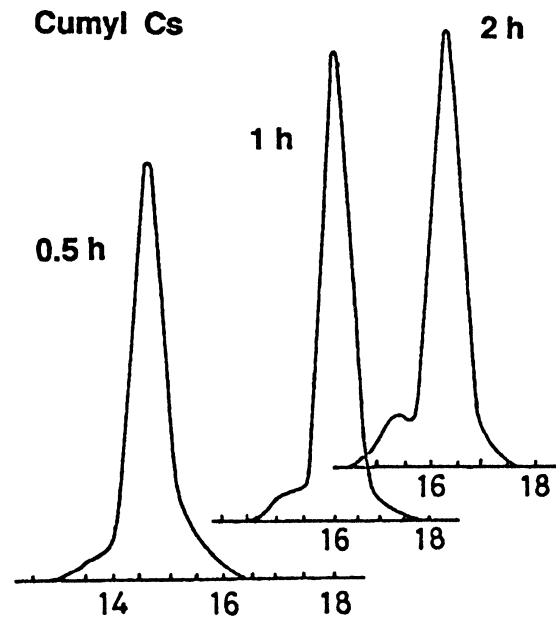
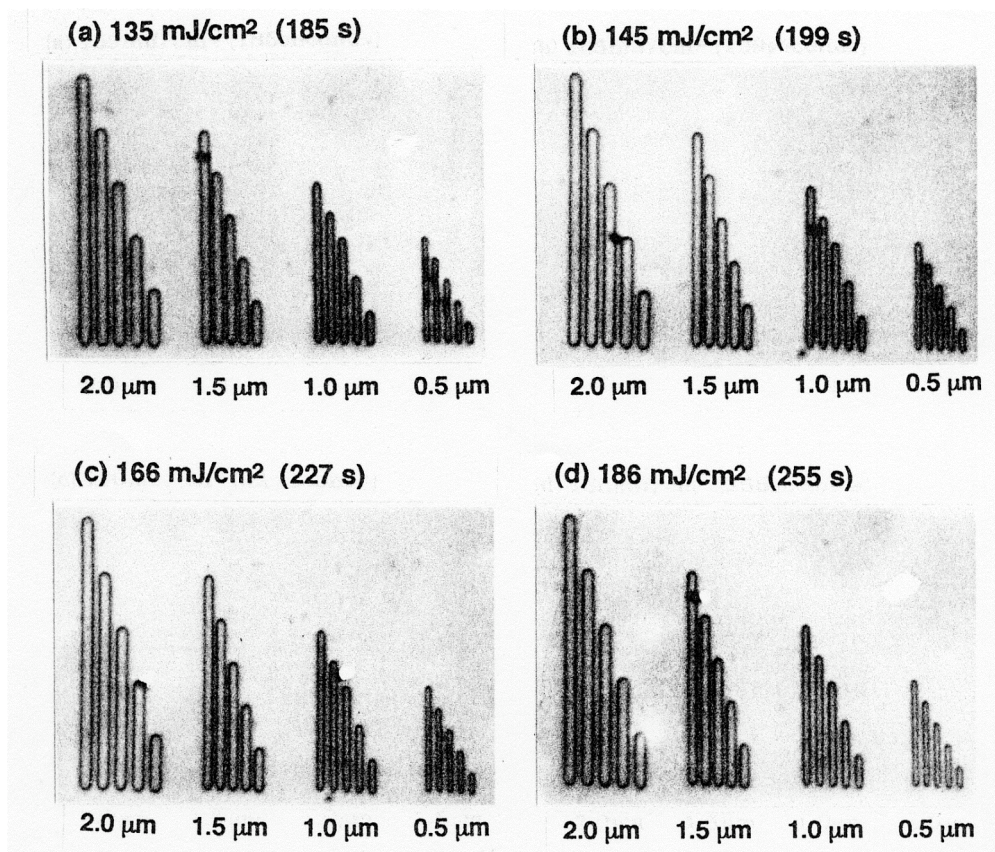


Fig. 29. GPC chromatograms of PVS prepared at a polymerization time between 0.5 h and 2 h, using Cumyl Cs as an initiator, and a mixture of Ether/1, 3-DX = 1/2 (a left figure) or Ether/1, 3-DX = 1/1 (a right figure) as a solvent.

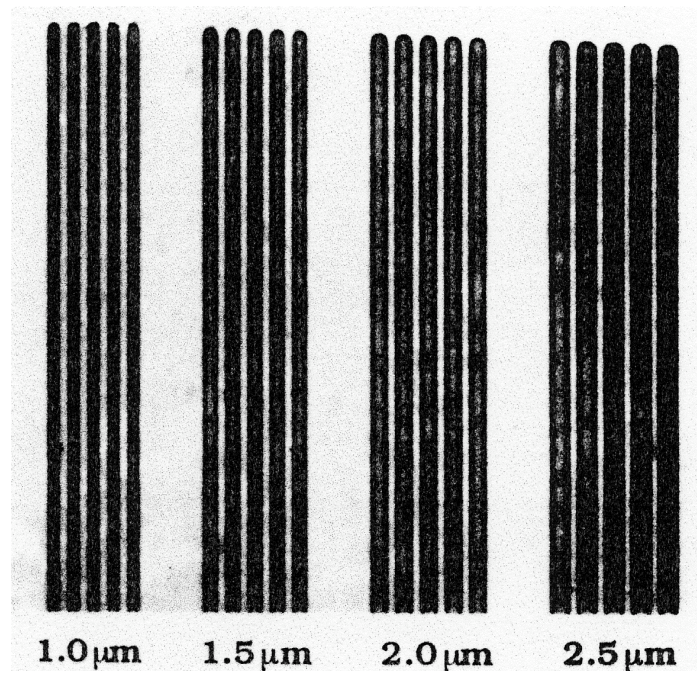


Please change:

Photograph of Fig. 34 in the Original Manuscript.

⇒ Here, Fig. 30 in the Revised Manuscript.

Fig. 30. Scanning electron micrographs of image lines from resists of PVS-4 exposed to a deep UV light of 270 nm. The developer is a mixture of xylene/methanol = 8/1. A number such as 2.0 μm appearing in this figure represents 2.0 μm lines, and all spaces between the lines are 0.75 μm . Intensities of a deep UV light are (a) 135 mJ/cm^2 (185 seconds), (b) 145 mJ/cm^2 (199 s), (c) 166 mJ/cm^2 (227 s), and 186 mJ/cm^2 (255 s).



Please change:

Photograph of Fig. 35 in the Original Manuscript.

⇒ Here, Fig. 31 in the Revised

Manuscript

Fig. 31. A scanning electron micrograph of image lines from a resist of PVS-4 exposed to an electron beam. A developer is a mixture of xylene/methanol = 8/1. A number such as 1.0 μm appearing in this figure represents 1.0 μm lines, and all spaces between the lines are 1.0 μm.

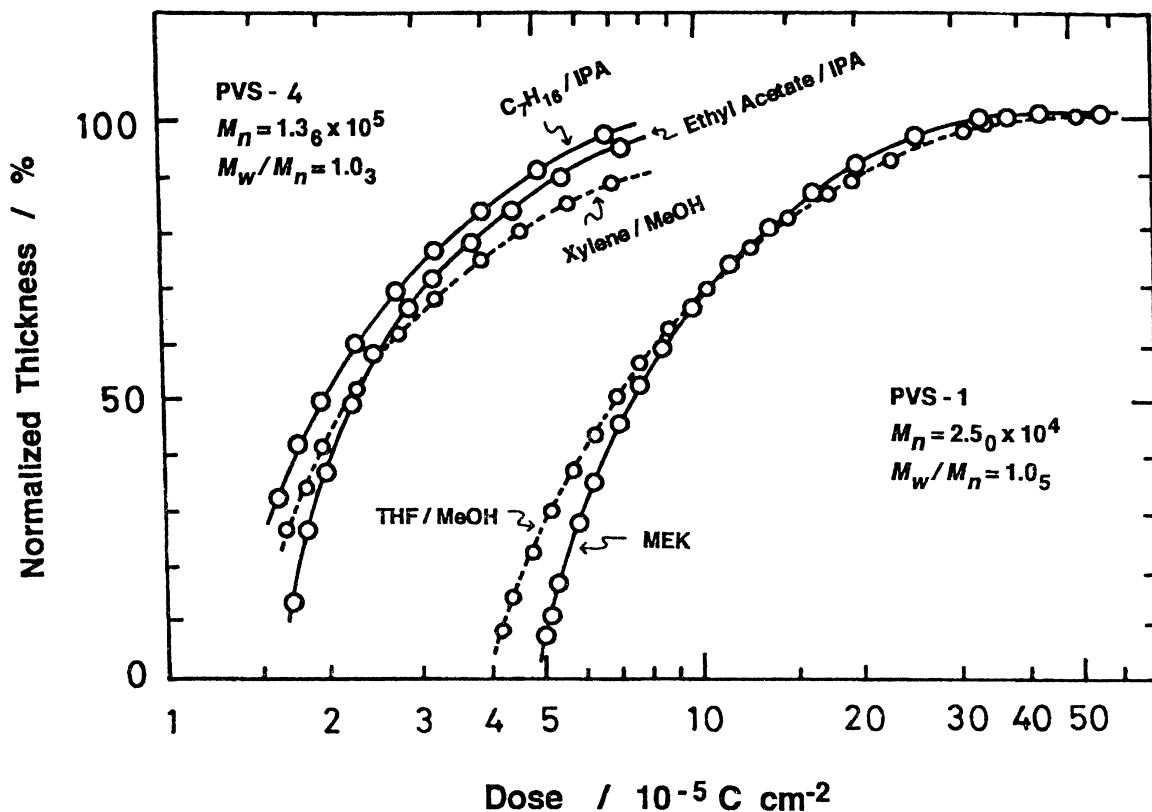


Fig. 32. Exposure response curves of PVS-1 and PVS-4 exposed to electron beams. Developers in the figure are *n*-heptane (C_7H_{16})/isopropyl acetate (IPA) = 1/1, ethyl acetate/isopropyl acetate (IPA) = 1/1, xylene/methanol (MeOH) = 8/1, tetrahydrofuran (THF)/methanol (MeOH) = 35/65, and methyl ethyl ketone (MEK).

(PVS-*g*-PIs)-*b*-PSt

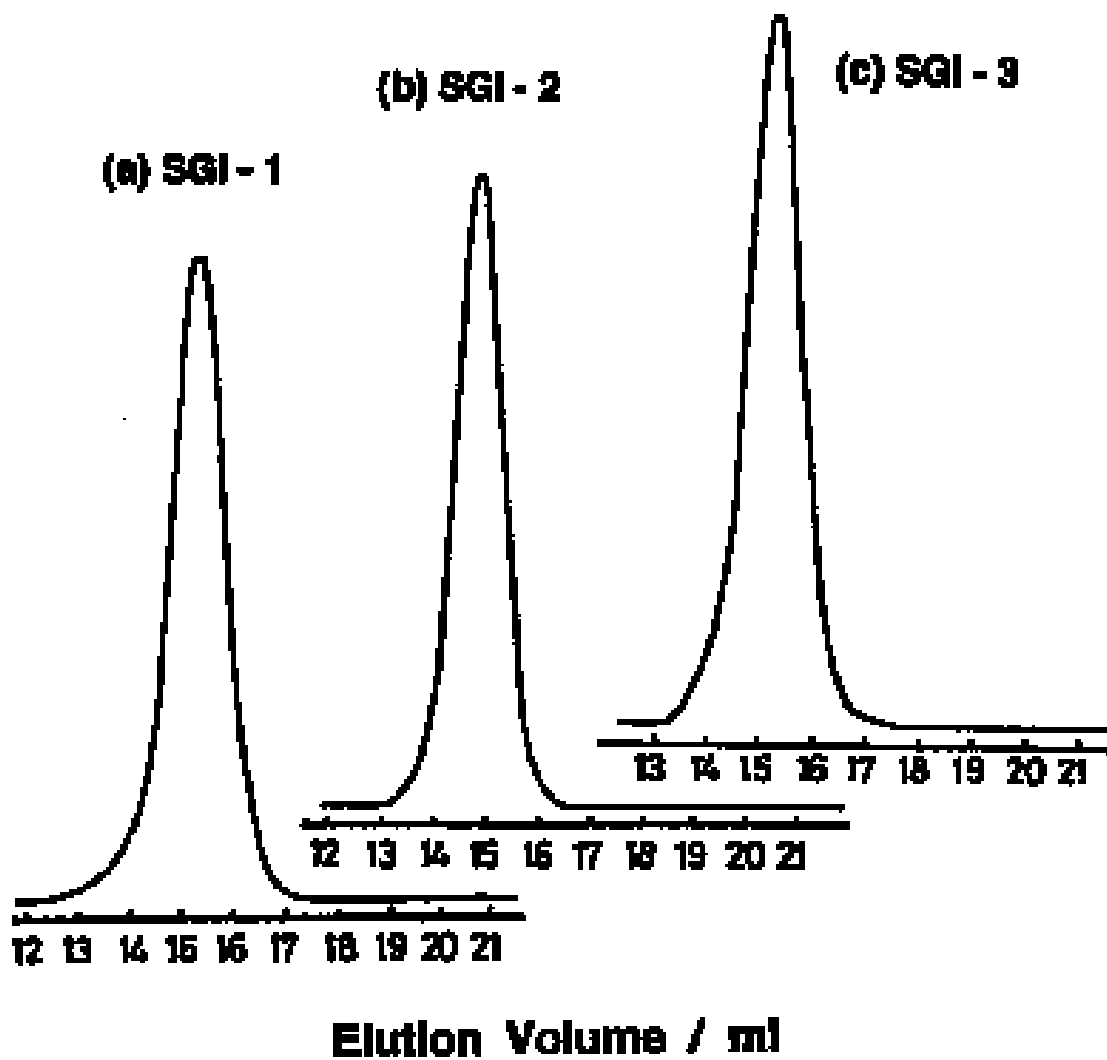
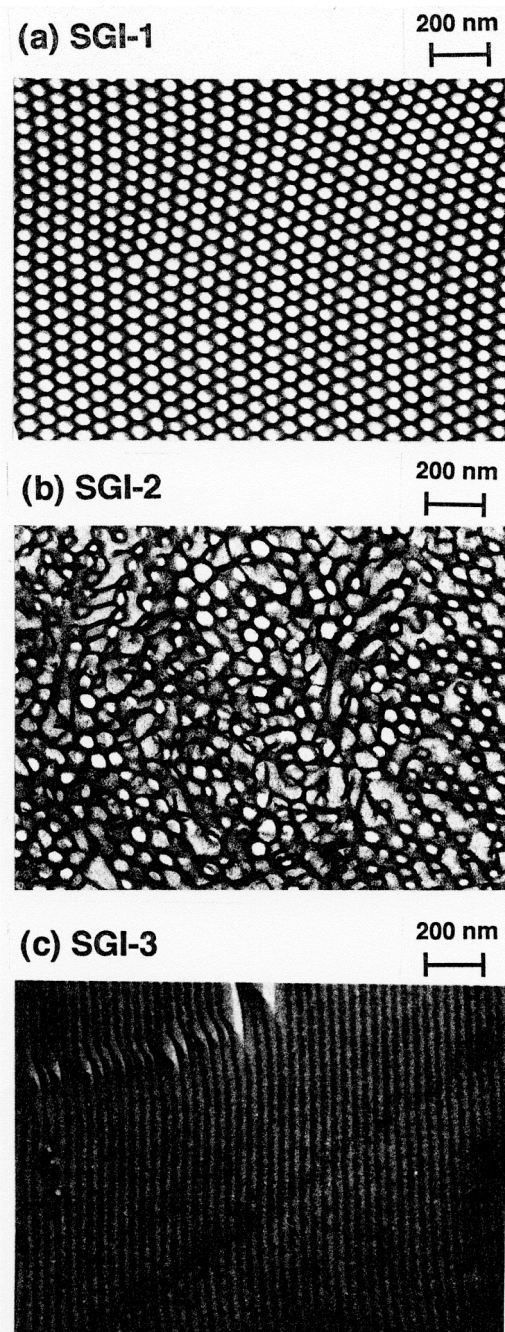


Fig. 33. GPC chromatograms of (PVS-*g*-PIs)-*b*-PSt block-graft copolymers of (a) SGI-1, (b) SGI-2, and (c) SGI-3 samples, prepared *via* a backbone coupling (a “grafting onto” process).



Please change:

**Photographs of Fig. 39 in
the Original Manuscript.**

**⇒ Here, Fig. 34 in the
Revised Manuscript.**

Fig. 34. Transmission electron micrographs of (PVS-*g*-PIs)-*b*-PSt block-graft copolymer films of (a) SGI-1, (b) SGI-2, and (c) SGI-3, which were cast from the respective benzene solutions and were subsequently stained with OsO₄. White and black regions correspond to PSt/PVS and PIs phases, respectively.

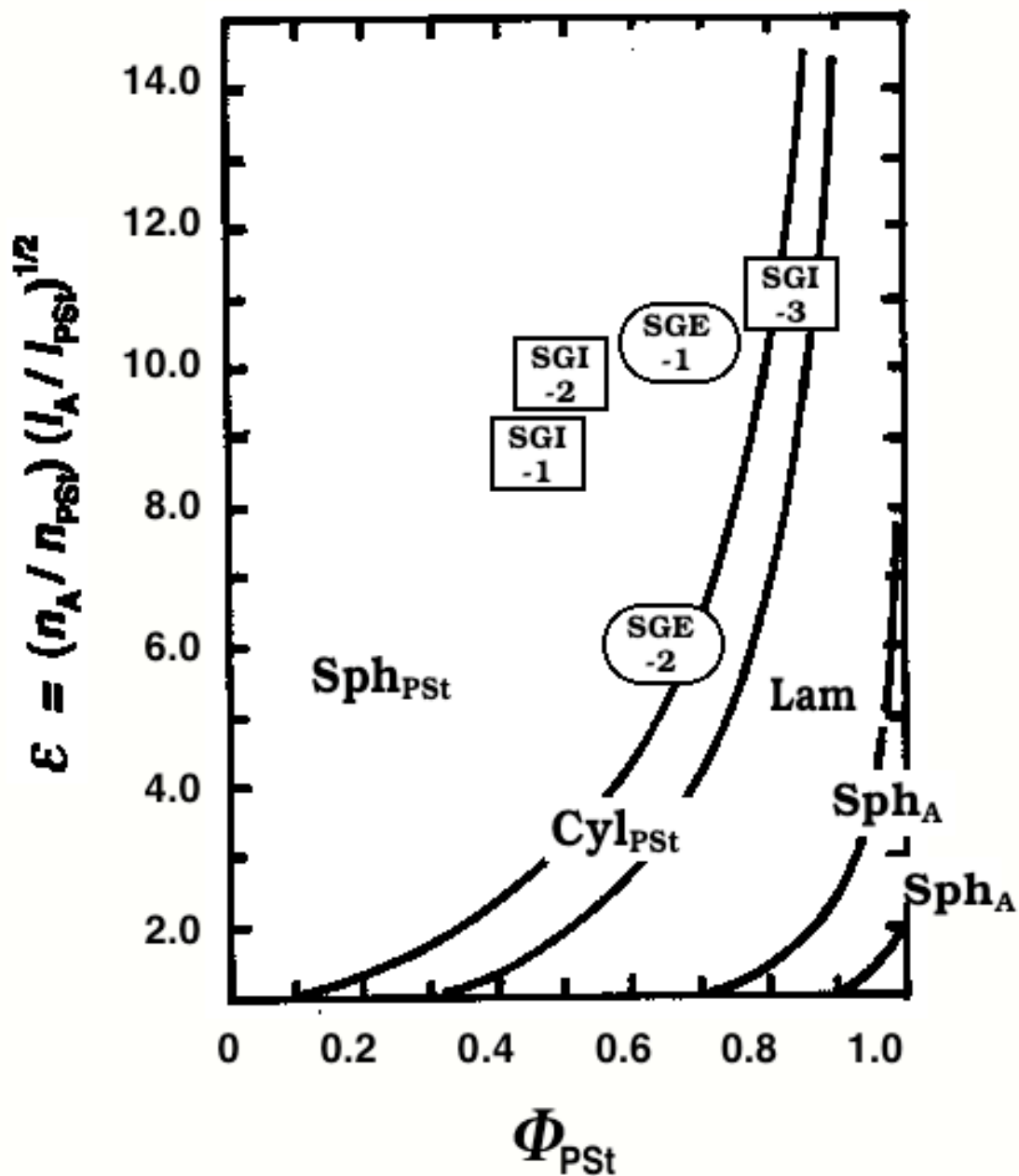


Fig. 35. Theoretical phase diagram of $(A)_m(PSt)_n$ calculated by Milner, where the bicontinuous phases are omitted due to being complicated. The A polymer is PIs for three SGI films or PEO for two SGE films. Symbols represent the MS structures of Sph_{PSt} (spheres of PSt), Cyl_{PSt} (cylinders of PSt), Lam (lamella), Cyl_A (cylinders of A polymer), and Sph_A (spheres of A polymer). Boldly outlined symbols indicate samples characterized in this study.

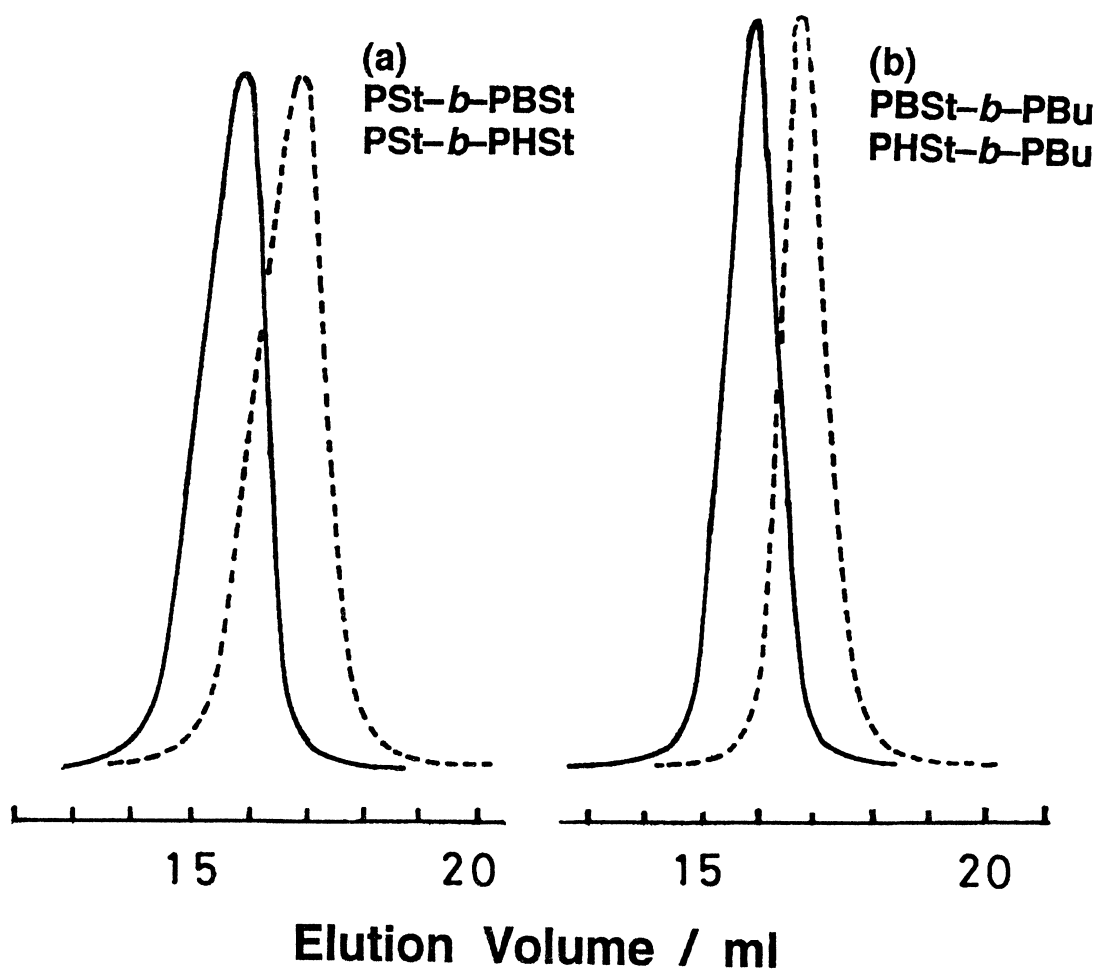


Fig. 36. GPC chromatograms of (a) PSt-*b*-PBSt block copolymer (—) and the resultant PSt-*b*-PHSt block copolymer (- - -) after removal of the *tert*-butyl group, and (b) PBSt-*b*-PBu block copolymer (—) and the resultant PHSt-*b*-PBu block copolymer (- - -).

PSt-*b*-PBSt-*b*-PSt

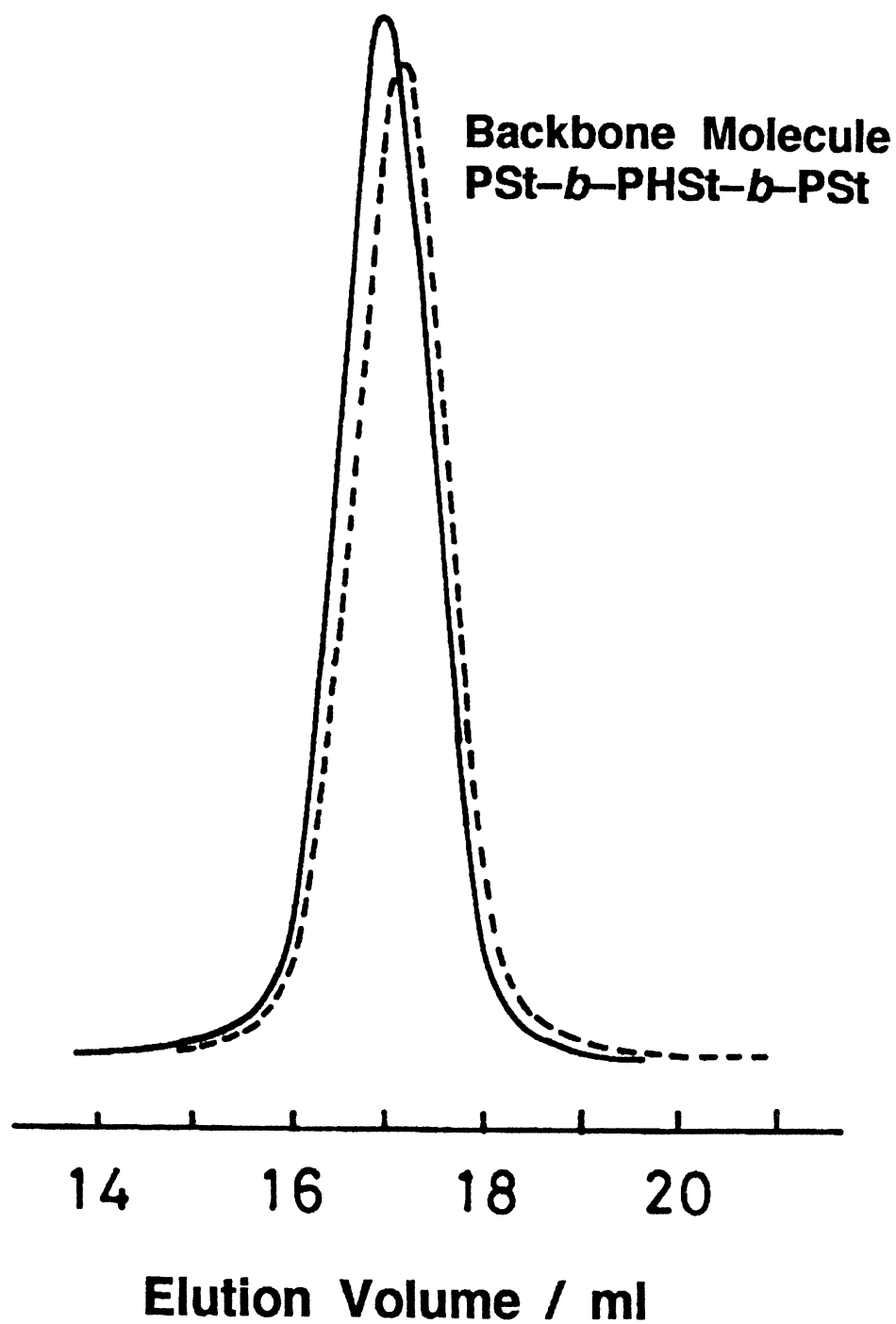


Fig. 37. GPC chromatograms of PSt-*b*-PBSt-*b*-PSt block copolymer (—) and the corresponding PSt-*b*-PHSt-*b*-PSt block copolymer (- - -) as a backbone chain deprotected by HBr.

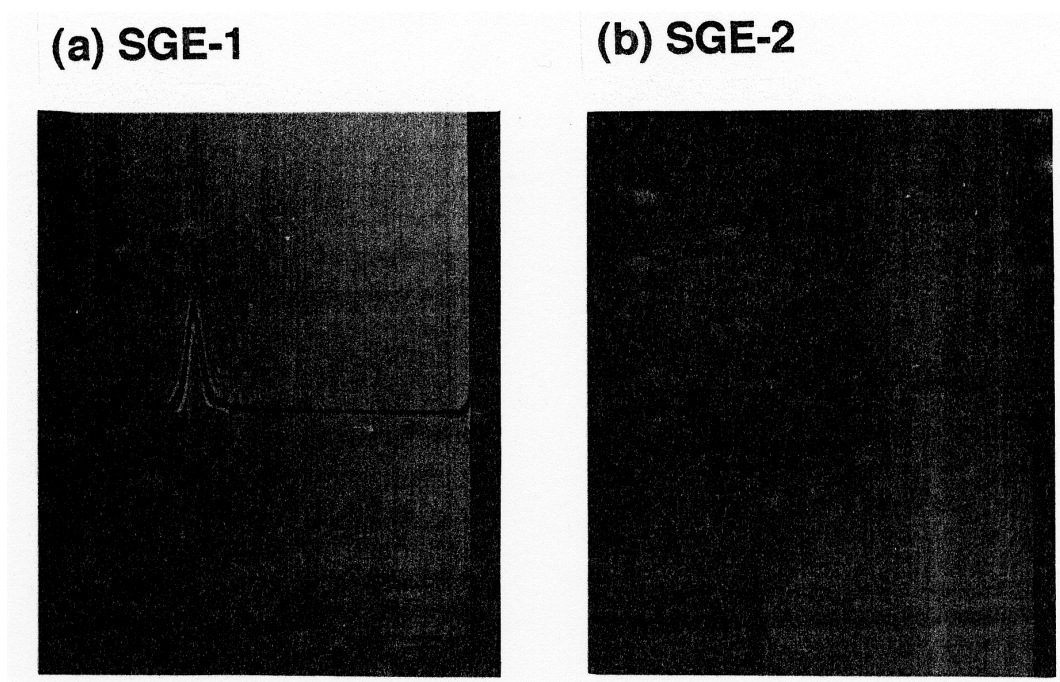


Fig. 38. Sedimentation patterns of two PSt-*b*-(PHSt-*g*-PEO)-*b*-PSt block-graft copolymers of (a) SGE-1 and (b) SGI-2: a concentration of 0.25 g dl⁻¹ and a time of 21 min for SGE-1, and a concentration of 0.20 g dl⁻¹ and a time of 18 min for SGE-2, THF solvent, a temperature of 25°C, a speed of rotation of 59,780 rpm, and an angle of 70 degrees.

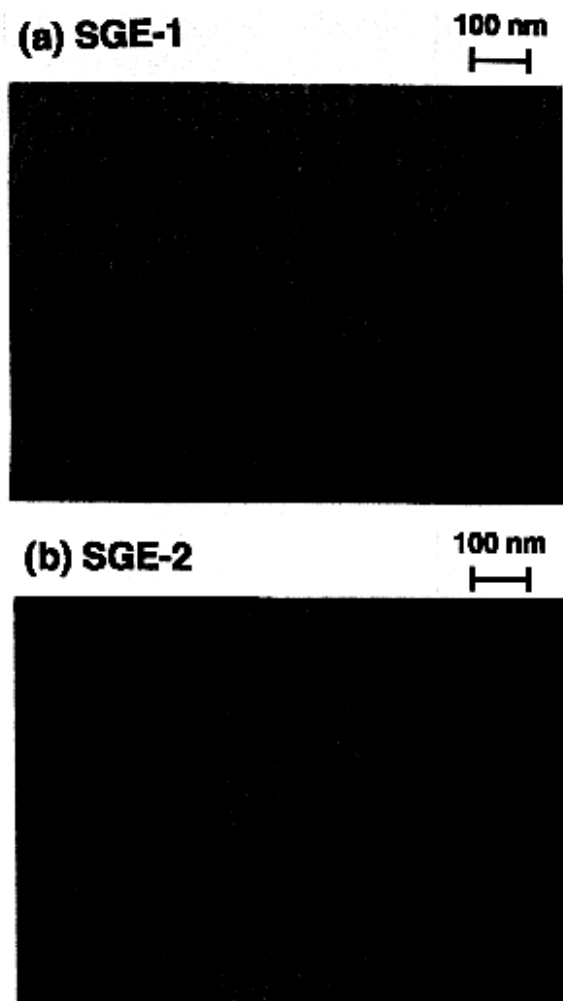


Fig. 39. Transmission electron micrographs of PSt-*b*-(PHSt-*g*-PEO)-*b*-PSt block-graft copolymer films of (a) SGE-1 and (b) SGE-2, which were cast from the respective benzene solutions and were subsequently stained with OsO₄ and RuO₄, respectively. White and black regions correspond to PSt/PHSt and PEO phases, respectively.